

THE UNIVERSITY OF MANITOBA
INTERACTION BETWEEN SHEAR WALLS
AND FLAT PLATE FLOOR SYSTEMS

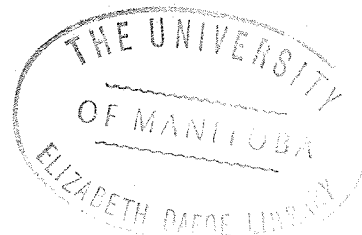
by

U. C. GOYAL

A THESIS
SUBMITTED TO THE FACULTY OF GRADUATE STUDIES
IN PARTIAL FULFILMENT OF THE REQUIREMENTS FOR THE DEGREE OF
MASTER OF SCIENCE IN CIVIL ENGINEERING

WINNIPEG, MANITOBA

OCTOBER, 1972



ACKNOWLEDGMENTS

The author would like to express his sincere gratitude to his advisor Dr. G. A. Morris for his invaluable guidance and encouragement throughout this thesis. Special thanks are due to Prof. R. B. Pinkney for his continued help in computer work. The author would also like to thank the Civil Engineering Laboratory staff for their help in the experimental work. The financial assistance of the National Research Council of Canada and of the University of Manitoba is gratefully acknowledged.

TABLE OF CONTENTS

Acknowledgment	i
List of Tables	iv
Notation	v
Chapter	Page
1 INTRODUCTION	1
1.1 Object of Study	1
1.2 Historical Background	6
1.3 Assumptions and Limitations	11
2 THEORETICAL CONSIDERATIONS	13
2.1 Stiffness Matrix	13
2.2 Bending Stiffness Coefficients	17
2.3 Measurement of Bending Stiffness Coefficients	18
2.3.1 Direct Bending Stiffness Coefficients For Flat Plate	20
2.3.2 Carry-Over Bending Stiffness Coefficients For Flat Plate	20
2.4 Behavior of Flat Plate Floor Systems	24
2.5 Contributions to Bending Resistance of Flat Plate Floor	29
3 ANALYTICAL AND EXPERIMENTAL STUDIES	36
3.1 Introduction	36
3.2 Analytical Procedure	38
3.2.1 Representation of Plate Model	38
3.2.2 Description of Analytical Models	45
3.3 Experimental Procedure	50
3.3.1 Description of Experimental Models	50
3.3.2 Loading Procedure	59
3.3.3 Photographic Technique	59
4 ANALYTICAL AND EXPERIMENTAL RESULTS	63
4.1 Results of Analytical Study	63
4.2 Results of Experimental Study	83

Chapter		Page
5	DISCUSSION OF RESULTS	85
	5.1 Effects of Column Size and Shear Wall Size	85
	5.1.1 Direct Bending Stiffness Coefficients	85
	5.1.2 Carry-Over Bending Stiffness Coefficients	89
	5.2 Contributions of Floor Plate Elements to Direct Bending Stiffness	90
6	ILLUSTRATIVE EXAMPLES	99
	6.1 Stiffness Coefficients For Basic Flat Plate Floor System	99
	6.2 Accuracy of Multiplying Factors	108
	6.3 Lateral Load Analysis of a Frame-Work	116
	6.3.1 Bending Stiffness Coefficients For the Floor Systems Supported Only on Columns	120
	6.3.2 Bending Stiffness Coefficients For Floor Systems with Shear Wall	125
7	CONCLUSIONS AND RECOMMENDATION FOR FURTHER STUDY	136
	7.1 Conclusions	136
	7.2 Recommendations for Further Study	138
	<u>References</u>	140
Appendix A:	Computer Program USER's Guide	142
Appendix B:	B-1 Basic Principle of the Moire' Method	159
	B-2 Determination of Slope Curve from Moire' Photograph	161
Appendix C:	Tables for Applied Moments and Resulting Rotations	182

LIST OF TABLES

Table	Page	
3.1	Dimensions of Models for Effect of Column Size	46
3.2	Dimensions of Models for Effect of Shear Wall Size	46
3.3	Dimensions of Models for Effect of Shear Wall Shape	47
3.4	Dimensions of Models for Second Phase of the Study	49
4.1	Effect of Column Size on Stiffness Coefficients	64
4.2	Effect of Shear Wall Size on Stiffness Coefficients	65
4.3	Effect of Shear Wall Shape on Stiffness Coefficients	66
4.4	Contribution of Different Panels and Joints to the Total Stiffness When Shear Wall Loaded	78
4.5(a)	Value of F_T	79
4.5(b)	Value of F_B	79
4.5(c)	Value of F_C	80
4.5(d)	Value of F_{TC}	80
4.5(e)	Value of F_{BC}	81
4.6	Effect of Different Parameters on Bending Stiffness Coefficients	82
4.7	Experimental Results	84
5.1	Stiffness Coefficients for Model P1	88
5.2	Percentage Contribution of Different Panels and Joints to the Total Stiffness when Shear Wall Loaded	91
5.3	Comparison of Experimental and Analytical Results	98
6.1(a)	Stiffness Coefficients for the Floor System of Example 1	106
6.1(b)	Stiffness Coefficients for the Floor System of Example 2	107
6.2(a)	Contribution of Different Panels and Joints to the Total Stiffness for Example 3	113
6.2(b)	Contribution of Different Panels and Joints to the Total Stiffness for Example 4	114

NOTATION

A	= member cross sectional area
B	= width of bending panel
b	= width of torsional panel
C	= column size
E	= modulus of elasticity
F_B	= multiplying factor for a bending panel
F_C	= multiplying factor for a corner panel
F_{BC}	= multiplying factor for a bending joint
F_T	= multiplying factor for a torsional panel
F_{TC}	= multiplying factor for a torsional joint
G	= modulus of rigidity
I	= moment of inertia about bending axis
K_B	= stiffness contribution due to a bending panel
K_C	= stiffness contribution due to a corner panel
K_{BC}	= stiffness contribution due to a bending joint
K_T	= stiffness contribution due to a torsional panel
K_{TC}	= stiffness contribution due to a torsional joint
K_{CC}	= direct bending stiffness coefficient at column
K_{SS}	= direct bending stiffness coefficient at shear wall
K_{SC}	= carry-over bending stiffness coefficient
L_B	= span of bending panel
L_C	= span of corner panel

L_T	=	span of torsional panel
M	=	applied moment
m	=	width of reference beam
SH	=	size of a square shear wall
SX	=	shear wall size in the X-X direction
SY	=	shear wall size in the Y-Y direction
S	=	clear span
TS	=	total span
TSX	=	total span in the X-X direction
TSY	=	total span in the Y-Y direction
t	=	floor thickness
θ	=	rotation

CHAPTER I

INTRODUCTION

1.1 Object of Study

During the past few decades, there has been a dramatic increase in the volume of construction of tall commercial and residential buildings throughout the world. This has necessitated the development of methods for accurate analysis of such structures.

One of the most important factors to be considered in the design of a tall building is its lateral stability in all directions when loaded by wind, earth tremors or blasts. Early in the twentieth century, tall structures generally employed rigid frames consisting of columns and beams. In these structures lateral stiffness was achieved by frame action. Later, flat slab and flat plate floor structures were adopted. Flat plate floor structures have no girders and employ a slab of uniform thickness which rests directly on columns. The flat-slab structure is similar, except that either the slab, the column, or both are thickened at their junction. A common procedure in the analysis of a flat plate multispan structure is to subdivide the whole structure into a series of parallel planar frames and assume the portion of the floor slab between the panel center lines on either side of the columns to be

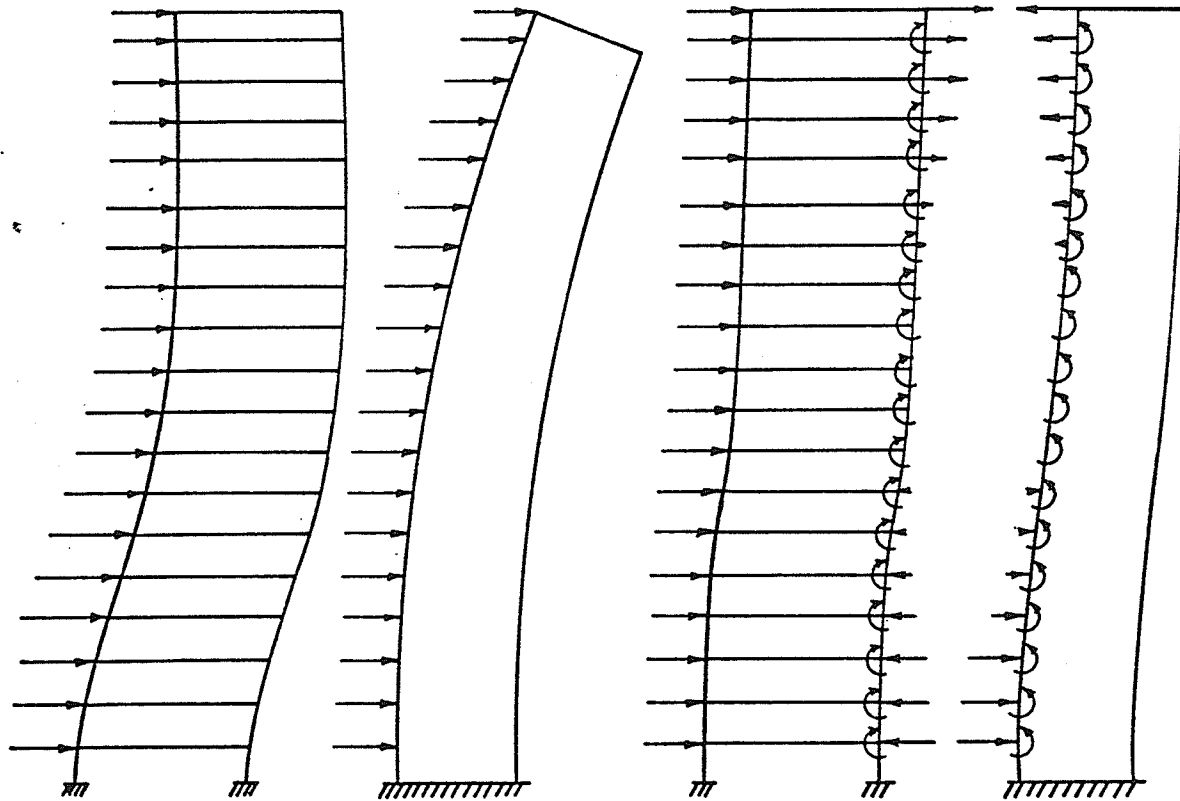
analogous to the beams in an ordinary frame. Each such planar frame is analyzed separately and the frames are then combined to form the complete structure. Assuming the floor slabs to act as rigid diaphragms for distributing in-plane forces, a trial and error procedure is then used to distribute the lateral loading among the frames in such a manner that equilibrium is everywhere satisfied and the lateral displacements of all frames at all floors are compatible.

Lateral stiffness in many tall buildings can be achieved most efficiently by shear wall construction which employs a combination of columns, floor systems and large shear walls which have high in-plane stiffness. Shear walls not only serve a structural function but also provide more flexibility in internal planning. Elevators, stairs and mechanical and electrical services can be grouped inside a central core which also acts as a shear wall and thus permits most economical use of space.

The two most complex aspects in the analysis of shear wall structures which employ flat plate floors are the shear-wall-frame interaction, and the interaction between the floor system (flat plate, flat slab, waffle slab, etc.) and the shear walls and columns. The former type of interaction has been thoroughly investigated and has been incorporated into shear wall-frame analysis computer programs⁽¹³⁾.

At one time, the practice was to design the shear walls for full lateral loads and to assume that the frame resisted only gravity loads. However, when shear wall-frame interaction was considered, it was found that each element obstructs the other from taking its natural free deflected shape. Typical deflected shapes due to lateral loading, for the frame only, the shear wall only and for the combined frame and shear wall are shown in Figure 1 (a), (b) and (c) respectively. Figure 1 (c) shows that toward the top of the structure, the frame resists the lateral deflection of the shear wall, while the opposite phenomenon occurs toward the bottom. Thus, resisting moments are applied to the shear wall by the frame, with a resulting significant reduction in lateral deflection of the structure, and hence, increased lateral stiffness.

The interaction between flat plate floors and shear walls and columns in laterally loaded structures has not yet been adequately investigated. Several studies (3,7,8,10) have been carried out to determine the moment-rotation characteristics for flat plate floors loaded by couples produced by transverse shears applied to columns. In most cases the investigators used effective slab width as a parameter for indicating the effective stiffness of the flat plate. Generally, effective slab width has been defined as the width of an imaginary beam with the same depth, span and stiffness against rotation of the columns, as those of the slab under



(a) Free Frame (b) Free Wall (c) Combined Frame & Shear Wall

Lateral Deflections for Elements in Shear
Wall-Frame Structure.

Fig. 1

consideration. However, for shear wall structures this parameter is unsuitable because the resisting moment applied to the shear wall by the floor slab is a function not only of the slab thickness (its moment of inertia) but also of the geometry of the floor plan. Its value is greatly affected by the shape, size and location of the shear wall and the columns.

Consequently, the objective of this study is to isolate the various geometric parameters which contribute to the stiffness of a flat plate floor system as it interacts with shear walls and columns in resisting lateral loading on the structure. An attempt is made to express, in nondimensional form, the effects of column size, shear wall shape and size and panel shape and size on the stiffness coefficients for flat plate floor systems. The mechanism by which the floor system resists the moment applied by a laterally loaded shear wall is examined and the moment resistance is subdivided into contributions from the various floor panels. The resistance provided by a given panel depends on its location relative to the shear wall, the direction of loading and the presence or absence of adjacent panels. Nondimensional parameters are presented, which can be used to calculate the bending stiffness coefficients for floor plate systems for various shear wall and column geometries. Moment-rotation characteristic for flat plate-shear wall plexiglass models, determined using the Moire technique, are presented. The values thus

obtained are correlated with corresponding relationships determined from finite element flat plate analyses.

1.2 Historical Background

The first flat slab building was constructed in 1906 by C.A.P. Turner and by 1913 over one thousand such structures had been constructed around the world. The details of development of flat slab design procedures given in different codes have been summarized in papers by Dowell and Hammil⁽¹⁾ and by Sozen and Siess⁽²⁾.

Early investigations included analyses of flat slab or flat plate structures for gravity load only and for moments produced by unbalanced gravity loads. Very little was said about lateral load analysis. During the past decade however, a number of investigations dealing with lateral loads have been carried out.

Frederic and Pullauf⁽³⁾ tested six reinforced concrete models of two way doubly reinforced square slabs with a six inch column extending through the slab. The important variable was distribution of reinforcement. Values of effective width of slab were reported. The effective width was defined as the width of flat plate floor that acts with the column in resisting the applied moment. It was noted that the effective width of the slab increased with a bunching of the steel. However, the ultimate moment capacity simultaneously decreased.

The behavior of three experimental flat plate structures under different types of loading was studied by the Commonwealth Scientific and Industrial Research Organization in Australia. Some of the interesting results have been summarized by Blakey⁽⁴⁾. The structures were designed according to the empirical method of the ACI building code⁽⁵⁾. One of the three structures was tested under lateral load, with bare columns and short brick walls in place on either side of the columns. It was noted that the lateral rigidity of the structure was increased by a factor of four by providing simple brick walls. It was also found that the moments produced in the slab by lateral loads were confined essentially to the column strips.

An investigation was carried out by Dista and VanBuren⁽⁶⁾ to determine maximum unit shearing stresses in the moment transfer region between the column and the flat plate floor, due to flexure and punching shear. Two critical sections were considered; one at a distance of $t - 1\frac{1}{2}$ " (where t represents the total slab thickness) from, and parallel to, the column faces for flexural shear, and one at the perimeter of the column for punching shear. Recommendations were also made for allowable stresses.

Tsuboi and Kawaguchi⁽⁷⁾ tested nine mortar plate floor models. Three were of plain mortar and the rest were reinforced in three different ways. The cross-sectional area of the reinforcement was the same for all slabs but the dis-

tribution of the reinforcement between column and middle strips was different. Results were reported in terms of effective width and were in good agreement with those obtained using elastic finite difference analyses. The effective width was defined here as the width of an imaginary beam with the same depth, span and stiffness against rotation of the column, as those of the slab under consideration. It was noted that, in the elastoplastic region, the distribution of the reinforcement has considerable effect on the slab stiffness.

Khan and Sbarounis⁽⁸⁾ investigated the problem of shear wall-frame interaction and suggested an iterative method of analysis. The whole structure was separated into two distinct systems; a frame, and one or more shear walls acting in parallel. The two systems were then combined in such a way that compatibility and equilibrium conditions were fully satisfied. Influence curves, to estimate the distribution of shear between the two systems, were developed for approximately 150 separate combinations of the four loadings considered (uniformly distributed, triangular, concentrated load at the top of the frame and base moment), for structures with various stiffnesses. The problem of slab-column interaction was also studied both analytically and experimentally, and graphs for effective width were presented. The findings of Khan and Sbarounis agreed quite well with those of Tsoboi and Kawaguchi.

Brotchie⁽⁹⁾, who carried out an analytical study of the elastic and elastoplastic behavior of flat plate floors, summarized his findings in a series of papers. He assumed the plate to be supported on a hypothetical elastic medium whose modulus of elasticity could be varied at will. Each loading and the corresponding column reactions were considered separately and the principle of superposition was used. He suggested a simple analysis procedure according to which the floor is subdivided into panel strips in each direction. Then each panel strip is considered as a continuous beam supported at the column center lines and is analysed by moment distribution. The relative stiffnesses of the slab and columns are then modified by multiplying factors which are given in tabular form. The procedure presumably could be used for lateral load analysis.

Carpenter⁽¹⁰⁾ conducted an analytical study of the behavior of a flat plate structure subjected to lateral loads in the elastic range. He also tested two plexiglass models and reported stiffness and carry-over factors for individual slab elements. The behavior of the structure as a whole was found by superimposing the results obtained by loading individual columns, with all other columns fixed. His experimental results agreed well with the analytical values. Carpenter's stiffness values, obtained by using Brotchie's stiffness definition, in which an entire transverse line of

columns is rotated simultaneously, were in good agreement with Brotchie's results. Stiffness values obtained analytically by Khan and Sbarounis also agreed reasonably well with those presented by Carpenter.

Bernard and Schweighofer⁽¹¹⁾ studied plexiglass models of coupled shear walls subjected to lateral loads and concluded that the entire slab width should be considered as effective in coupling the shear walls.

Nantasarn⁽¹²⁾ conducted Moiré tests on four 1/24 scale plexiglass models. In addition, two similar 1/16 scale microconcrete models were tested by Parnichkul⁽¹²⁾. The purpose of these tests was to obtain the values of effective width, stiffness and carry-over stiffness factors for flat plate floor panels loaded by an interior column or shear wall and by an exterior column. The loading was applied in the form of couples produced by loads applied transversely to columns and shear walls. The main variable considered was shape and size of the shear wall. The effective width was considered to be the width of a hypothetical beam whose flexural stiffness is equal to that of flat plate floor panel. Effective widths for the panels loaded through shear walls ranged from 3 to 12 times the true panel width and it was concluded that effective slab width is a function not only of the slab thickness and panel size, but also of the geometry of the whole structure and therefore is not a suitable criterion for specifying plate stiffness. The effective widths

obtained using the concrete models were fairly close to the values reported by Brotchie⁽⁹⁾.

There is no mention in the ACI code⁽⁵⁾ of effective width of slab or stiffness and carry-over coefficients in shear wall structures. However, recommendations are made regarding effective widths for flat slabs for transferring bending moment between columns and slab. Section 2102 (g) states that "A slab width between lines that are $1.5t$ each side of the column may be considered effective." Where, t is the thickness of the floor slab.

1.3 Assumptions and Limitations

The assumptions and limitations employed in this study are:

1. Linearly elastic behavior has been assumed for both experimental and analytical work. Hence, the principle of superposition is assumed to be valid.

2. The finite element computer program, used for analytical work, is based on classical thin plate bending theory.

3. Externally applied moments are simulated by couples formed by concentrated point loads.

4. In both the analytical and the experimental models, the slab is extended through the shear wall. Thus, the models should exhibit somewhat more continuity than the corresponding actual structures in which stairs, elevators and duct openings would occupy the space enclosed by the shear wall.

5. In the finite element analysis, shear wall and column elements have been represented by stiff beam elements.

6. Only flat plate floors (as opposed to flat slabs, waffle slabs, etc.) have been considered.

7. Neither possible shear failure of the slab (punching shear or diagonal tension) nor possible buckling of the slab is considered in the analytical studies.

CHAPTER II

THEORETICAL CONSIDERATIONS

2.1 Stiffness Matrix

The analysis of a structure by the displacement method requires the determination of force-displacement relationships for each member in the form:

$$P = KD \quad (2.1)$$

where,

P is a vector of force components applied at the ends of the member,

D is a vector of corresponding displacement components, and

K is the member stiffness matrix. Each element K_{ij} in the stiffness matrix represents the force component in direction i corresponding to a unit displacement in direction j, with all other displacement components equal to zero.

For example, the force-displacement relationships for a prismatic bar AB from a planar structure, as illustrated in Figure 2.1(a), are:

$$\begin{Bmatrix} PA_1 \\ PA_2 \\ PA_3 \\ PB_1 \\ PB_2 \\ PB_3 \end{Bmatrix} = \begin{bmatrix} \frac{EA}{L} & 0 & 0 & -\frac{EA}{L} & 0 & 0 \\ 0 & \frac{12EI}{L^3} & -\frac{6EI}{L^2} & 0 & -\frac{12EI}{L^3} & -\frac{6EI}{L^2} \\ 0 & -\frac{6EI}{L^2} & \frac{4EI}{L} & 0 & \frac{6EI}{L^2} & \frac{2EI}{L} \\ -\frac{EA}{L} & 0 & 0 & \frac{EA}{L} & 0 & 0 \\ 0 & -\frac{12EI}{L^3} & \frac{6EI}{L^2} & 0 & \frac{12EI}{L^3} & \frac{6EI}{L^2} \\ 0 & -\frac{6EI}{L^2} & \frac{2EI}{L} & 0 & \frac{6EI}{L^2} & \frac{4EI}{L} \end{bmatrix} \begin{Bmatrix} \delta A_1 \\ \delta A_2 \\ \delta A_3 \\ \delta B_1 \\ \delta B_2 \\ \delta B_3 \end{Bmatrix}$$

where,

(2.2)

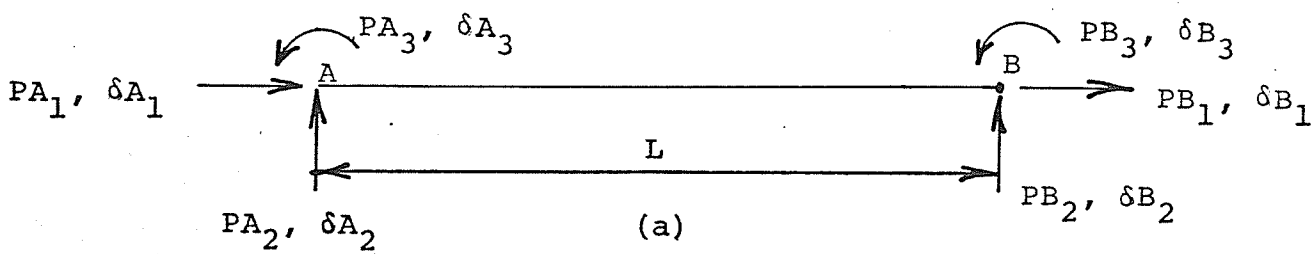
E = modulus of elasticity

I = moment of inertia of member about bending axis,

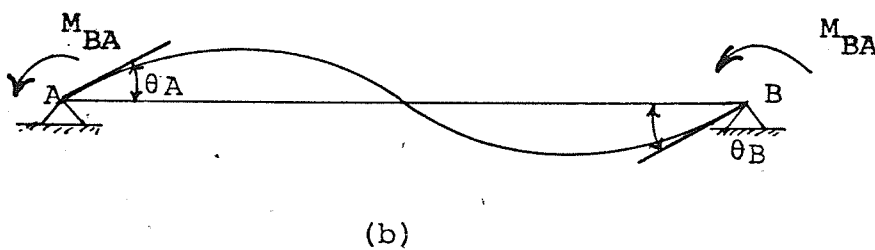
and A = member cross sectional area.

In the above relationships, the effects of shearing deformation are assumed to be negligible compared to those of flexural deformations.

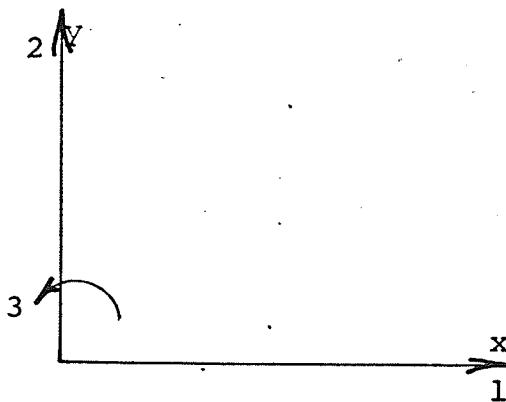
The axial forces in floor members in a rectangular frame, and consequently their axial deformations, are generally relatively small, and they are commonly assumed to be negligible. When this assumption is made, the member force-deformation relationships can be reduced to:



End Forces and Displacements for Member AB.



End Moments and Rotations for Member AB.



SIGN CONVENTION - Positive directions for displacements and forces.

Fig. 2.1

$$\begin{Bmatrix} PA_2 \\ PA_3 \\ PB_2 \\ PB_3 \end{Bmatrix} = \begin{bmatrix} 12EI/L^3 & -6EI/L^2 & -12EI/L^3 & -6EI/L^2 \\ -6EI/L^2 & 4EI/L & 6EI/L^2 & 2EI/L \\ -12EI/L^3 & 6EI/L^2 & 12EI/L^3 & 6EI/L^2 \\ -6EI/L^2 & 2EI/L & 6EI/L^2 & 4EI/L \end{bmatrix} \begin{Bmatrix} \delta A_2 \\ \delta A_3 \\ \delta B_2 \\ \delta B_3 \end{Bmatrix}$$

(2.3)

If, further, the axial deformations of columns and vertical displacements of shear walls are ignored, only the end moments and end rotations need to be related in the structural analysis, and the force-deformation relationships take the form:

$$\begin{Bmatrix} PA_3 \\ PB_3 \end{Bmatrix} = \begin{bmatrix} 4EI/L & 2EI/L \\ 2EI/L & 4EI/L \end{bmatrix} \begin{Bmatrix} \delta A_3 \\ \delta B_3 \end{Bmatrix} \quad (2.4)$$

Equation 2.4 can be expressed in the form:

$$\begin{Bmatrix} M_{AB} \\ M_{BA} \end{Bmatrix} = \begin{bmatrix} K_{AA} & K_{AB} \\ K_{AB} & K_{BB} \end{bmatrix} \begin{Bmatrix} \theta A \\ \theta B \end{Bmatrix} \quad (2.5)$$

where,

M_{BA} , M_{AB} , θA and θB are end moments and rotations for the member, as illustrated in Figure 2.1(b). K_{AA} and K_{BB} may be termed direct bending stiffness coefficients, since they relate forces and displacements at a single point, and K_{AB} and K_{BA} may be termed carry-over bending stiffness coefficients, since they relate forces at one point to displacements at another.

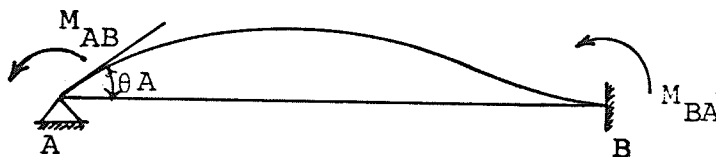
2.2 Bending Stiffness Coefficients

The bending stiffness coefficients, K_{AA} , the direct stiffness coefficient at end A, and K_{BA} , the carry-over bending stiffness coefficient, for the prismatic bar shown in Figure 2.2.1 are defined as follows:

$$\begin{aligned} K_{AA} &= M_{AB}/\theta A \\ K_{BA} &= M_{BA}/\theta A \end{aligned} \tag{2.6}$$

where,

M_{AB} is the counterclockwise moment applied at end A of the bar, θA is the counterclockwise rotation at end A and M_{BA} is the counterclockwise moment induced at fixed end B.



Fixed End Moment for A Prismatic Bar

Fig. 2.2.1

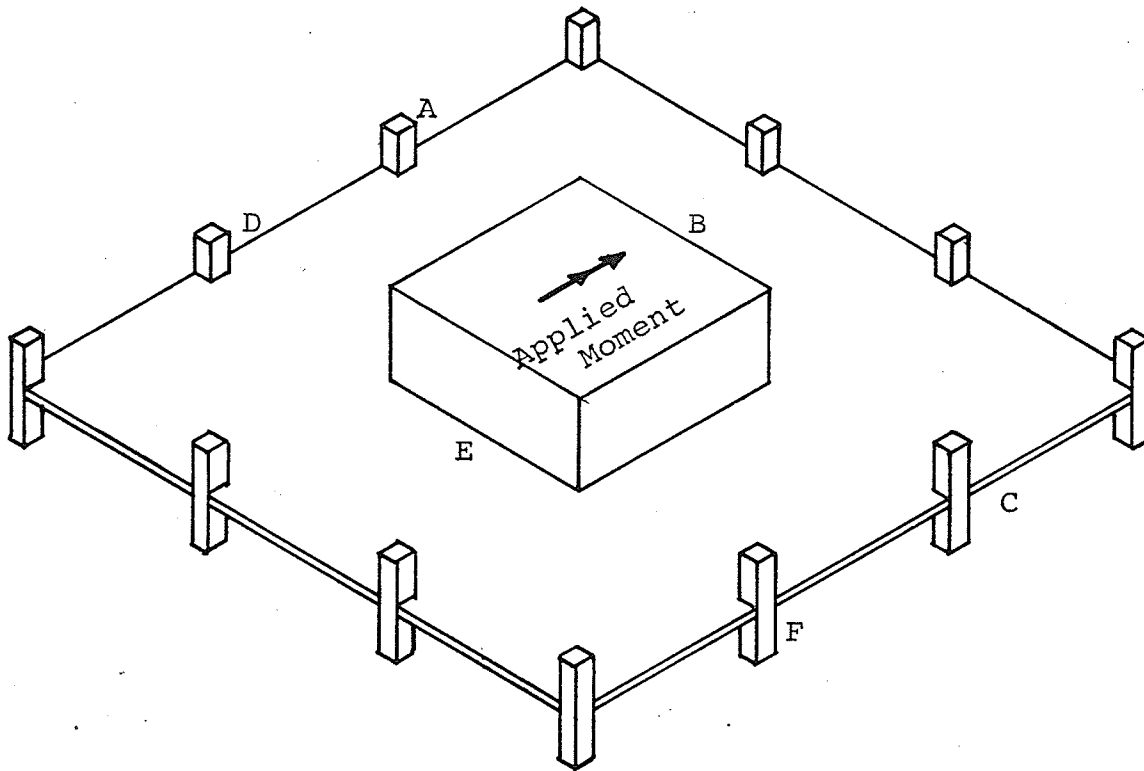
Analogously, in this study the bending stiffness coefficients for flat plate floor system shown in Figure 2.2.2 will be defined as follows:

The direct bending stiffness coefficient for the flat plate at the shear wall is the ratio of the moment applied to the shear wall to the resulting rotation of the shear wall and floor plate at B, normal to line ABC, when all columns are fixed. The carry-over bending stiffness from the shear wall to columns A or C is the ratio of the fixed-end moment produced at the column supports A or C due to the moment applied to the shear wall, to the resulting rotation of the shear wall and floor plate at B, normal to line ABC.

Likewise, the direct bending stiffness coefficient for the floor at column A is the ratio of the moment applied to the column to the corresponding rotation of column A normal to line ABC, when the shear wall and all other columns are fixed. Finally, the carry-over bending stiffness from column A to the shear wall is the ratio of the fixed-end moment produced at the shear wall when moment is applied to column A to the resulting rotation of column A normal to line ABC.

2.3 Measurement of Bending Stiffness Coefficients

While stiffness coefficients can be readily calculated for a bar, those for flat plate elements such as are used for the floors of shear wall-frame structures cannot be easily calculated. It is therefore necessary to apply couples of known magnitude to the shear wall and columns and to measure



Determination of Direct Bending
Stiffness Coefficients

Fig. 2.2.2

the resulting plate rotation in order to determine direct bending stiffness coefficients for the flat plate elements. The determination of carry-over stiffness coefficients requires, in addition, the application of the principle of superposition, as described in Section 2.3.2.

2.3.1 Direct Bending Stiffness Coefficients for Flat Plate

The direct bending stiffness coefficient at the shear wall for the flat plate floor shown in Figure 2.2.2 can be obtained by applying a known moment to the shear wall with all column supports fixed, and measuring the rotation of the floor section ABC at the shear wall. Similarly, the direct bending stiffness at columns A or C can be obtained by applying equal moments to columns A, C, D and F shown in Figure 2.2.2 and keeping the other column and shear wall supports fixed.

2.3.2 Carry-Over Bending Stiffness Coefficients For Flat Plate

Since it is difficult to measure directly the fixing moments at the various supports, the principle of superposition is used in obtaining the values of carry-over stiffness coefficients.

The procedure used to obtain carry-over stiffness coefficients can be illustrated with the help of Figure 2.3, which shows cross sections along line ABC of the floor system

shown in Figure 2.2.2. The support conditions at A and C for each structure shown in Figure 2.3 are such that antisymmetrical deflection patterns are obtained and the structure is symmetrical about support B.

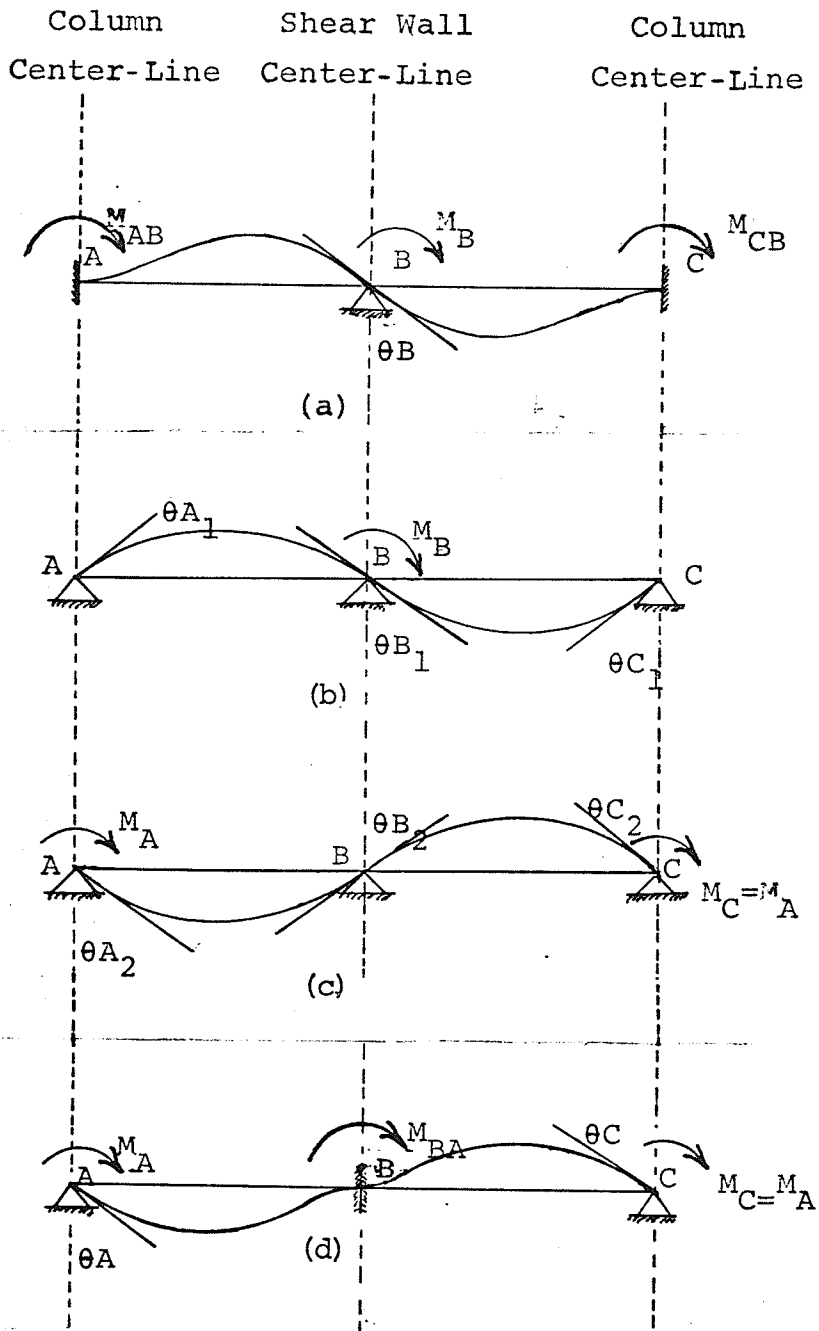
In Figure 2.3 (a), a clockwise moment M_B is applied at B. It causes a rotation θ_B at B and equal clockwise moments M_{AB} and M_{CB} at the fixed supports A and C. By definition, the carry-over bending stiffness coefficient for external moments applied at the shear wall are:

$$K_{CB} = K_{AB} = \frac{M_{AB}}{\theta_B} = \frac{M_{CB}}{\theta_B} \quad (2.7)$$

Since it is difficult to measure M_{AB} or M_{CB} directly, they can be determined using the principle of superposition, as follows.

In Figure 2.3 (b) an external moment M_B is applied to the structure with pinned supports at A, B and C, and rotations θ_{B_1} and $\theta_{A_1} = \theta_{C_1}$ are measured. Then the pin supported structure is loaded by moment M_A at A and moment $M_C = M_A$ at C as shown in Figure 2.3 (c) and the corresponding rotations θ_{B_2} and θ_{A_2} are measured. Finally, if all moments and rotations for the structure in Figure 2.3 (c) are multiplied by $\theta_{A_1}/\theta_{A_2}$ and added to those in Figure 2.3 (b), a structure with a deflected shape that is identical to that shown in Figure 2.3 (a) results. The final rotations at A and C are:

$$\begin{aligned} \theta_A &= -\theta_{A_1} + \theta_{A_2} (\theta_{A_1}/\theta_{A_2}) = 0 \\ \theta_C &= -\theta_{C_1} + \theta_{C_2} (\theta_{C_1}/\theta_{C_2}) = 0 \end{aligned} \quad (2.8)$$



Determination of Carry-Over Stiffness Coefficients Using Principle of Superposition.

Fig. 2.3

Also:

$$M_{AB} = M_A * \theta_{A1} / \theta_{A2} = M_{CB} \quad (2.9)$$

Hence, from equation 2.7, the carry-over stiffness coefficients for moment applied at the shear wall are:

$$K_{CB} = K_{AB} = (M_A * \theta_{A1}) / (\theta_B * \theta_{A2}) \quad (2.10)$$

Similarly, the carry-over stiffness coefficient for external moments applied at columns A or C. are:

$$K_{BC} = K_{BA} = \frac{M_{BA}/2}{\theta_A} = \frac{M_{BA}/2}{\theta_C} \quad (2.11)$$

where

$M_A = M_C$ = external moments applied at columns A and C for the structure shown in Figure 2.3 (d)

M_{BA} = resisting moment at fixed support B.

$\theta_A = \theta_C$ = rotations produced at support A and C.

A structure with a deflected shape that is identical to that shown in Figure 2.3 (d) can be obtained if all moments and rotations for the structure in Figure 2.3 (b) are multiplied by θ_{B2}/θ_{B1} and added to those in Figure 2.3 (c).

Therefore,

$$M_{BA} = \frac{M_B * \theta_{B2}}{\theta_{B1}} \quad (2.12)$$

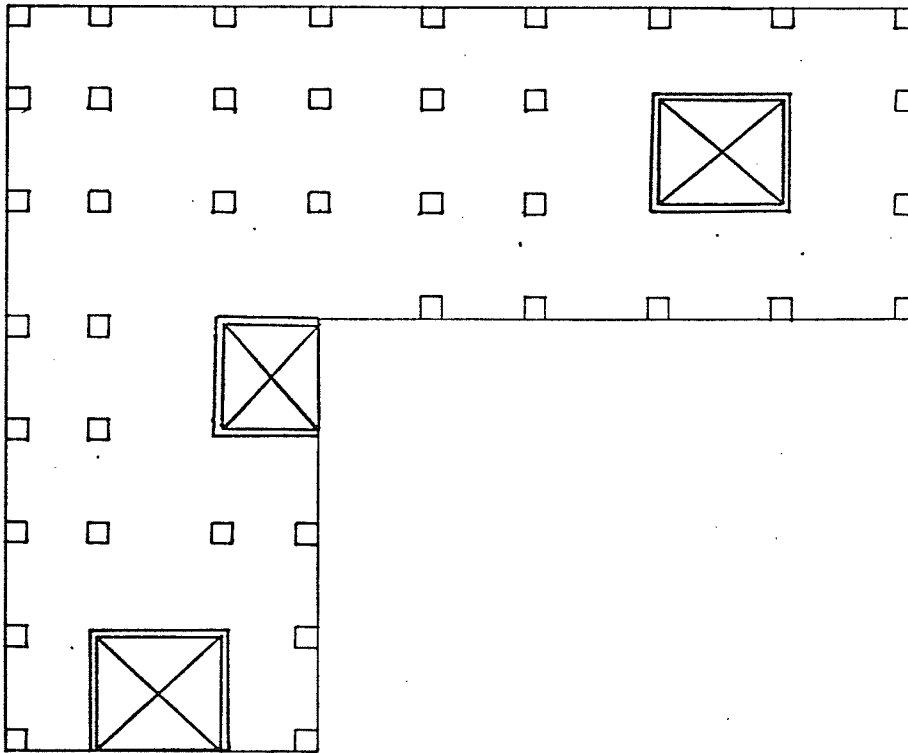
Hence, from eq (2.11), the carry-over stiffness coefficient for moment applied at the columns are

$$K_{BC} = K_{BA} = \frac{M_B * \theta_{B2}}{2 * \theta_A * \theta_{B1}} \quad (2.13)$$

Equation 2.10 can be used to determine the carry-over stiffness coefficients from the shear wall to the column, while equation 2.13 can be used to determine the carry-over stiffness coefficient from the column to the shear wall.

2.4 Behaviour of Flat Plate Floor Systems

Figures 2.4.1 (a), (b), (c), and (d) show typical floor plans for flat plate shear wall-frame structures. Such structures generally have one or more "box type" shear walls and columns located approximately on a rectangular grid. This arrangement of supporting members tends to subdivide the floor slab into a series of rectangular panels. When the structure is subjected to lateral loads, transverse moments are applied to the flat plate floor by the shear walls and columns. The various floor panels offer different resistance to these moments depending on their size, shape and location relative to the shear walls.



Typical Floor Plan For Flat Plate
Shear Wall-Frame Structure.

Fig. 2.4.1 (a)

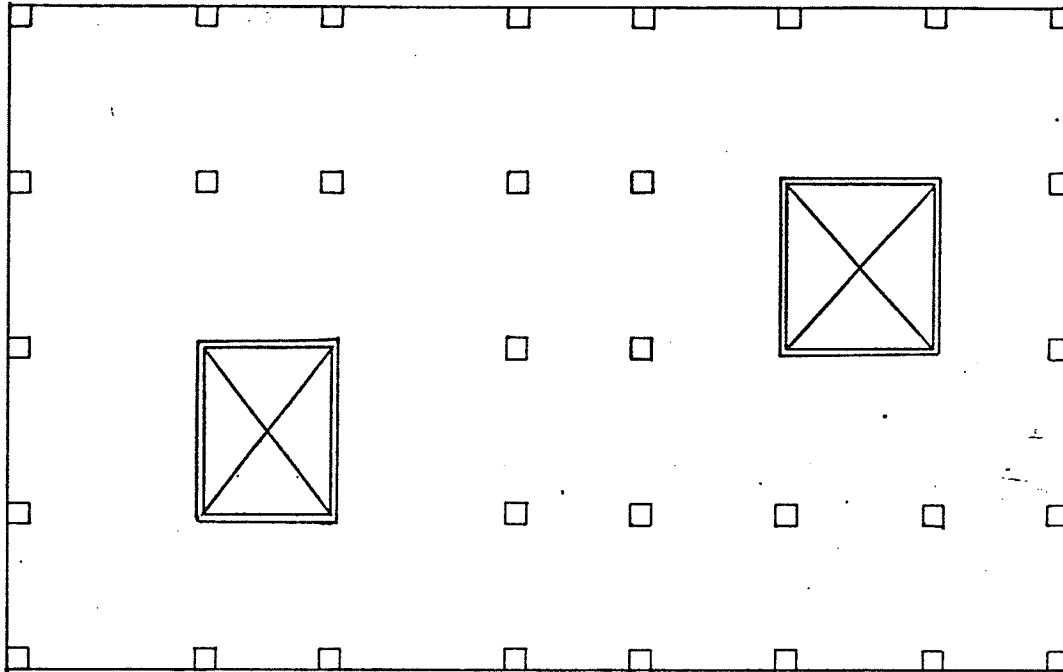


Fig. 2.4.1 (b)

Typical Floor Plan For Flat Plate Shear
Wall-Frame Structure.

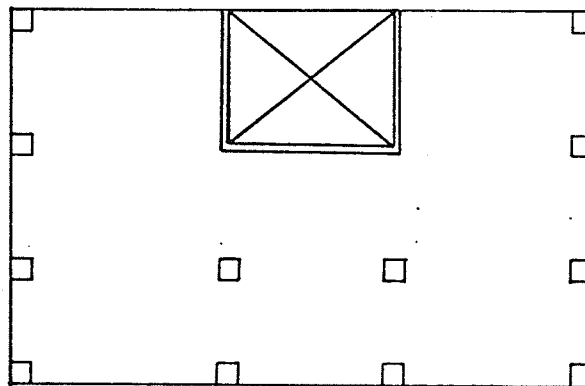
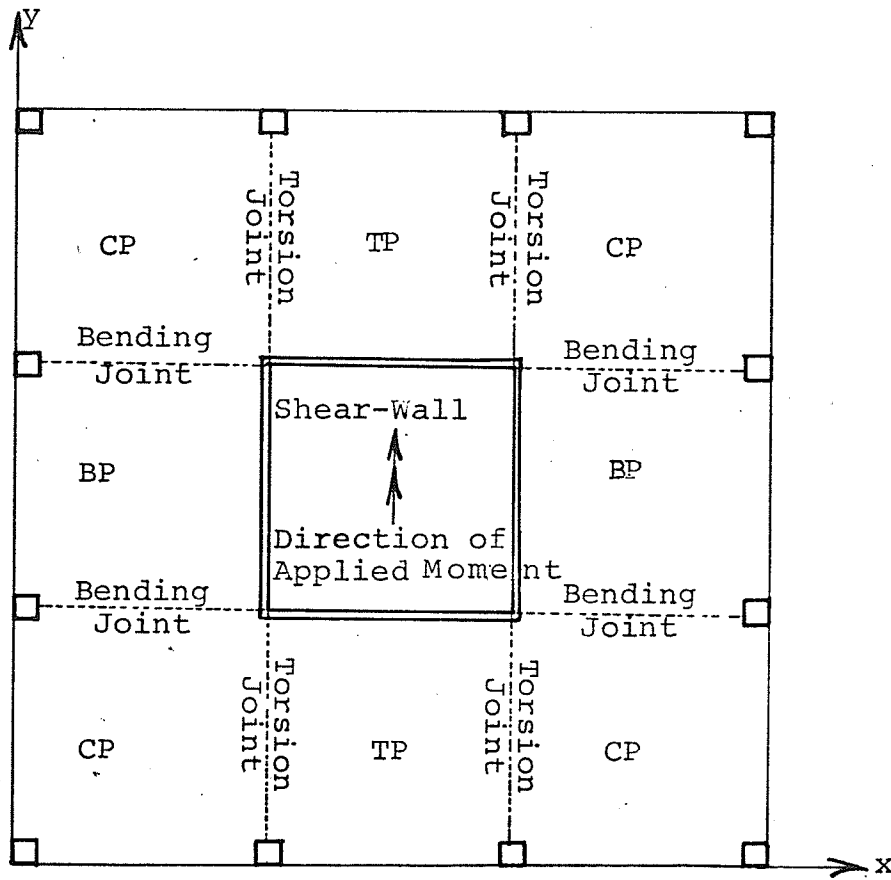


Fig. 2.4.1 (c)

Typical Floor Plan For Flat Plate Shear
Wall-Frame Structure.



TP = Torsional Panel

CP = Corner Panel

BP = Bending Panel

Basic Flat Plate Floor Plan

Fig. 2.4.1. (d)

The basic flat plate floor plan considered in this study is shown in Figure 2.4.1 (d). It is relatively simple, but includes most of the possible positions of the rectangular flat plate floor panels relative to the shear walls and columns. Assuming this basic flat plate floor to be subjected to an external moment about an axis parallel to the Y-Y axis and applied by the shear wall, the whole floor can be subdivided into three types of floor panels, depending upon their behavior. These will be referred to as torsional panels, which are subjected mainly to torsion, bending panels, which resist primarily bending, and corner panels, which are subjected to both bending and torsion. The resistance offered to transverse moment by the different panel types is greatly affected by the continuity between adjacent panels. For example, the torsional resistance of a torsion panel is increased by the addition of a corner panel, since the continuity between the two results in bending in the corner panel. Similarly, the resistance of a bending panel is increased by torsion in an adjacent corner panel. In this study, the joint between a corner panel and a torsional panel will be referred to as a torsion joint while the joint between a bending panel and a corner panel will be called a bending-joint.

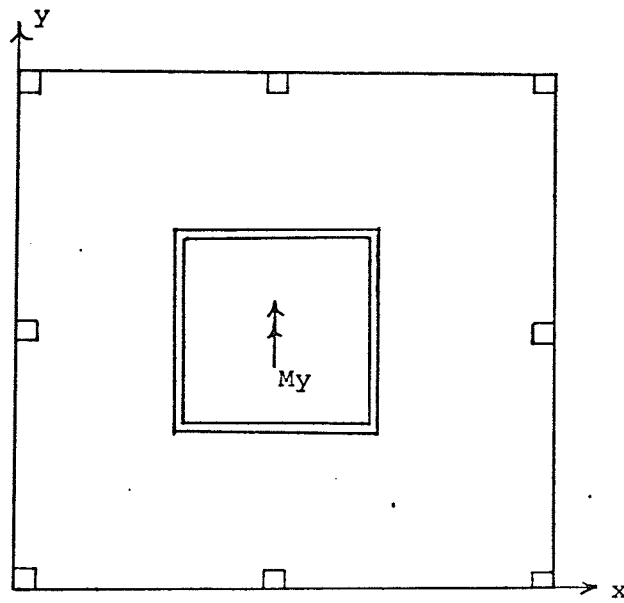
The moment resistance offered by a given floor system is also highly dependent on the location of the support-

ing columns, as demonstrated in Figure 2.4.2. The resistance of the floor slab shown in Figure 2.4.2(a) to a shear wall moment M_y will be less than that of the slab in Figure 2.4.2(b) because of the absence of torsion panels in the former case. The behavior of the latter system will be almost the same as that of the floor slab shown in Figure 2.4.1(d). The presence of the additional columns for the system in Figure 2.4.2(b) will slightly increase the stiffness of the torsional panels and hence the over all stiffness of the floor slab.

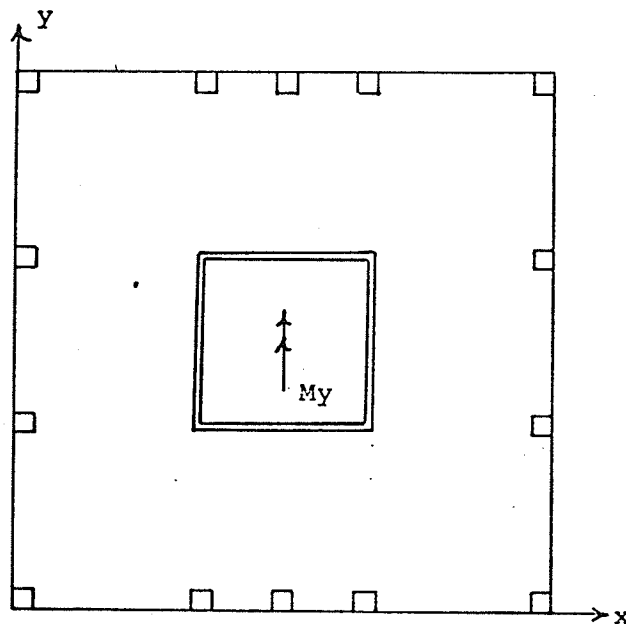
Further, the behavior of a particular floor panel depends upon the direction of the external moment. For example, if the flat plate floor in Figure 2.4.1(d) is subjected to a shear wall moment parallel to the X-X axis, the torsional panel will become a bending panel and the bending panel will become a torsional panel.

2.5 Contributions to Bending Resistance of Flat Plate Floor

The stiffness contributions of individual panels of the basic floor slab shown in Figure 2.5(a) and of continuity between adjacent panels can be obtained by carrying out load-displacement analyses for the basic structure and a series of eight related structures. The related structures, which are shown in Figure 2.5(b) to (j), are obtained by removing various panels from the basic structure and by destroying continuity between adjacent panels.



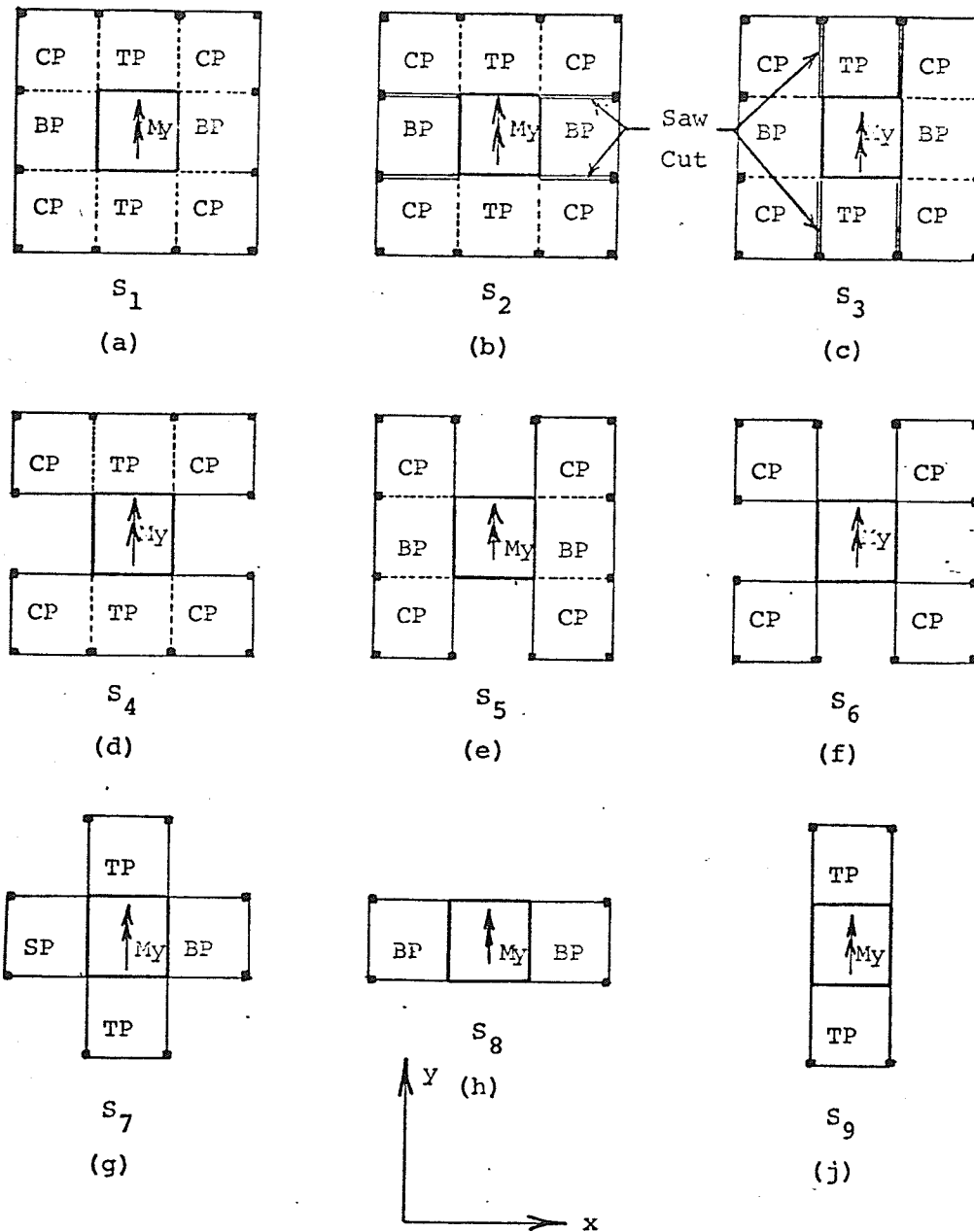
(a)



(b)

Different Column Locations

Fig. 2.4.2



Determination of Contributions to Bending
Resistance of Floor System

BP = Bending Panel
 TP = Torsional Panel
 CP = Corner Panel

Fig. 2.5

It is convenient to define the "direct stiffness coefficient" (the ratio of moment M_y applied through the shear wall, to resulting rotation θ_y of shear wall) for the basic structure in Figure 2.5(a) as K_1 . Similarly, the corresponding direct stiffness coefficients for the related structures S_2, S_3, S_9 in Figure 2.5(b) to J will be designated K_2 to K_9 , respectively.

The principle of superposition can be used to establish relationships among the direct stiffness coefficients for the various structures shown in Figure 2.5 and to isolate the stiffness contributions of the various elements in the basic floor structure.

For example, the moment resistance of structure S_7 can be obtained by superimposing those for structures S_8 and S_9 . Hence

$$K_7 = K_8 + K_9 \quad (2.5.1)$$

Similarly, by considering the superposition of structures S_9 and S_5 , it can be seen that

$$K_3 = K_5 + K_9 \quad (2.5.2)$$

Finally, the superposition of structures S_8 and S_4 leads to the relationship

$$K_2 = K_4 + K_8 \quad (2.5.3)$$

By considering structure S_8 only, it can be seen that the direct stiffness coefficient for a single bending panel, with no continuity with adjacent panels, is

$$K_B = \frac{1}{2} K_8 \quad (2.5.4)$$

Likewise, considering structure S_9 , it is seen that the direct stiffness factor for a single torsion panel is

$$K_T = \frac{1}{2} K_9$$

By comparing structures S_1 and S_2 , it can be seen that the direct stiffness contribution due to a bending joint (due to the continuity along a single boundary between a bending panel and a corner panel) is

$$K_{BC} = \frac{1}{4} (K_1 - K_2) \quad (2.5.5)$$

Similarly, by considering structures S_1 and S_3 , it can be seen that the stiffness contribution due to a torsion joint (due to continuity along a single boundary between a corner panel and a torsion panel) is

$$K_{TC} = \frac{1}{4} (K_1 - K_3) \quad (2.5.6)$$

Finally, by comparing structures S_3 and S_7 , the contribution of one corner panel can be obtained as

$$K_C = \frac{1}{4} [K_3 - K_7 - 4 K_{BC}] \quad (2.5.7)$$

It is convenient to express the direct stiffness coefficients for various elements making up the floor system, in terms of stiffness factors for equivalent beam elements.

Therefore, define for the panel contributions

$$K_{EB} = \frac{4EI}{L_B} = \frac{E t^3 B}{3L_B}$$

$$K_{EC} = \frac{4EI}{L_C} = \frac{E t^3 L_T}{3L_C}$$

$$K_{ET} = \frac{I_1 G t^3 b}{L_T}$$

and by analogy, for the joint stiffness contributions

$$K_{EBC} = \frac{E t^3 L_B}{B}$$

$$K_{ETC} = \frac{E t^3 L_T}{b}$$

where,

E = modulus of elasticity

I = moment of inertia of beam

L_B = span of bending panel

B = width of bending panel

L_C = span of corner panel,

G = modulus of rigidity

b = width of torsion panel

t = floor thickness

L_T = span of torsion panel

$$I_1 = \frac{1}{3} (1 - 0.63 \frac{t}{b})$$

= shape factor (16)

The direct bending stiffness coefficients for various elements of a basic floor plan can then be defined as

- (i) DIRECT STIFFNESS COEFFICIENT
FOR ONE BENDING PANEL $= K_B = F_B * K_{EB}$
- (ii) DIRECT STIFFNESS COEFFICIENT
FOR ONE TORSION PANEL $= K_T = F_T * K_{ET}$
- (iii) DIRECT STIFFNESS COEFFICIENT
FOR ONE CORNER PANEL $= K_C = F_C * K_{EC}$
- (iv) DIRECT STIFFNESS COEFFICIENT
DUE TO ONE BENDING JOINT $= K_{BC} = F_{BC} * K_{EBC}$
- (v) DIRECT STIFFNESS COEFFICIENT
DUE TO ONE TORSION JOINT $= K_{TC} = F_{TC} * K_{ETC}$

F_B , F_T , F_C , F_{BC} and F_{TC} are dimensionless multiplying factors.

The values of these multiplying factors for a basic flat floor with the geometry shown in Figure 2.5(a), can be obtained by determining the direct stiffness coefficients for structures S_1 , S_4 , S_5 , S_8 , and S_9 , shown in Figure 2.5.

CHAPTER III

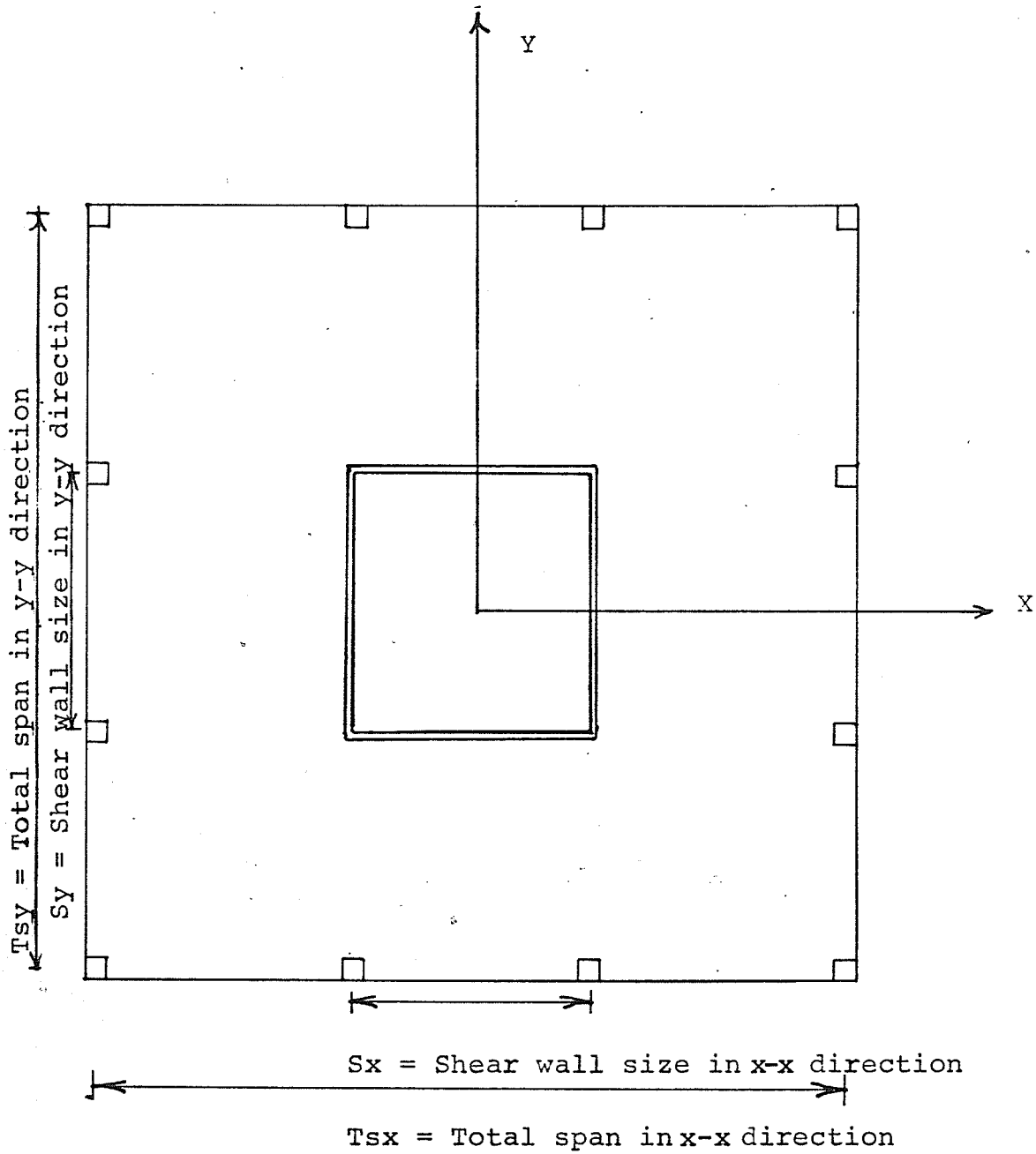
ANALYTICAL AND EXPERIMENTAL STUDIES

This chapter describes the analytical finite element study and the Moiré experimental work carried out in order to evaluate the bending stiffness properties for various geometries of flat plate floors.

3.1 Introduction

The analytical study consisted of two phases. The first of these dealt with the effects of column size and shear wall size and shape on the bending stiffness of the floor plate. The purpose of the second phase was to derive values for the multiplying factors, described in Section 2.5, for indicating the contributions of the various floor elements to the bending resistance of a flat plate floor system. In the first phase, direct bending-stiffness coefficients and carry-over stiffness coefficients for both shear wall loading and column loading were studied. The second phase was limited to the study of direct stiffness coefficients only, for shear wall loading. The Moiré experimental study was limited to the second phase.

The basic prototype structure, on which both the experimental and the analytical models were based is shown



Prototype Floor Plan

Fig. 3.1.1

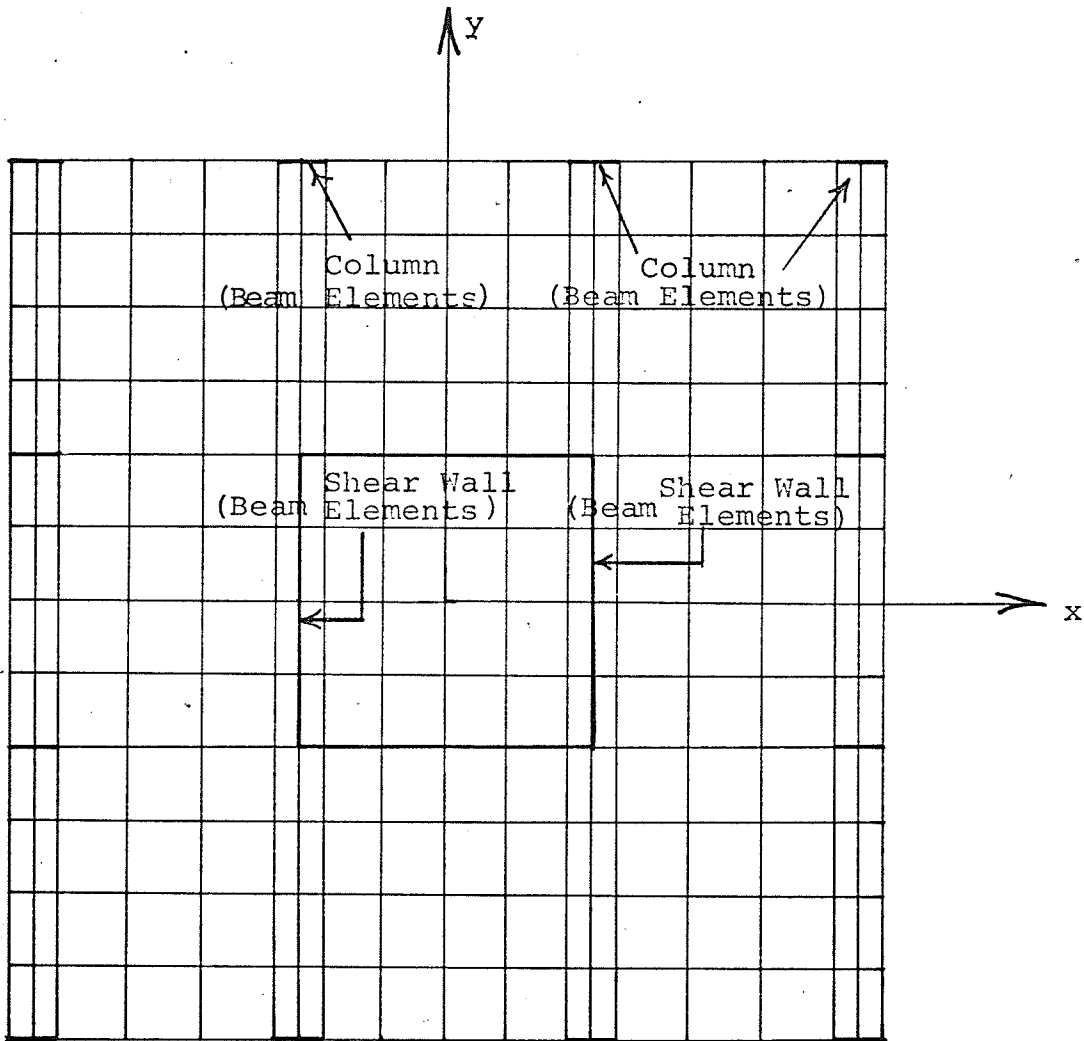
in Figure 3.1.1. Its proportions and dimensions were designed to be within the practical ranges for flat plate structures of the type being considered. All columns were square. For the first phase study, the column size was varied from 12 inches to 36 inches while it was kept at 24 inches for all structures analyzed in the second phase. Both rectangular and square shear wall shapes were considered. For both phases, the shear wall size was varied from 4.5 feet to 48 feet in the X-X direction and 9 feet to 24 feet in the Y-Y direction. The ratio of the shear wall size to total span was varied from $1/5$ to $1/2.5$. A 6-inch slab thickness was assumed throughout. In all cases moments were applied to the structures about axes parallel to the Y-Y axis.

3.2 Analytical Procedure

A computer program titled "The Finite Element Analysis of Stiffened Plates", developed by Ian G. Buckle at the University of California, was employed in the analytical work. The principal features of this program have been summarized in Appendix A. The double precision version of the program was used.

3.2.1 Representation of Plate Model

The finite element grid for the typical model is shown in Figure 3.2.1. The column and shear wall elements were represented by stiff beam elements whose depths were made larger than those of the plate elements. The thick-



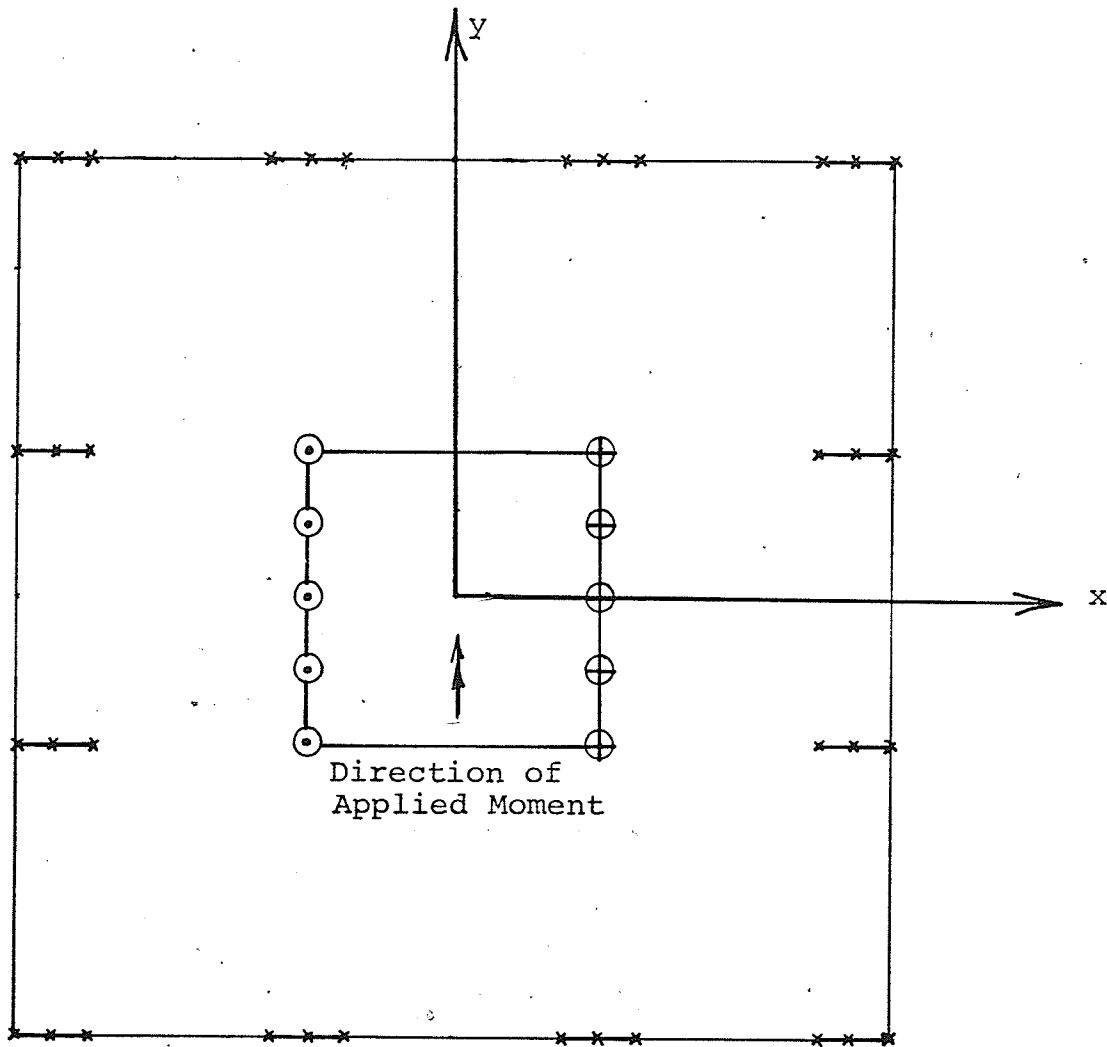
Finite Element Grid for Typical Plate Model.

Fig. 3.2.1

nesses of the beam elements were made sixteen times as large as those for the plate elements. The purpose of using stiff beam elements was to obtain a rigid bending behavior of the shear wall and columns compared to that of the flat plate. The external moment loading was simulated by a couple produced by equal and opposite point loads as illustrated in Figure 3.2.2. Each column was represented by two beam elements and three nodes as illustrated in Figure 3.2.1. The hinged support at the column was obtained by restraining the transverse deflection of the central node and leaving the other two nodes completely free. For a fixed column support, all three movements (transverse deflection and two rotations) were restrained for all three nodes.

To obtain the values of direct and carry-over stiffness coefficients, the models were analyzed for four types of loading as illustrated in Figures 3.2.2, 3.2.3, 3.2.4 and 3.2.5. However, for obtaining the values of multiplying factors F_B , F_T , F_C , F_{TC} and F_{BC} described in Chapter 2, the models were analyzed for type A loading only, as shown in Figure 3.2.2.

All models analyzed were symmetrical about both X-X and Y-Y axes passing through the centroids of the floor areas and only one quarter of each model was analyzed. This reduced the number of elements and nodes to be dealt with in the finite element analysis, hence reducing the cost of the computational work. Each loading was symmetrical about the



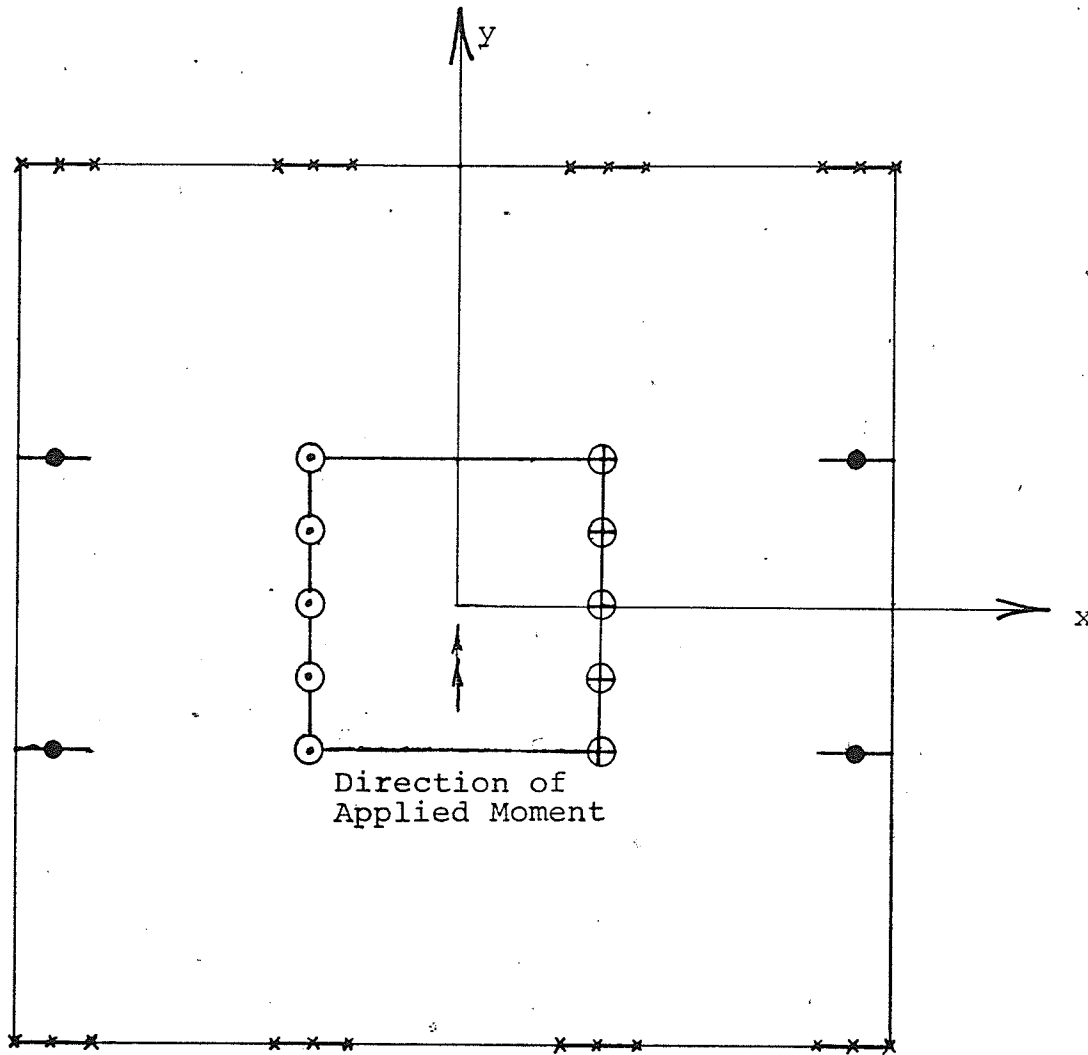
× Completely fixed node.

⊙ Upward Point Load.

⊕ Downward Point Load.

Loading Type A

Fig. 3.2.2.



x Completely fixed node.

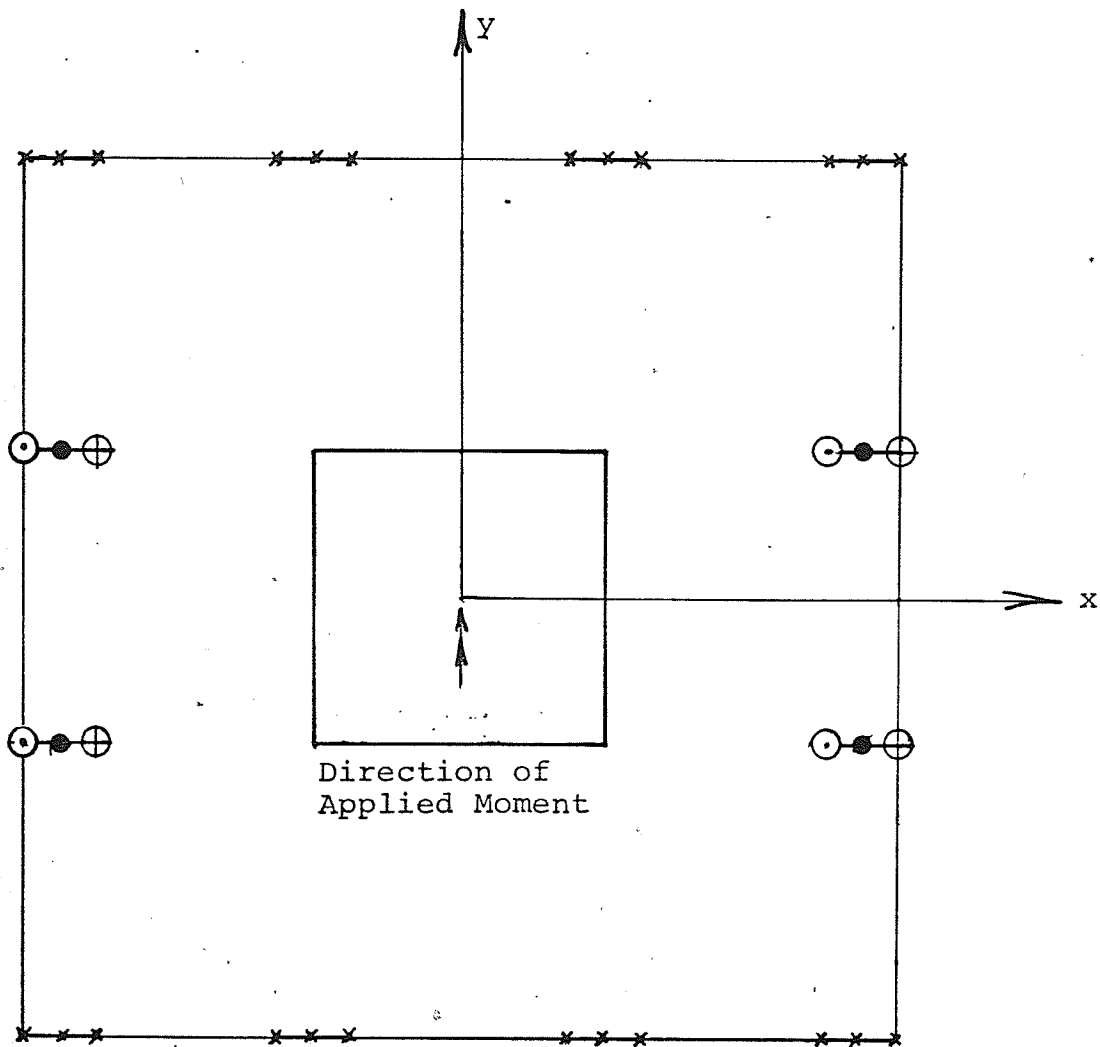
● Node for which only transverse deflection is restrained.

⊙ Upward Point Load.

⊕ Downward Point Load.

Loading Type B

Fig. 3.2.3



× Completely fixed node.

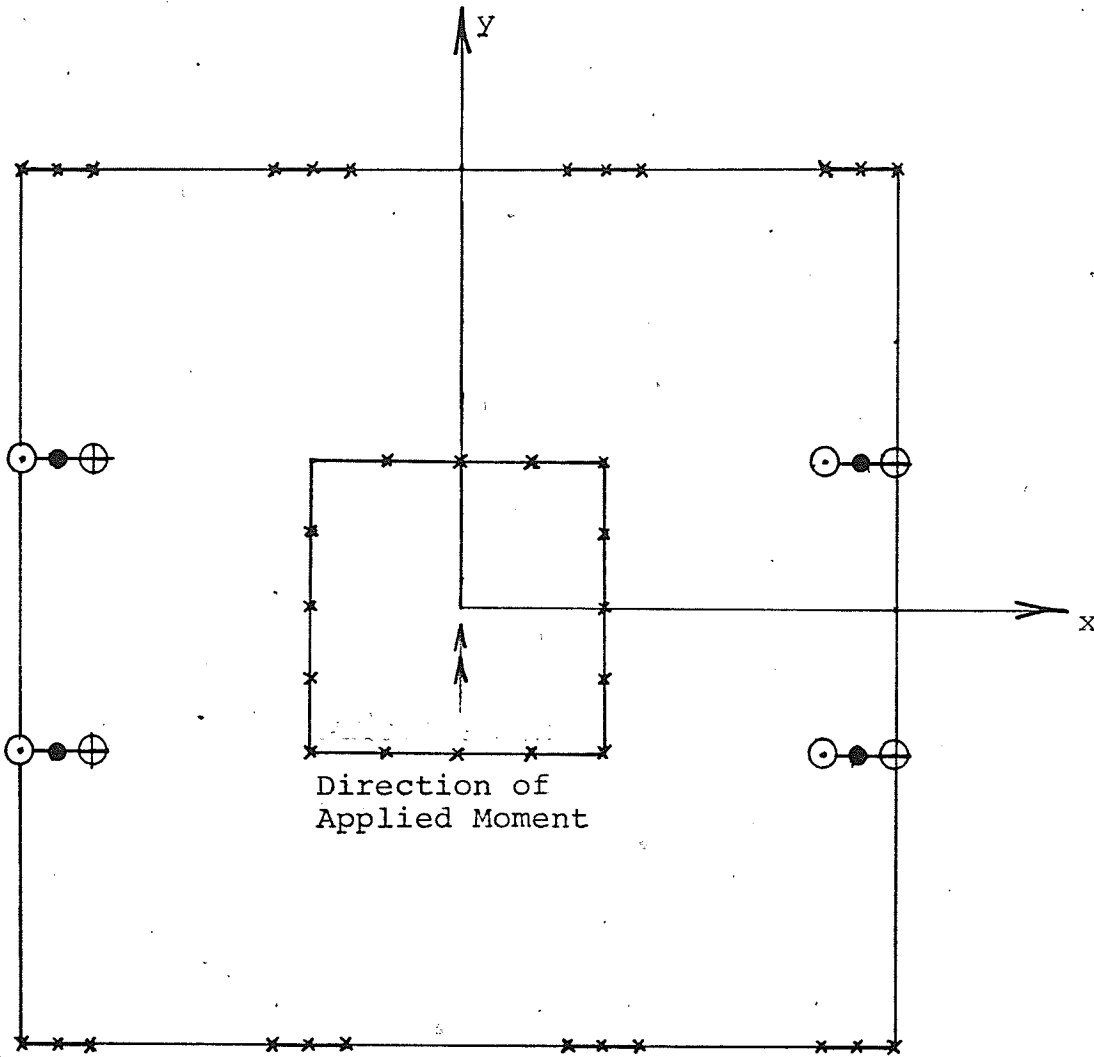
● Node for which only transverse direction is restrained.

○ Upward Point Load.

⊕ Downward Point Load.

Loading Type C

Fig. 3.2.4



× Completely fixed node.

● Node for which only transverse deflection is restrained.

⊙ Upward Point Load.

⊕ Downward Point Load.

Loading Type D

Fig. 3.2.5.

Y-Y axis and antisymmetrical about the X-X axis. Hence, the transverse plate deflection, and the rotation θ_X were zero along the Y-Y axis passing through the centroid of the floor plan and rotation θ_X about the X-X axis was zero along the X-X axis passing through the centroid. Locally, suitable boundary conditions were adopted for obtaining fixed or hinged supports.

3.2.2 Description of Analytical Models

The first phase study involved ten finite element representations of 1/24 scale plexiglass models, designated P1, P2, ----- P10, and analyzed for the four types of loading shown in Figures 3.2.2, 3.2.3, 3.2.4, and 3.2.5. The dimensions of these models are given in Tables 3.1, 3.2, and 3.3. In the second phase, sixteen series of models were analyzed for Type A loading shown in Figure 3.2.2. Nine 1/24 scale models corresponding to the nine floor plans shown in Figure 2.5 were considered in each series. The models of each series were designated using double subscripts, the first of which indicates the series number while the second designates model number in that series. For example, the models of the first series were designated as PS1-1, PS1-2 ----- PS1-9. In fact, models corresponding to the shapes of models S1, S4, S5, S8 and S9 only, in Figure 2.5, were analyzed, as the results for the models S2, S3, S6 and S7 were obtained by

TABLE NO. 3.1

DIMENSIONS OF MODELS FOR EFFECT OF COLUMN SIZE

For all Models,
Clear Span in Both X-X and Y-Y Direction = 9.0 Inch
Thickness of Floor = 0.25 Inch

Model	Shear Wall Size		Total Span		Column Size	$\frac{SX}{SY}$	$\frac{\text{Column Size}}{\text{Clear Span}}$	$\frac{SY}{TSX}$
	SX	SY	TSX	TSY				
P1	9"	9"	27"	27"	0.5"	1.0	0.0555	$\frac{1}{3}$
P2	9"	9"	27"	27"	0.75"	1.0	0.0833	$\frac{1}{3}$
P3	9"	9"	27"	27"	1.0"	1.0	0.1111	$\frac{1}{3}$
P4	9"	9"	27"	27"	1.5"	1.0	0.1666	$\frac{1}{3}$

TABLE NO. 3.2

DIMENSIONS OF MODELS FOR EFFECT OF SHEAR WALL SIZE

For all Models,
Clear Span in Both X-X and Y-Y Direction = 9 Inch
Thickness of Floor = 0.25 Inch

Model	Shear Wall Size		Total Span		Column Size	$\frac{SX}{SY}$	$\frac{\text{Column Size}}{\text{Clear Span}}$	$\frac{SY}{TSX}$
	SX	SY	TSX	TSY				
P5	4.5"	4.5"	22.5"	22.5"	0.5"	1.0	0.0555	$\frac{1}{5}$
P6	6"	6"	24"	24"	0.5"	1.0	0.0555	$\frac{1}{4}$
P1	9"	9"	27"	27"	0.5"	1.0	0.0555	$\frac{1}{3}$
P7	12"	12"	30"	30"	0.5"	1.0	0.0555	$\frac{1}{2.5}$

where,

SX and SY are shear wall size in the X-X and Y-Y direction respectively, TSX and TSY are total span in the X-X and Y-Y direction respectively.

TABLE NO. 3.3

DIMENSIONS OF MODELS FOR EFFECT OF SHEAR WALL SHAPE

For all Models,
 Clear Span in Both X-X and Y-Y Direction = 9 Inch
 Thickness of Floor = 0.25 Inch

Model	Shear Wall Size		Total Span		Column Size	$\frac{SX}{SY}$	Column Size Clear Span	$\frac{SY}{TSY}$
	SX	SY	TSX	TSY				
PS8	4.5"	9.0"	22.5"	27"	0.75"	0.5	0.0833	1/3
P2	9.0"	9.0"	27"	27"	0.75"	1.0	0.0833	1/3
P9	13.5"	9.0"	31.5"	27"	0.75"	1.5	0.0833	1/3
P10	18"	9.0"	36"	27"	0.75"	2.0	0.0833	1/3

SX and SY are shear wall size in X-X and Y-Y direction respectively TSX and TSY are total span in X-X and Y-Y direction respectively.

using the principle of superposition. The dimensions of the first model of each series are given in Table 3.4. In the Tables S_X and S_Y represent overall shear wall dimensions in the X-X and the Y-Y directions respectively while T_{SX} and T_{SY} represent total span in the X-X and Y-Y directions respectively as shown in Figure 3.1.1.

TABLE 3.4

DIMENSIONS OF MODELS FOR SECOND PHASE OF THE STUDY

For all Models,

- (i) Column Size = 1 Inch Square
(ii) Thickness of Floor = 0.25 Inch

Model	Shear Wall Size		Total Span		$\frac{SX}{SY}$	$\frac{SY}{TSY}$	=	$\frac{SX}{TSX}$
	SX	SY	TSX	TSY				
PS1-1	2.25"	4.5"	11.25"	22.5"	0.5			1/5
PS2-1	4.5"	4.5"	22.5"	22.5"	1.0			1/5
PS3-1	6.75"	4.5"	33.75"	22.5"	1.5			1/5
PS4-1	9.0"	4.5"	45"	22.5"	2.0			1/5
PS5-1	3.0"	6"	12"	24"	0.5			1/4
PS6-1	6.0"	6"	24"	24"	1.0			1/4
PS7-1	9.0"	6"	36"	24"	1.5			1/4
PS8-1	12.0"	6"	48"	24"	2.0			1/4
PS9-1	4.5"	9"	13.5"	27"	0.5			1/3
PS10-1	9.0"	9"	27"	27"	1.0			1/3
PS11-1	13.5"	9"	40.5"	27"	1.5			1/3
PS12-1	18.0"	9"	54"	27"	2.0			1/3
PS13-1	6.0"	12"	15"	30"	0.5			1/2.5
PS14-1	12.0"	12"	30"	30"	1.0			1/2.5
PS15-1	18.0"	12"	45"	30"	1.5			1/2.5
PS16-1	24"	12"	60"	30"	2.0			1/2.5

where,

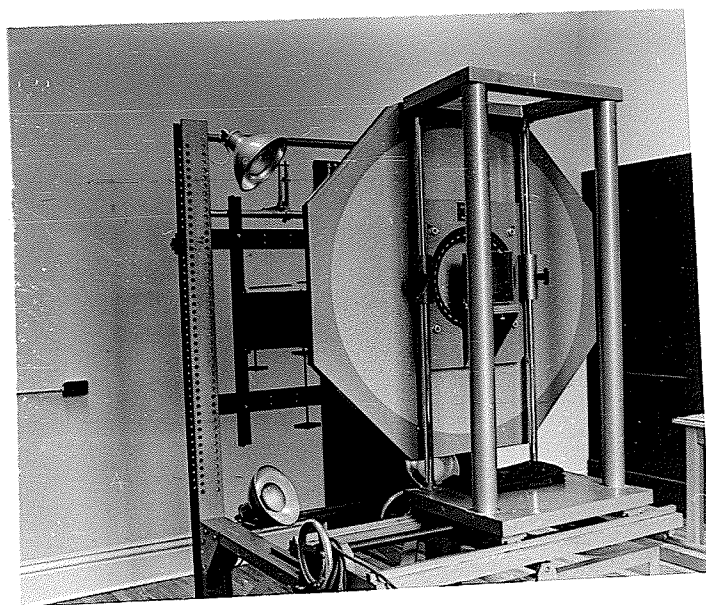
SX and SY are shear wall size in the X-X and Y-Y direction respectively, and TSX and TSY are total span in the X-X and Y-Y direction respectively.

3.3 Experimental Procedure

The Moiré apparatus shown in Figure 3.3.1 was used for the experimental work. The principles of the Moiré technique have been summarized in Appendix B. Since, for all models, the variation of the plate slope about horizontal axes was desired, the Moire screen was always positioned such that the ruled lines were horizontal.

3.3.1 Description of Experimental Models

Seven 1/24 scale plexiglass models, designated ES1, ES2, ES3, ES4, ES5, ES6, ES7, were tested. These models were similar to the analytical models of the tenth series of the second phase study, designated PS10-1, PS10-2, PS10-3, PS10-4, PS10-5, PS10-8 and PS10-9. The dimensions of the experimental models are shown in Figures 3.3.3 to 3.3.9. The models were fabricated from 1/4 inch thick black plexiglass (acrylic sheet) and were designed in such a way that loading could be applied through the shear wall, keeping all columns fixed. The columns were cut from 1 inch square steel bar and 1/4 inch diameter holes were drilled through their centers to clamp them to the plate and the loading frame. The columns in the line of loading were 3/4 inch in height while others were 1/2 inch in height. Eight plexiglass sheet panels, all of the shape and size shown in Figure 3.3.2, were cut and cemented together to form two boxes. These boxes were cemented to



Moiré Apparatus

Fig. 3.3.1

the top and the bottom of the plate to simulate a box type shear wall passing through a flat plate floor. Jaybond GC-2 acrylic adhesive cement, which produced the required strength in 48 hours, was used for cementing all joints. Model ES1 was fabricated and tested first. Model ES2 was then obtained by making saw cuts in the original model. Model ES3 was obtained by rotating model ES2 through 90° in a vertical plane and thereby changing the direction of loading. ES4 was then obtained by removing two panels from model ES2. Model ES5 was obtained by rotating model ES4 to again change the loading direction. Similarly, model ES6 and ES7 were obtained by removing panels.

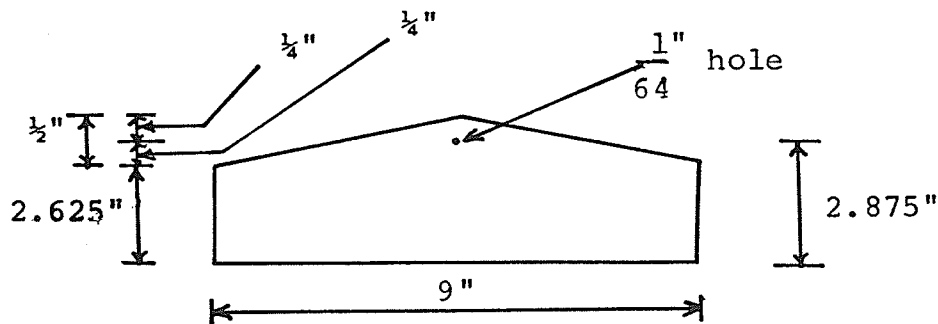
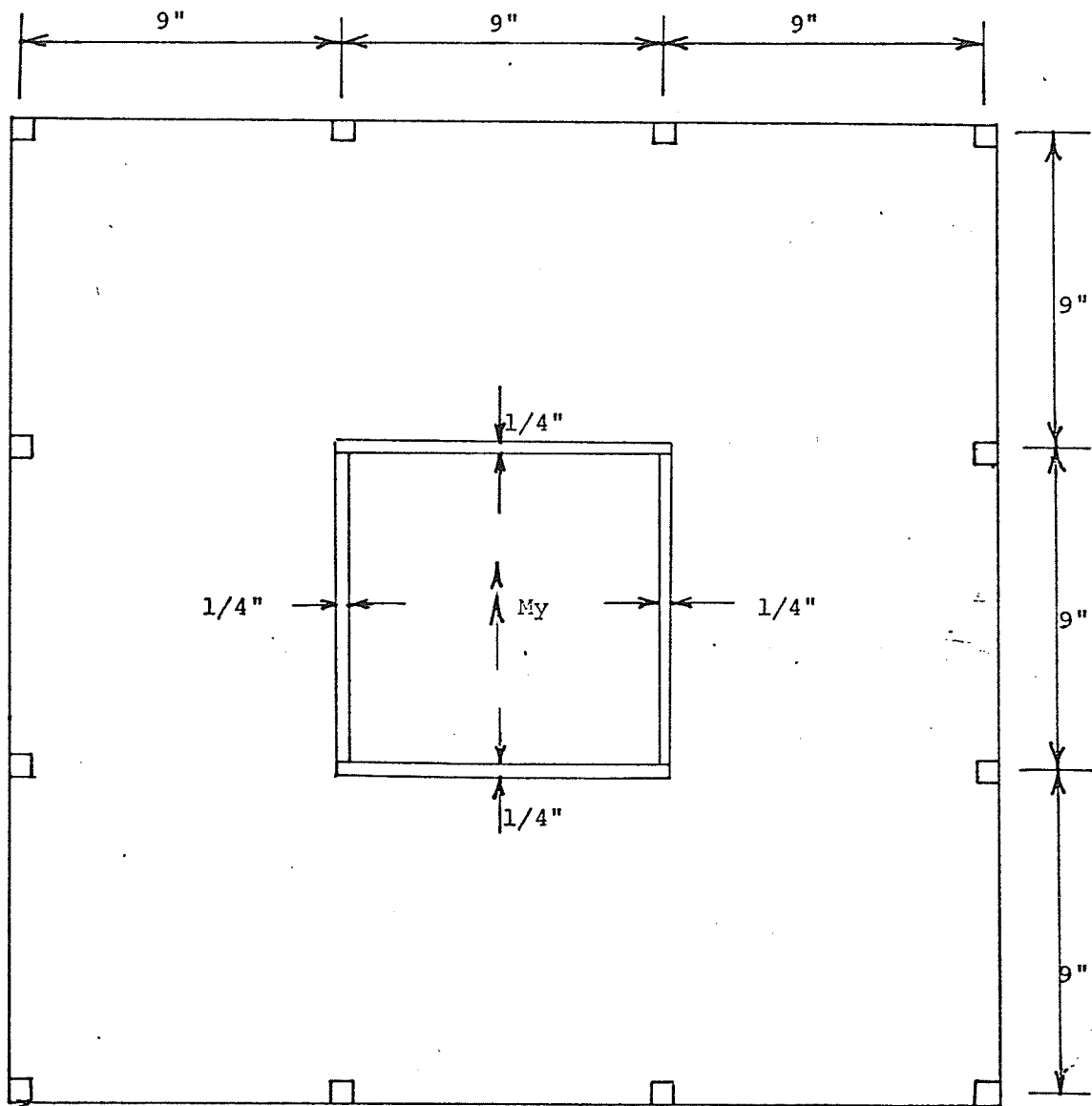
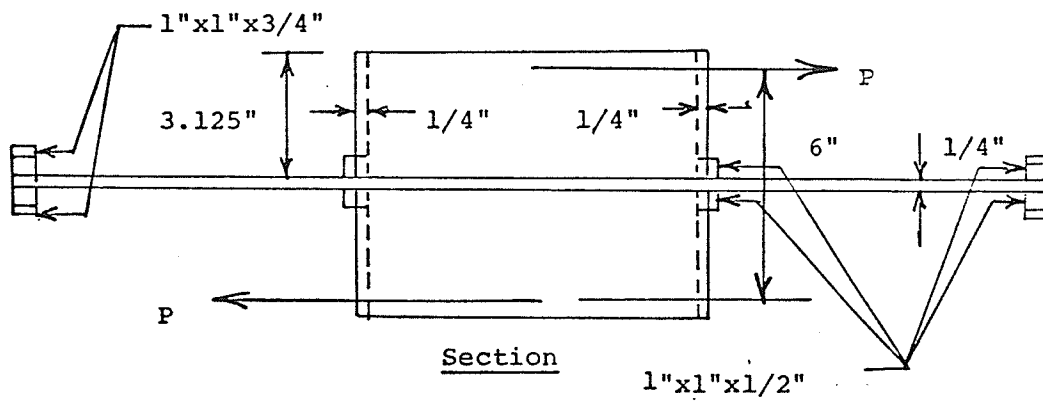


Plate Section Used In Fabricating Shearwall
Fig. 3.3.2

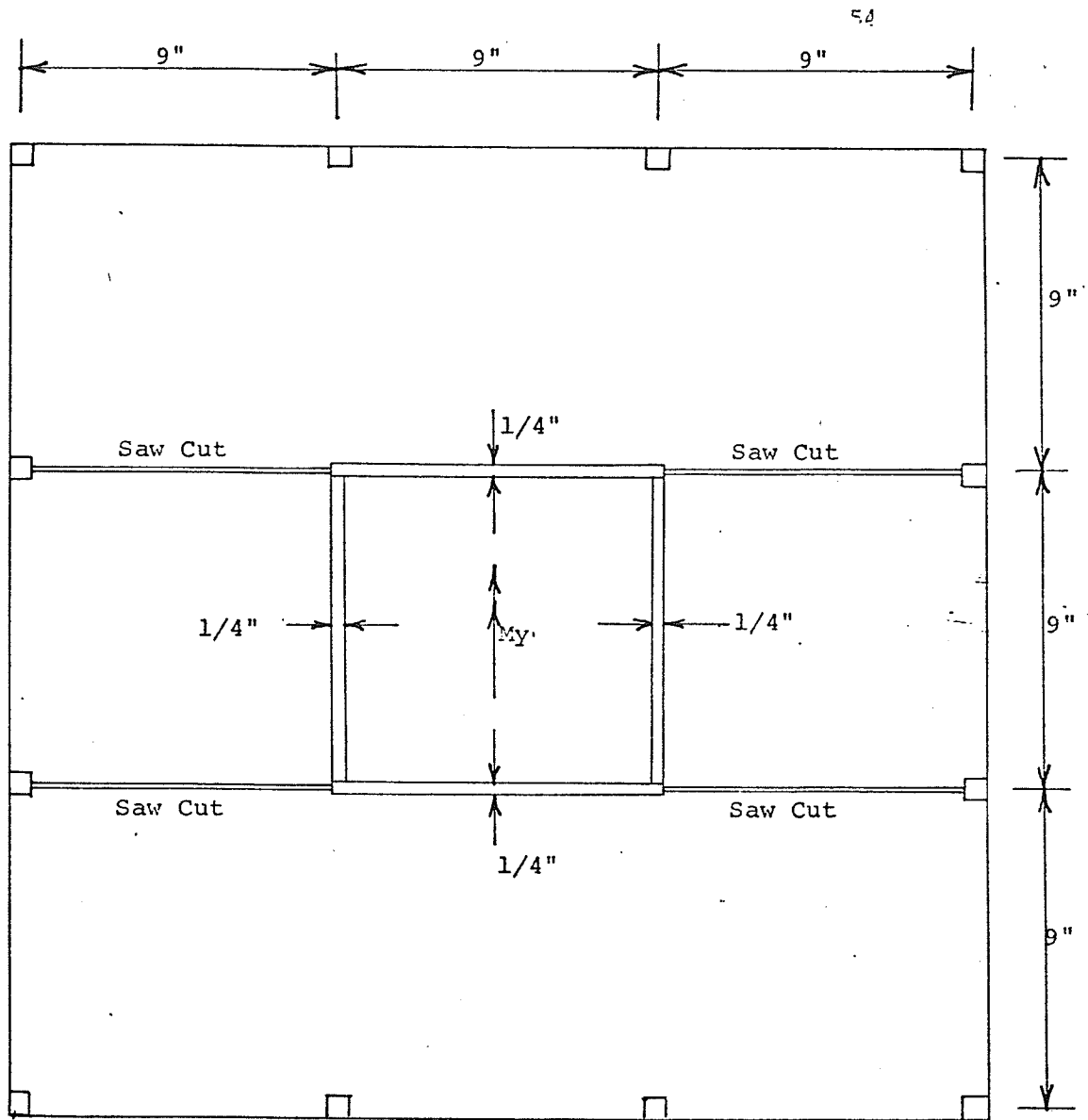


Plan



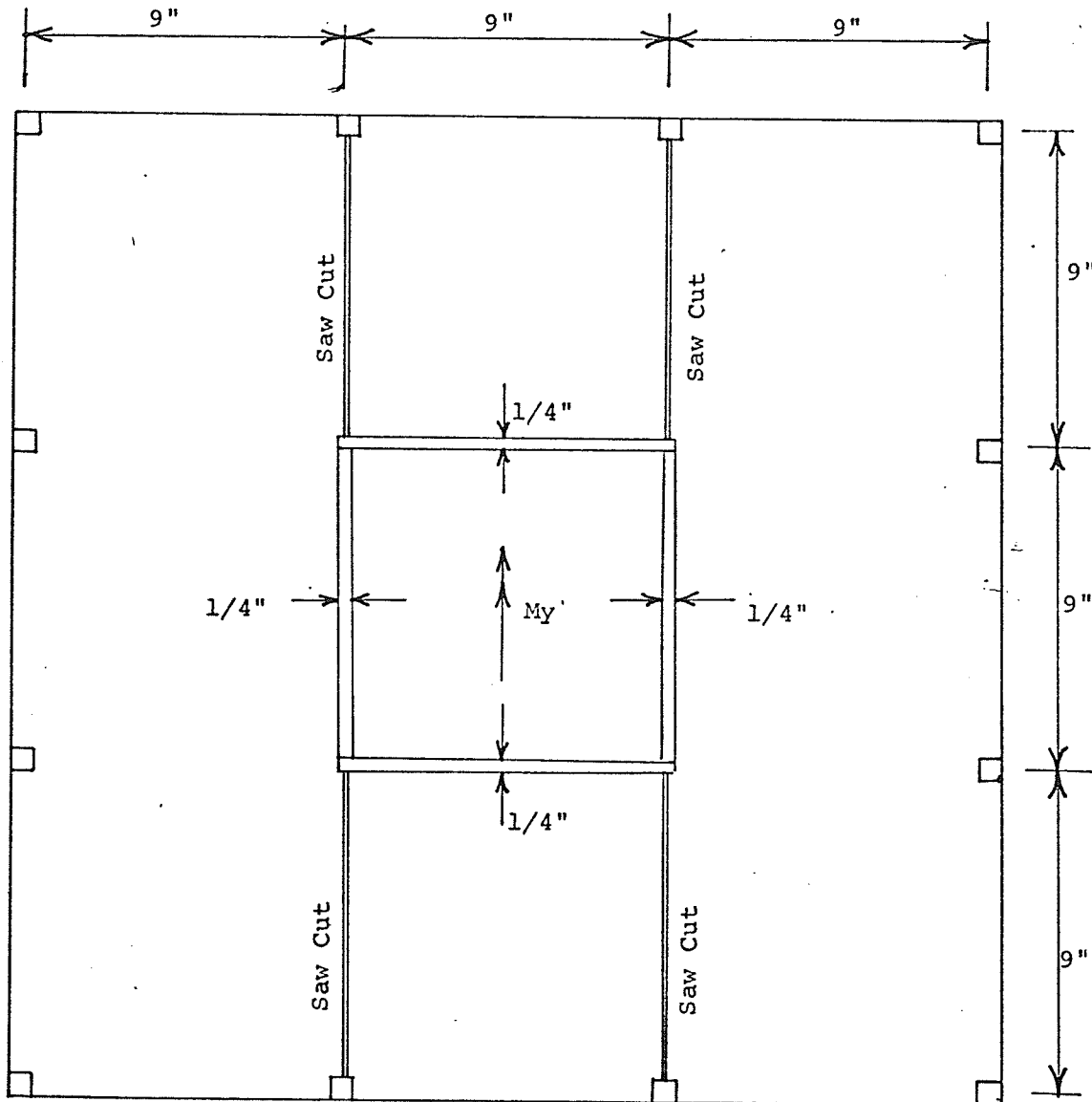
Section

Model ES1
Fig. 3.3.3



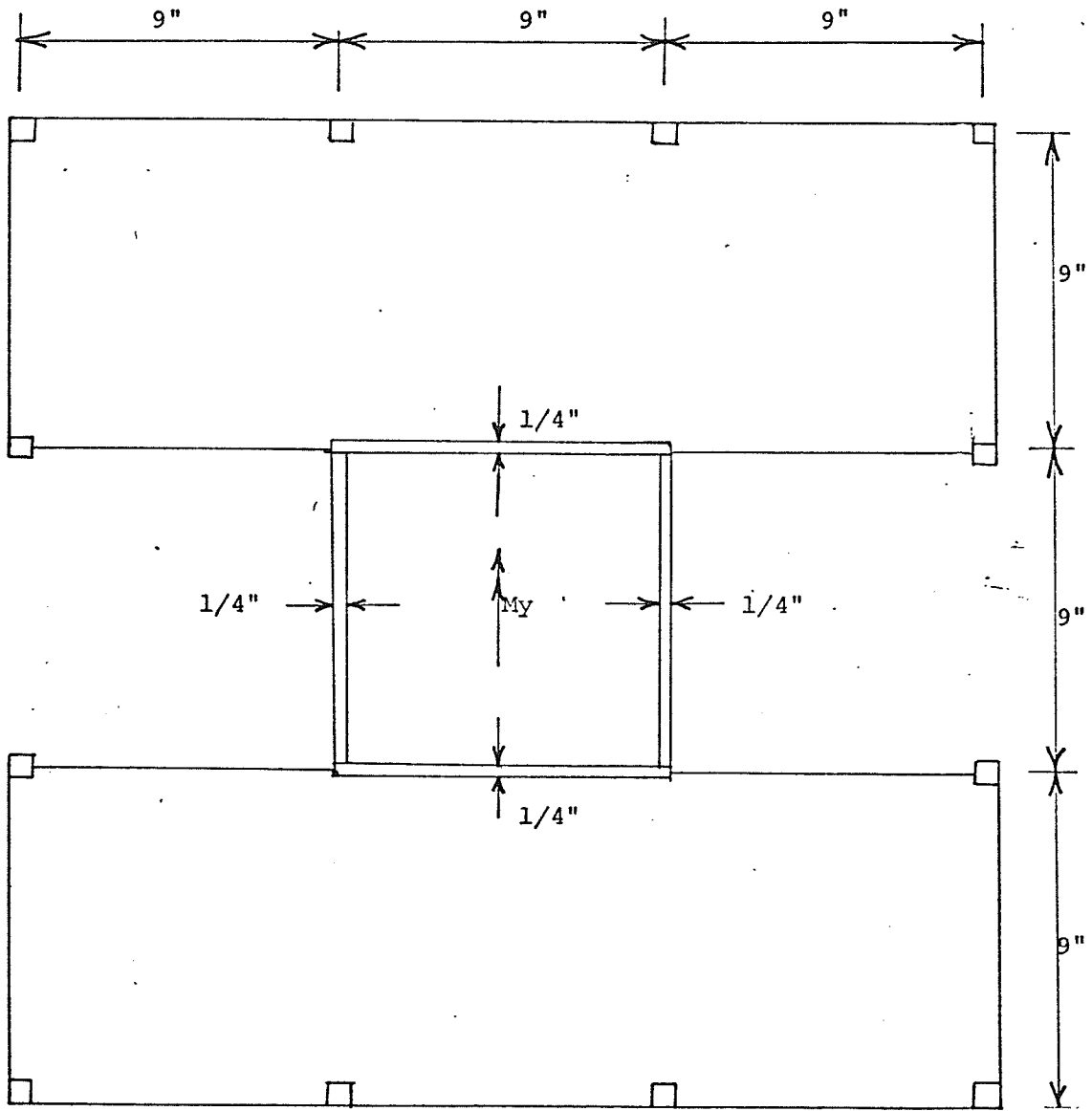
Model ES2

Fig. 3.3.4



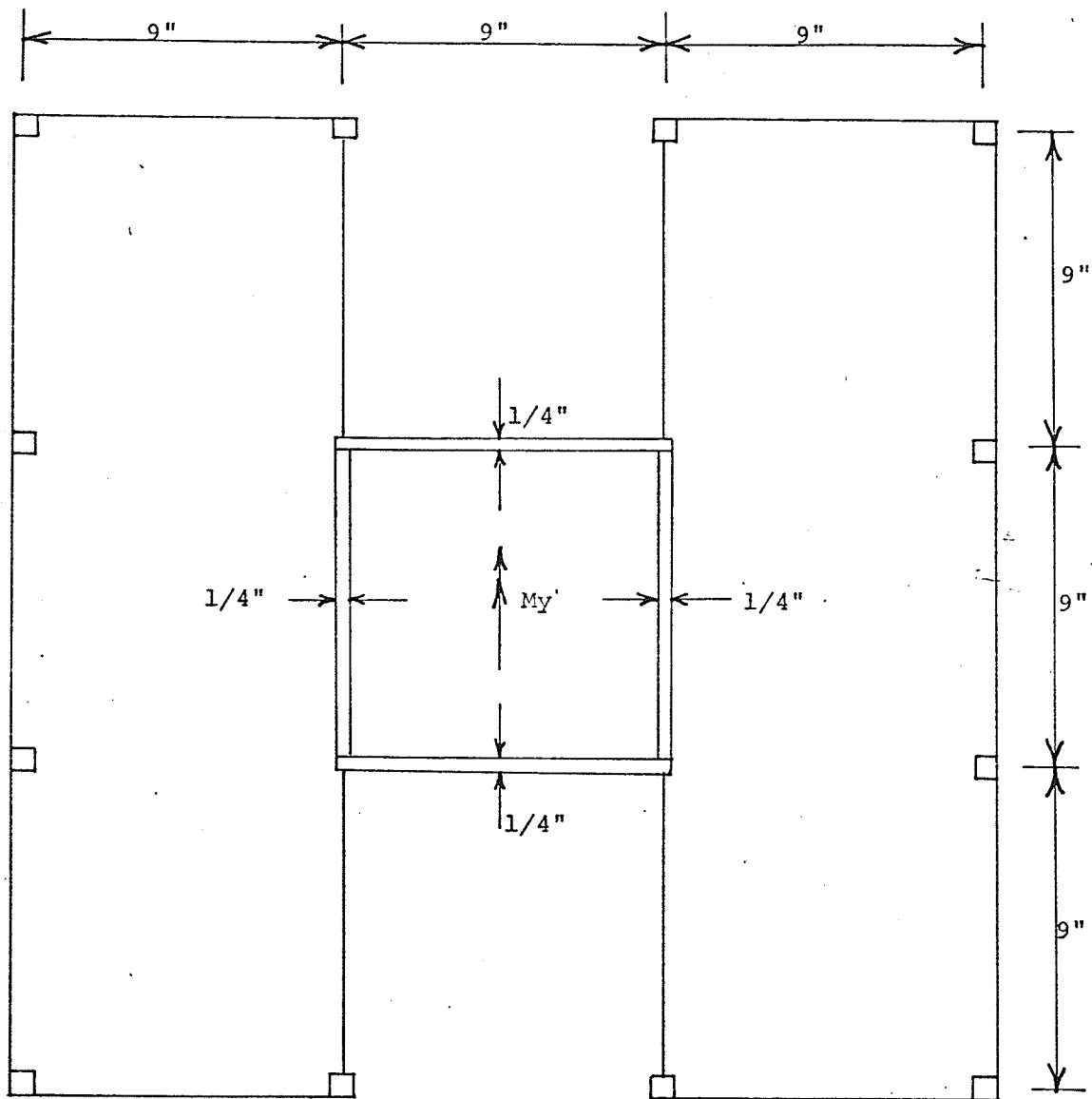
Model ES3

Fig. 3.3.5



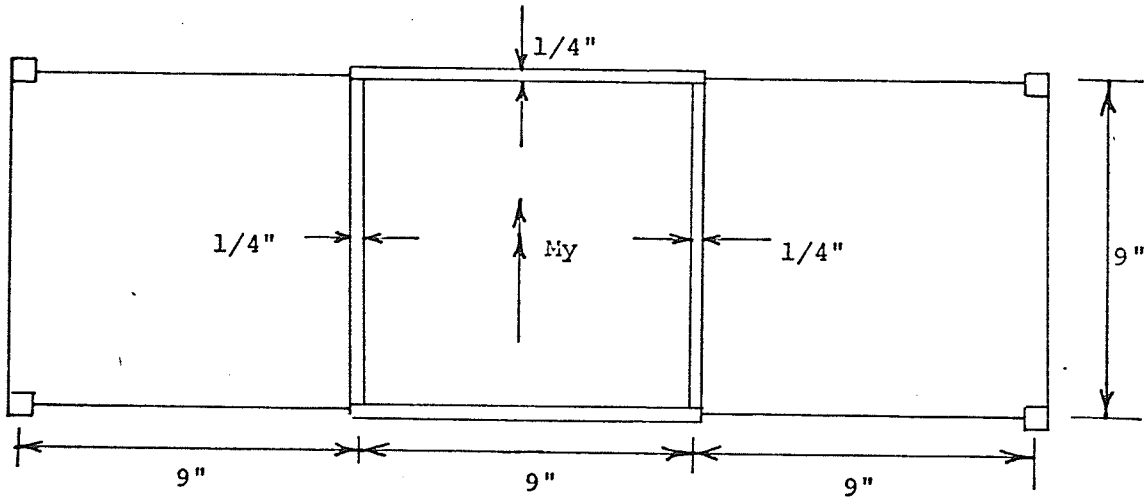
Model ES4

Fig. 3.3.6



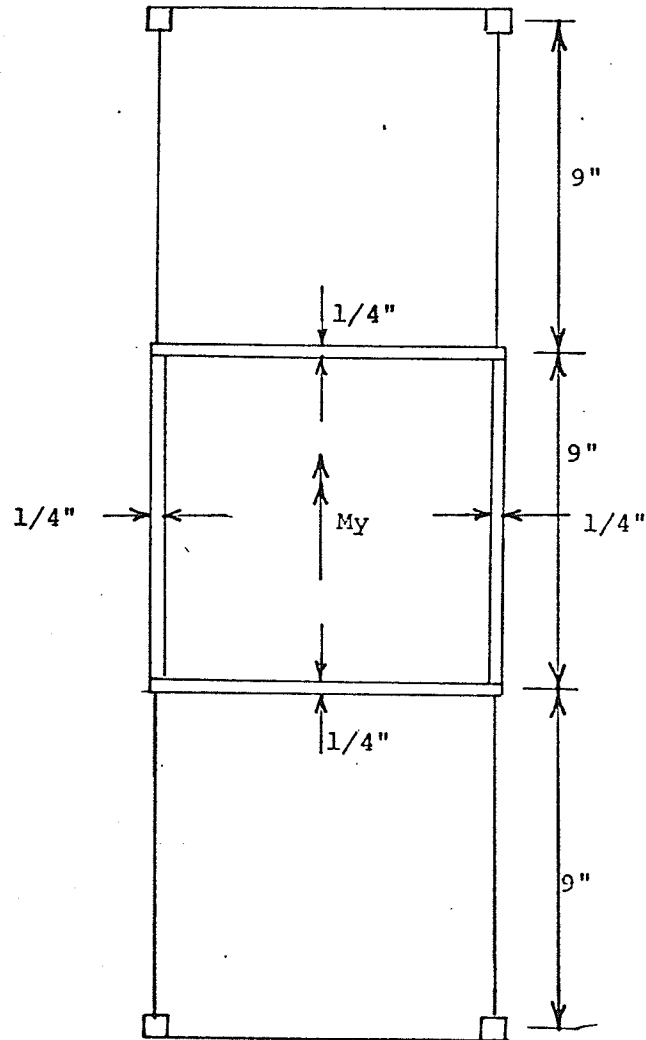
Model ES5

Fig. 3.3.7



Model ES6

Fig. 3.3.8



Model ES7

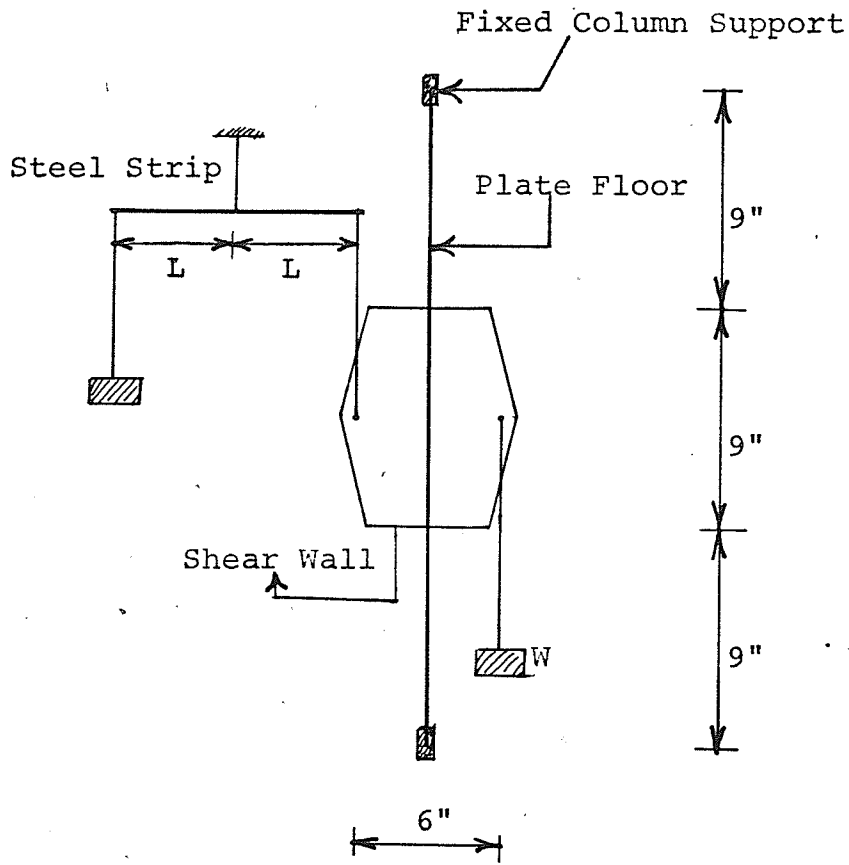
Fig. 3.3.9

3.3.2 Loading Procedure

Each model was loaded by a couple applied to the shear wall, and produced by forces 6 inches apart as illustrated in Figure 3.3.3. Since the models were mounted with the plate in a vertical plane in the Moiré apparatus, the loads were applied vertically. The downward forces were provided by applying weights to loading hangers which were attached to strings passing through the holes in either side of the shear wall. The upward forces were similarly applied using a simple lever system, as shown in the Figure 3.3.10. Figure 3.3.11 shows the loading arrangement for model ES9.

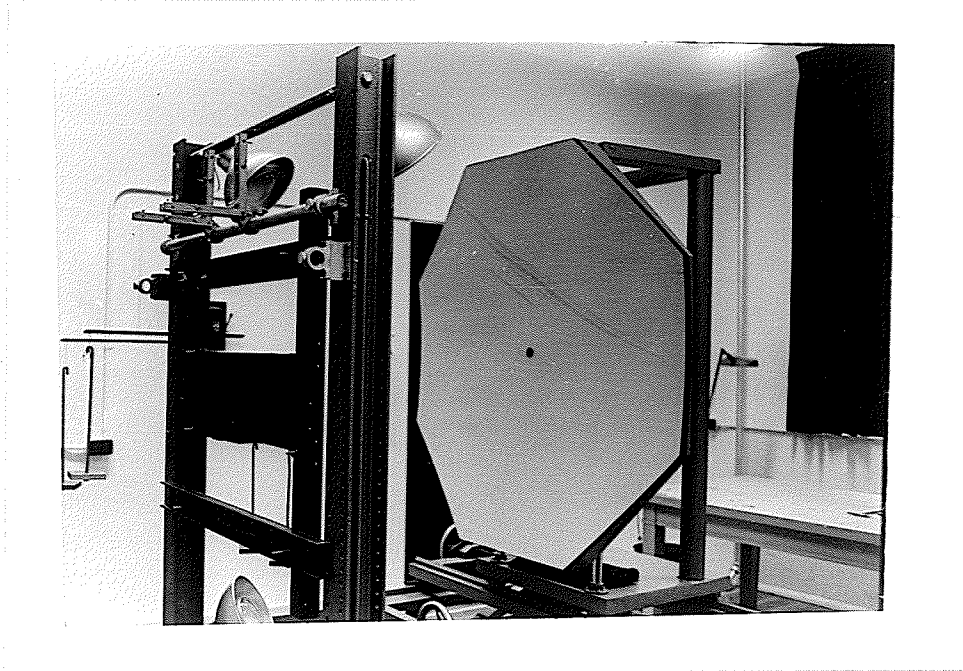
3.3.3 Photographic Technique

The Moiré screen, with the ruled lines in the horizontal position, was placed in the proper position at a distance of 85 centimeters from the model. The screen was illuminated by four R₂ super flood DXC 120V lamps. The camera was focused by viewing the image of the screen on the ground glass screen with a magnifying glass. While focusing the camera, the diaphragm was opened completely and photo flood lights were switched on. After focusing, the diaphragm was set to its smallest opening (f:32) to obtain good sharpness. The first exposure was taken with no load applied to the model, and the second exposure was made on the same negative after applying the loads. During exposure time, the room lights were switched off. Different combinations of exposure



Loading Arrangement

Fig. 3.3.10



Loading Arrangement For Model ES9

Fig. 3.3.11

and developing times for both prints and photographic plates were tried and the combination yielding the best results was chosen. Kodak metallographic plates were used. Kodak Bromide F-3 single weight paper was used for all prints and Dektol developer was used for both plates and prints. Prints were made to one-half scale. The positions of the photo flood lights were adjusted to obtain uniform illumination of the screen. The most important precaution taken was to keep the reflecting surface of the model clean and dust free, to obtain sharp and clear fringe patterns.

CHAPTER IV

ANALYTICAL AND EXPERIMENTAL RESULTS

The results for both the analytical and experimental studies are summarized in this Chapter. The complete listing of the data is included in Appendix C.

4.1 Results for Analytical Study

The first phase study involved the determination of the effects of column size and shear wall size and shape on the direct and carry-over stiffness coefficients for the plate floor. These coefficients were determined by applying known moments to either the shear wall or to the external column for models P1, P2 ----P10 and measuring corresponding plate rotations.

The applied moments and resulting rotations for the four loading conditions described in Section 2.3.2. for the first phase of the analytical study are given in Tables C1, C2 and C3 in Appendix C. The corresponding stiffness coefficients are presented in Tables 4.1, 4.2 and 4.3. Wherever possible, results are presented in the non-dimensional form by using size parameters such as column size to clear span ratio , ratio of shear wall size in the X-X direction to that in the Y-Y direction and shear wall size to total span ratio. Table 4.1 shows the calculated stiffness coefficients for four different column size to clear span ratios for a 9-inch square shear wall and a shear wall size to total span ratio of one third. Table 4.2 shows the stiffness coefficients

TABLE 4.1

EFFECT OF COLUMN SIZE ON
STIFFNESS COEFFICIENTS

Model	Column Size Clear Span	Shear Wall Loading		Exterior Column Loading		Average Carry-Over Stiffness Coefficient
		Direct Stiffness Coefficient	Carry-Over Stiffness Coefficient	Direct Stiffness Coefficient	Carry-Over Stiffness Coefficient	
P1	0.0555	28915	1590	1562	1618	1604
P2	0.0833	29593	1760	1760	1791	1776
P3	0.1111	31421	2026	2010	2060	2043
P4	0.1666	31872	2278	2383	2331	2305

TABLE 4.2

EFFECT OF SHEAR WALL SIZE ON STIFFNESS COEFFICIENTS

Model	Shear Wall Size	Shear Wall Loading		Exterior Column Loading		Average Carry-Over Stiffness Coefficient
		Direct Stiffness Coefficient	Carry-Over Stiffness Coefficient	Direct Stiffness Coefficient	Carry-Over Stiffness Coefficient	
P5	1/5	13223	938	1383	943	941
P6	1/4	17732	1152	1445	1163	1157
P1	1/3	28915	1590	1562	1618	1604
P7	1/2.5	42123	1979	1584	2006	1992

TABLE 4.3

EFFECT OF SHEAR WALL SHAPE ON STIFFNESS COEFFICIENTS

Model	Shear Wall Size in X-X Direction (SX)	Shear Wall Loading		Exterior Column Loading		Average Carry-Over Stiffness Coefficient
		Direct Stiffness Coefficient	Carry-Over Stiffness Coefficient	Direct Stiffness Coefficient	Carry-Over Stiffness Coefficient	
P8	0.5	16536	1215	1755	1230	1223
P2	1.0	29593	1760	1760	1791	1776
P9	1.5	51903	2569	1892	2611	2590
P10	2.0	70652	2896	1794	2960	2928

for four different square shear wall size to total span ratios for 0.5 inch columns. The values of stiffness coefficients for four rectangular shear walls for 0.75 inch square columns are given in Table 4.3. According to the Maxwell-Betti reciprocal theorem the carry-over stiffness coefficients from the shear wall to the exterior column are equal to the corresponding carry-over stiffness coefficients from the column to the shear wall. It can be seen from Tables 4.1 to 4.3 that a good agreement between corresponding values was obtained. Hence, the average of the two carry-over stiffness coefficients for each model is listed in the last column of each of Tables 4.1, 4.2 and 4.3.

The direct stiffness coefficients and the average carry-over stiffness coefficients from Table 4.1 are plotted for each column size to clear span ratio in Figures 4.1.1, 4.1.2 and 4.1.3. While the values from Table 4.2 are plotted for each shear wall size to total span ratio in Figures 4.2.1, 4.2.2 and 4.2.3. Similarly, the values given in Table 4.3 are plotted for each ratio of shear wall size in the X-X direction to that in the Y-Y direction, in Figures 4.3.1, 4.3.2 and 4.3.3. These plots are approximated by simple algebraic equations derived using the least square method of curve fitting. The plots shown in Figures 4.1.1, 4.1.2, 4.1.3, 4.2.1, 4.2.2, 4.2.3, 4.3.1 and 4.3.3 are represented by straight lines given by equations 4.1.1, 4.1.2, 4.1.3, 4.2.1, 4.2.2, 4.2.3, 4.3.1 and 4.3.3 respectively in Table 4.6. Figure 4.3.2 shows that the direct stiffness coefficient when the floor is loaded through the exterior column, does not vary with the ratio of the shear

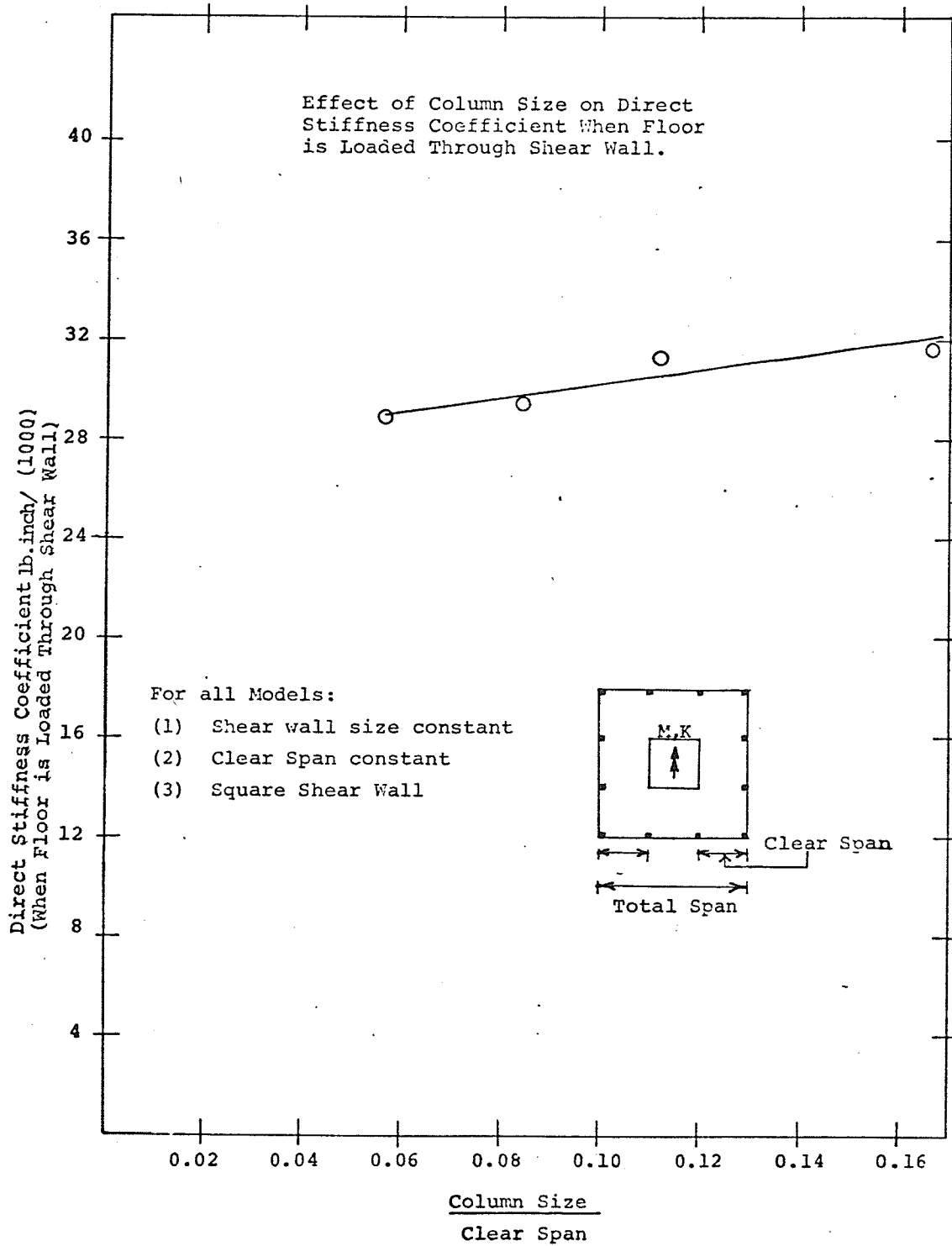
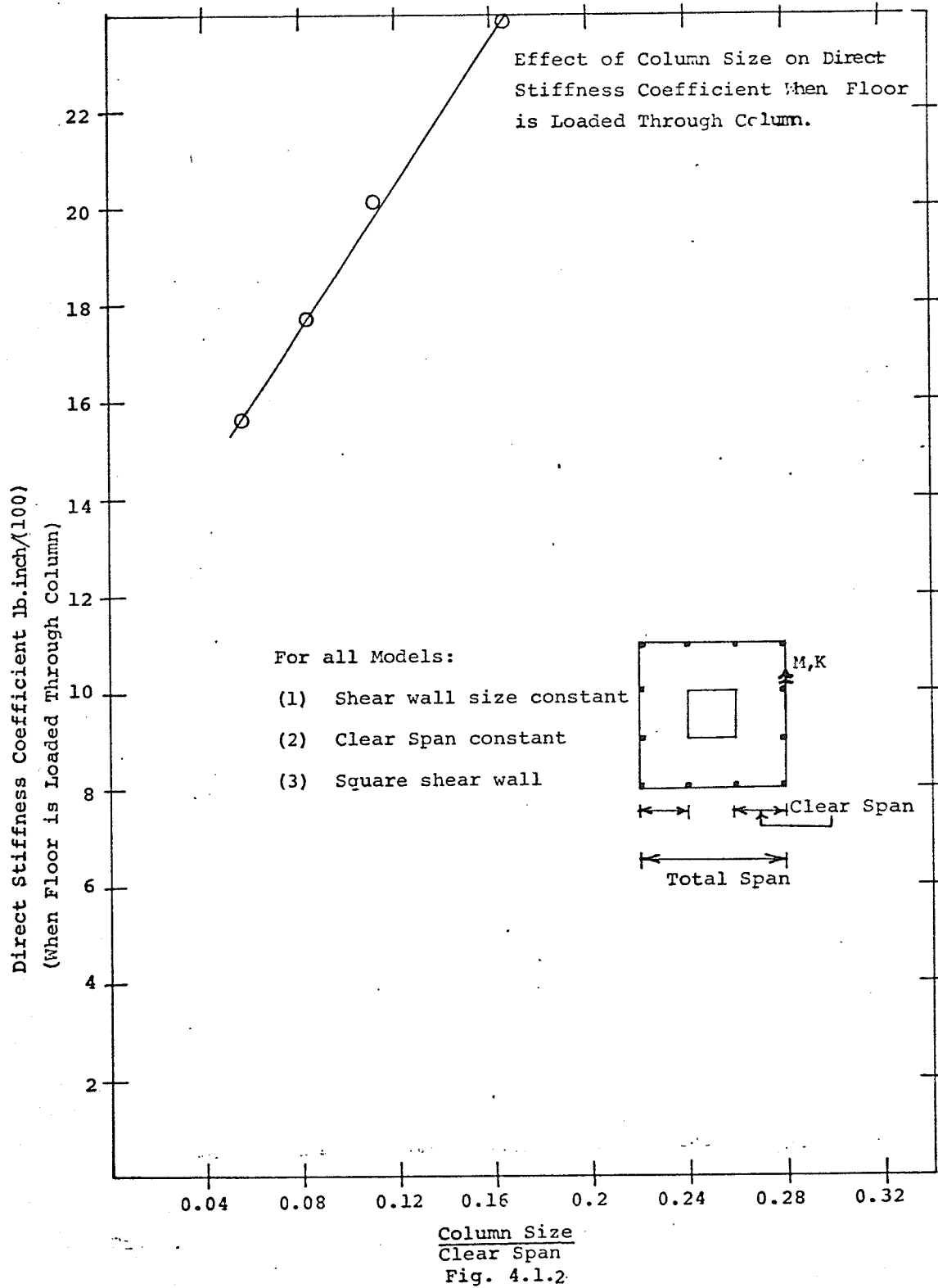


Fig. 4.1.1



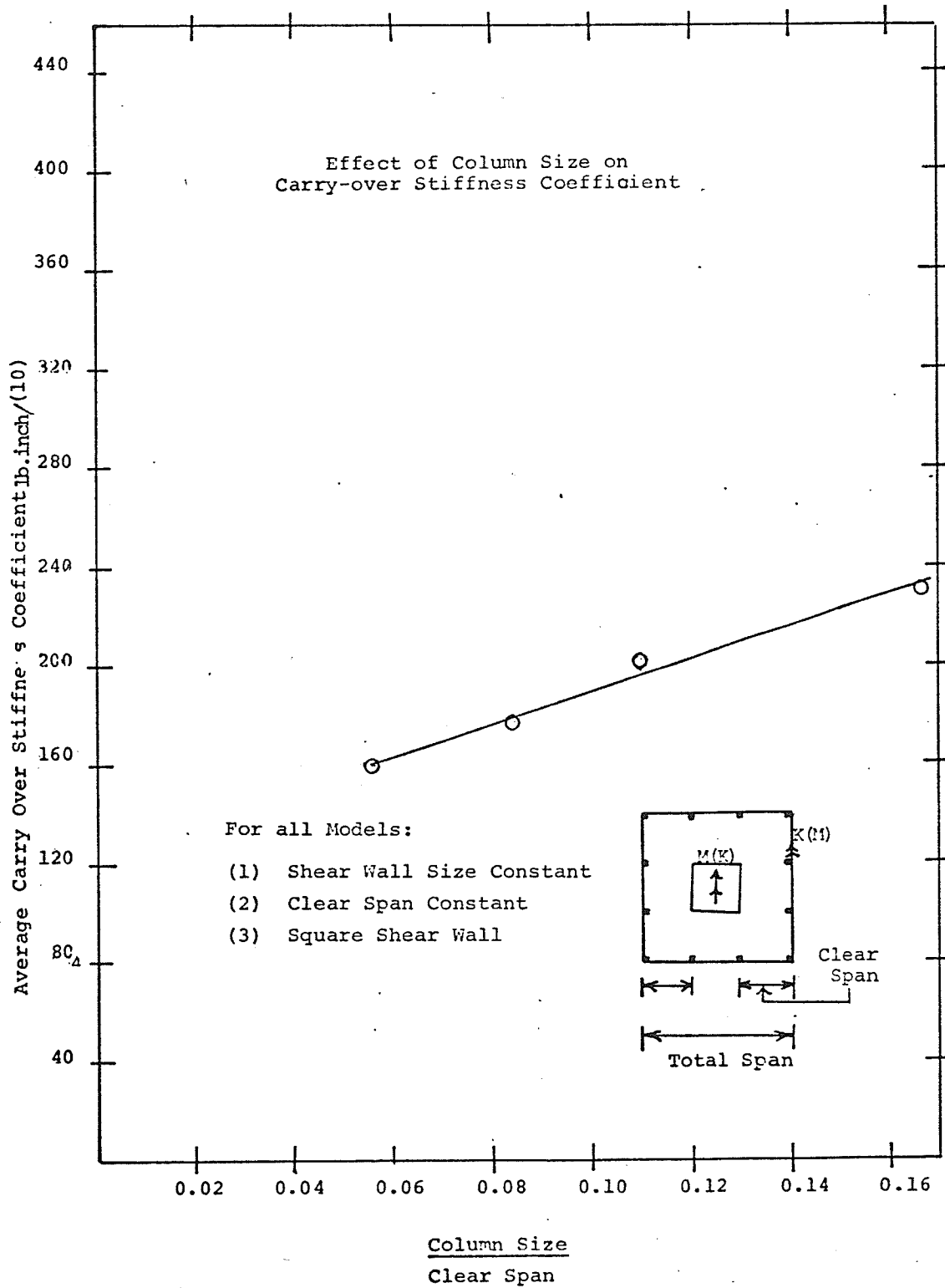


Fig. 4.1.3

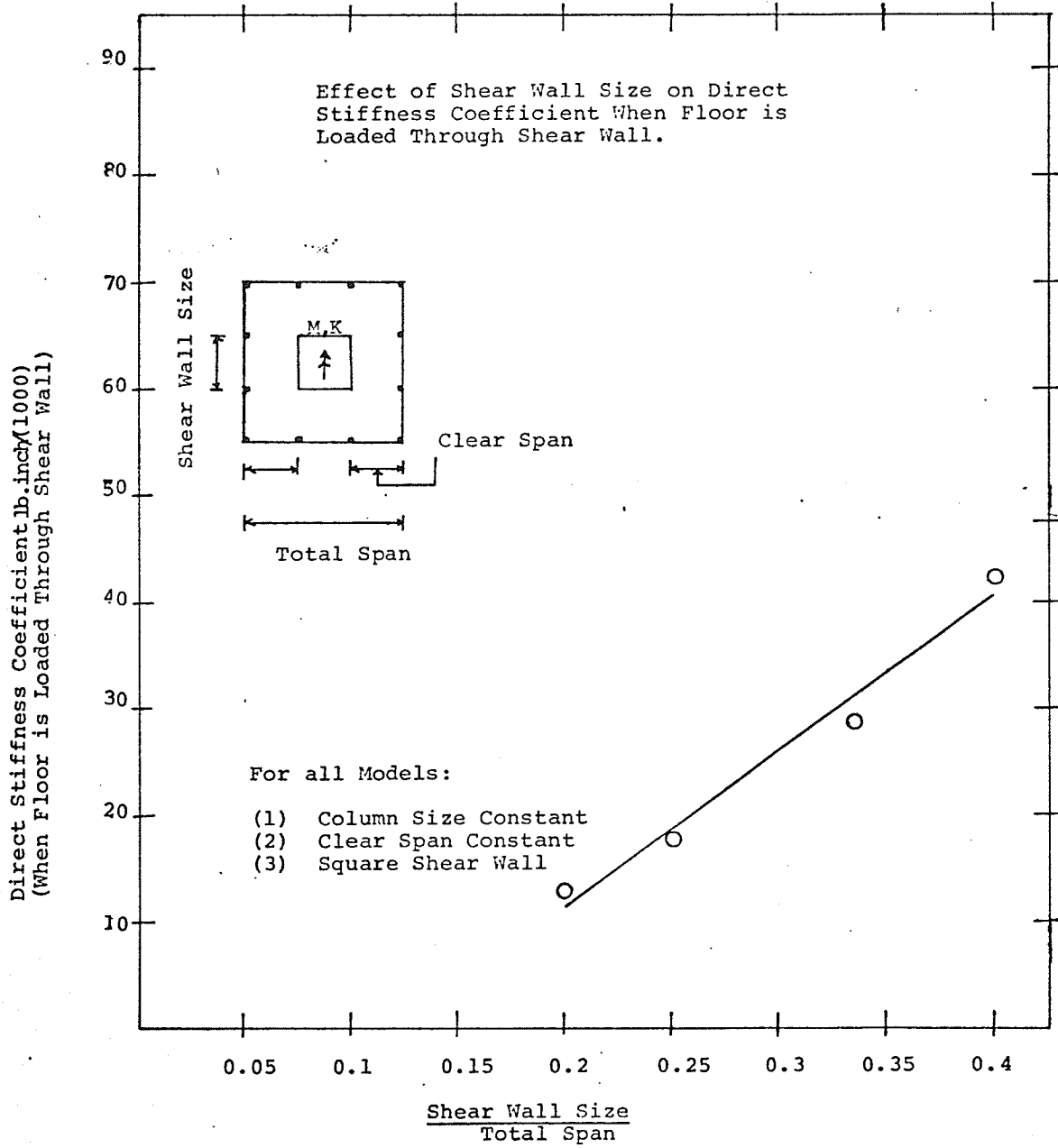


Fig. 4.2.1

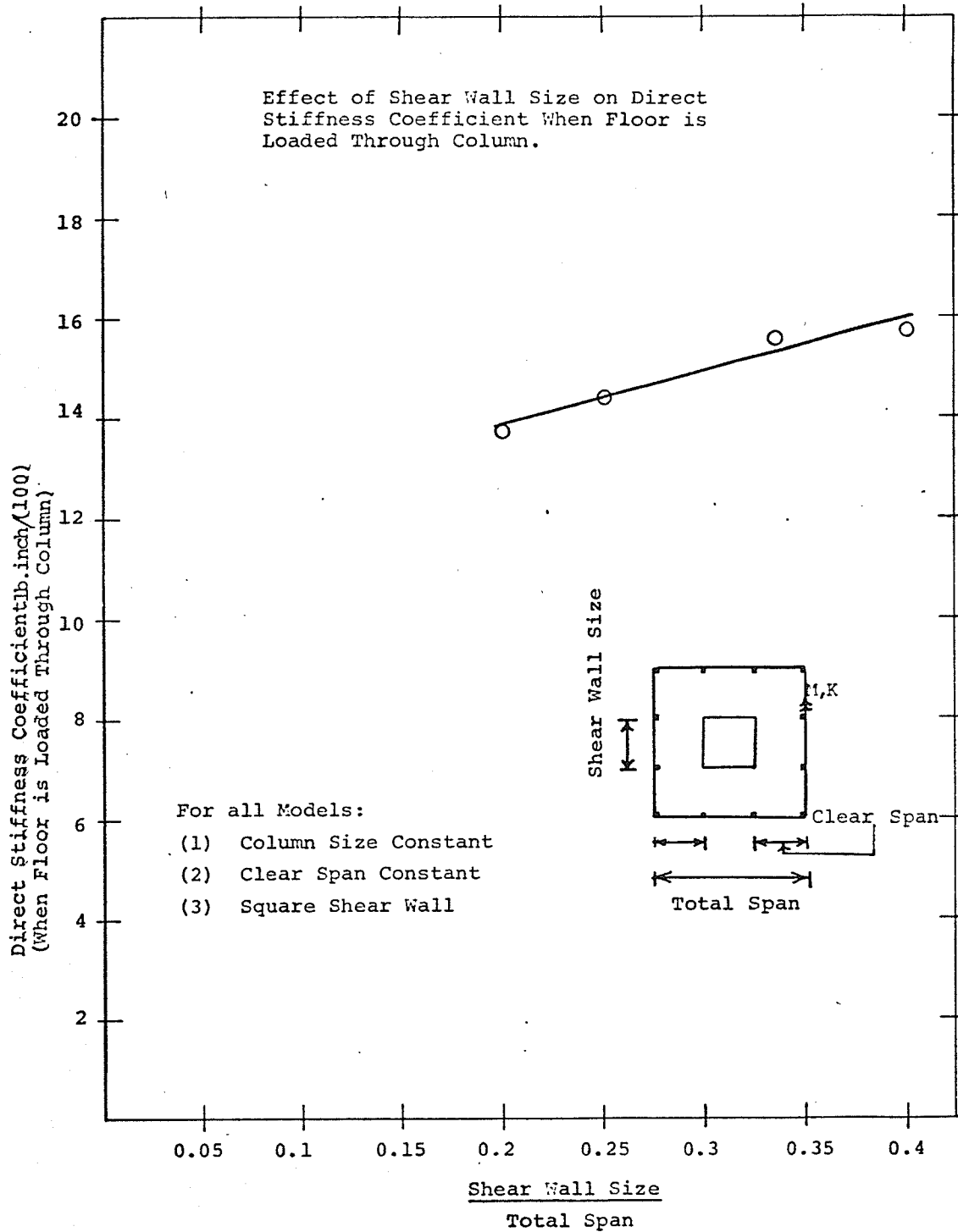


Fig. 4.2.2

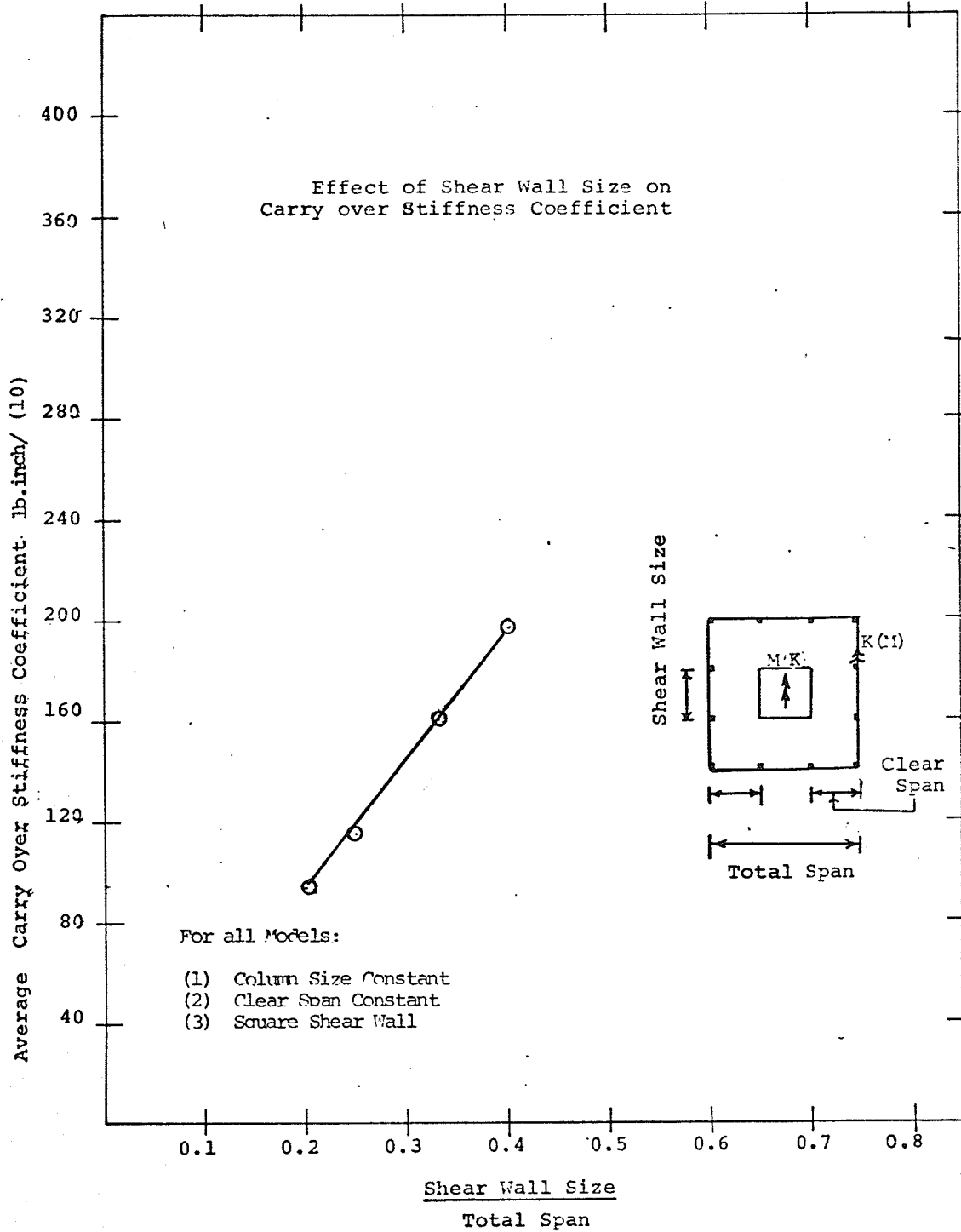


Fig. 4.2.3

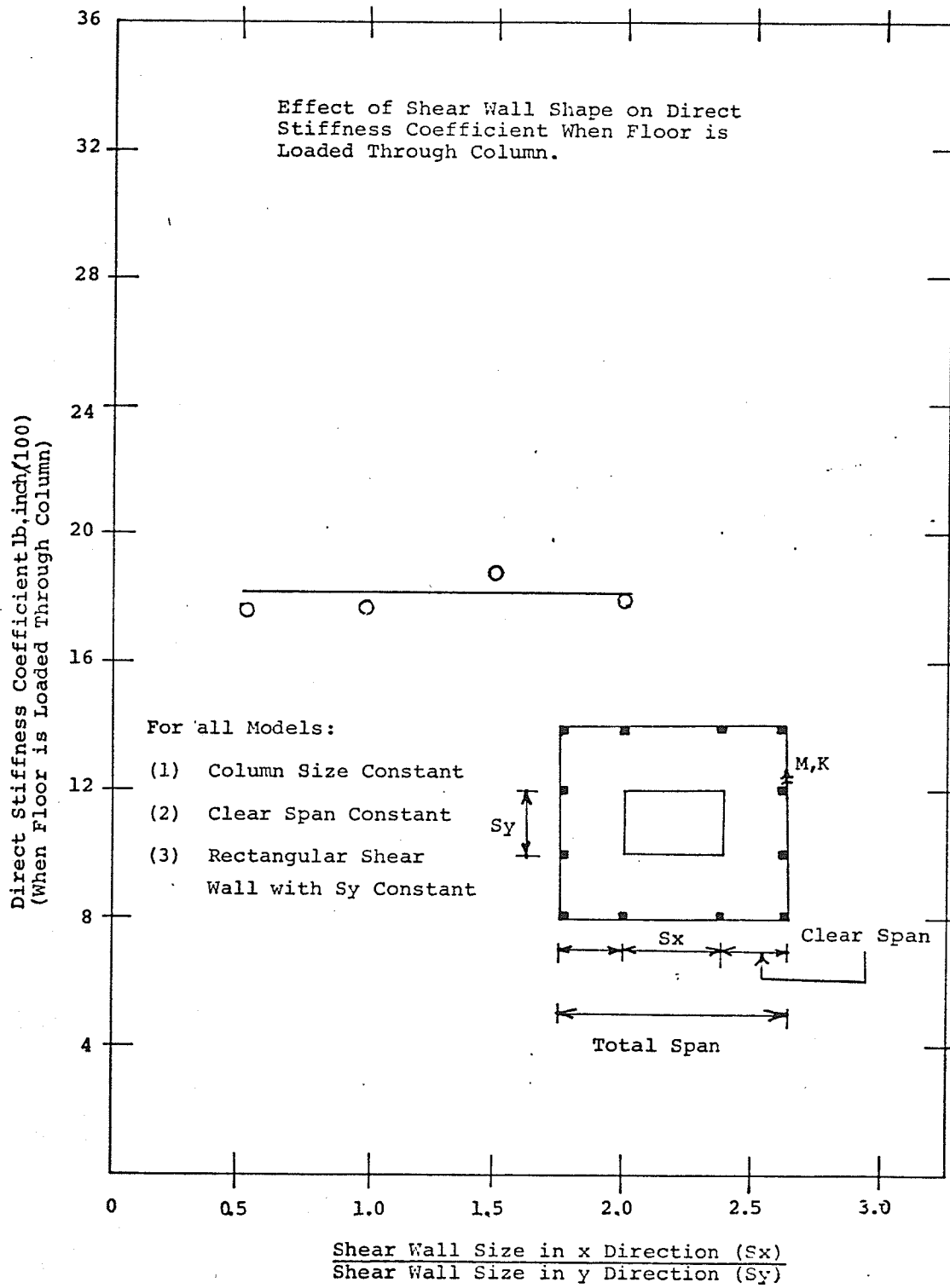


Fig. 4.3.2

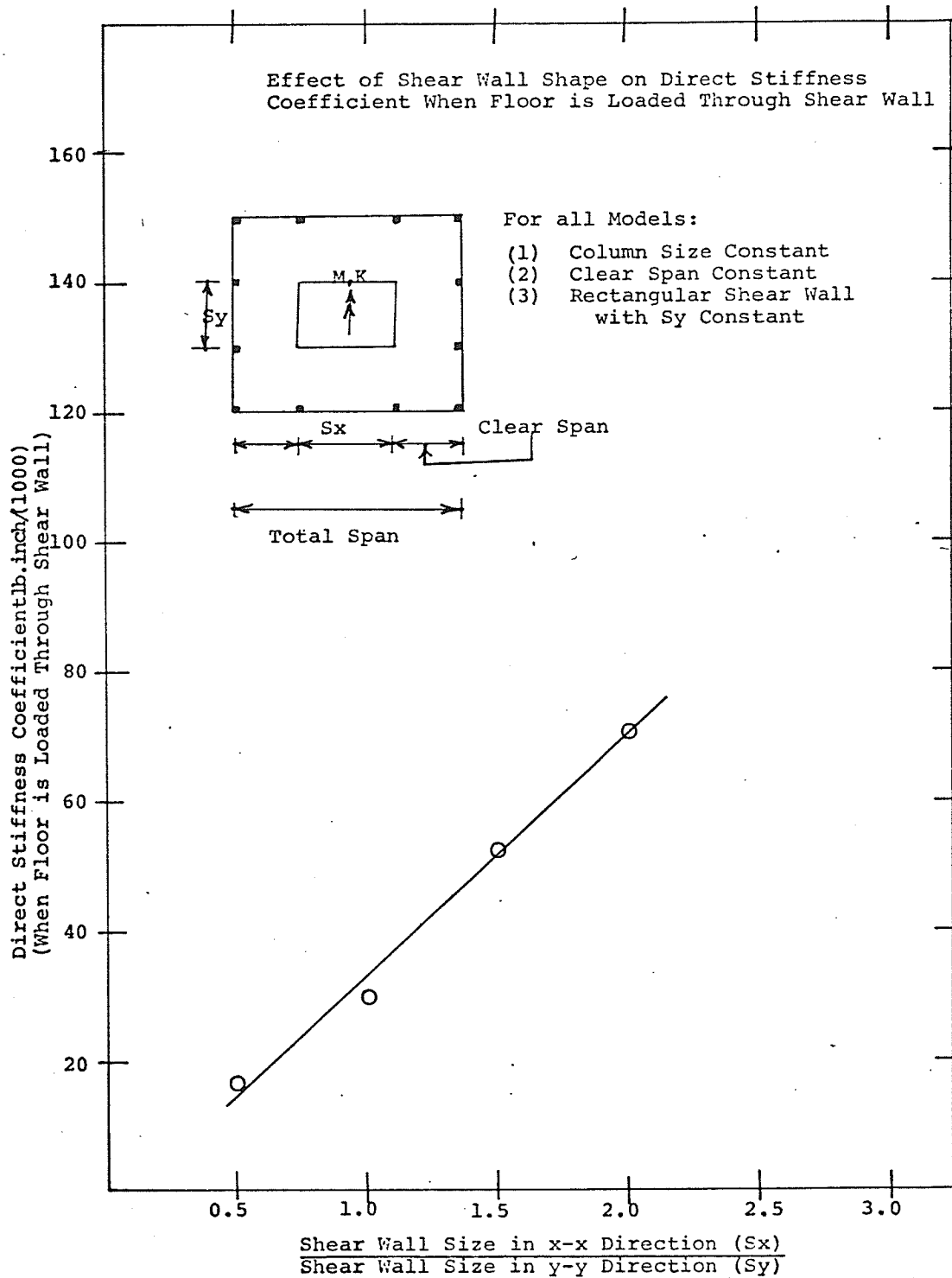


Fig. 4.3.1

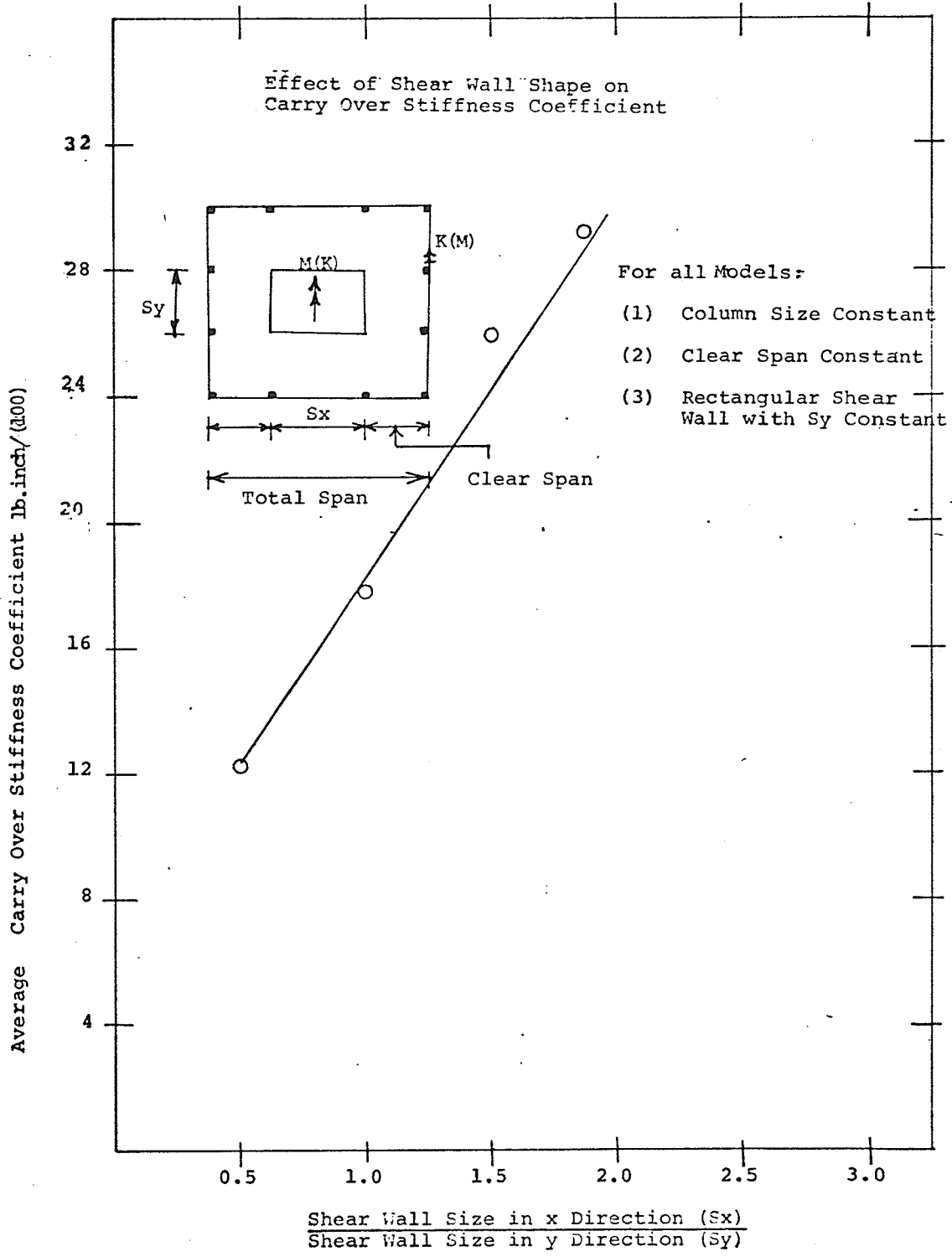


Fig. 4.3.3

wall dimension in the X-X direction to that in the Y-Y direction. Hence, no attempt is made to approximate this curve by an algebraic equation.

The analytical portion of the second phase study involved the application of known moments to each of the analytical models PS1-1, ----, PS16-1 and the calculation of the resulting plate rotations. The moments and rotations were then used to calculate direct stiffness coefficients which in turn were used in obtaining the multiplying factors described in section 2.5.

The applied moments and resulting rotations (for loading condition A, described in section 2.3.2), along with the calculated direct stiffness coefficients for the phase two models are included in Tables C4, C5, C6 and C7 in Appendix C.

The contribution of the various slab panels and joints to the direct bending stiffness, calculated as described in section 2.5, are listed in Table 4.4.

Finally, the multiplying factors are given in Tables 4.5(a), (b), (c), (d) and (e) for models with four different shear wall to total span ratios ranging from 1/5 to 1/2.5 for shear wall size in the X-X direction to shear wall size in the Y-Y direction ratios ranging from 0.5 to 2.0 and for 1 inch square columns.

The values of multiplying factor, F_T , given in Table 4.5 (a) are used to calculate the contribution of the torsional panels to the total stiffness while the values of F_B in Table 4.5 (b) are used for calculating the contribution of bending panels. Likewise, the values of F_C , F_{TC} and F_{BC} in Tables 4.5 (c), 4.5 (d) and 4.5 (e) are used for obtaining the stiffness due to the corner panels, torsion joints and bending joints respectively.

TABLE 4.4
 CONTRIBUTION OF DIFFERENT PANELS AND JOINTS
 TO THE TOTAL STIFFNESS WHEN SHEAR WALL LOADED

Model	Contribution of Different Panels			Contribution of Different Joints		Total Stiffness
	Torsional Panels	Bending Panels	Corner Panels	Bending Joints	Torsion Joints	
PS1-1	580	8633	3758	1725	3968	18666
PS2-1	1171	4455	3130	2038	2847	13642
PS3-1	1980	3015	3437	2672	2339	13445
PS4-1	3033	2280	4078	3696	2201	15290
PS5-1	753	12321	4713	2210	4881	24880
PS6-1	1685	6666	4102	2580	3486	18521
PS7-1	3033	4604	4729	3482	2932	18782
PS8-1	4878	3529	5884	4947	2873	22113
PS9-1	1170	20547	7166	3239	6862	38986
PS10-1	3032	11934	6594	3882	4893	30336
PS11-1	6012	8555	8153	5452	4316	32490
PS12-1	10364	6719	10751	8030	4501	40367
PS13-1	1683	30003	10058	4670	9019	55435
PS14-1	4878	18312	9839	5418	6474	44923
PS15-1	10368	13501	12805	7786	5855	50316
PS16-1	18750	10810	17500	11747	6302	65111

TABLE 4.5(a)

Value of F_T

$SX/SY \backslash SH/TS$	1/5	1/4	1/3	1/2.5
0.5	1.467	1.330	1.377	1.486
1.0	1.50	1.487	1.78	2.15
1.5	1.55	1.785	2.358	3.05
2.0	1.784	2.15	3.04	4.136

TABLE 4.5(b)

Value of F_B

$SX/SY \backslash SH/TS$	1/5	1/4	1/3	1/2.5
0.5	1.879	2.01	2.236	2.450
1.0	1.939	2.177	2.598	2.990
1.5	1.97	2.255	2.793	3.306
2.0	1.985	2.304	2.925	3.530

where,

SH = Shear Wall Size,
 TS = Total Span, and
 SX and SY = Shear Wall Size in Y-Y and X-X direction
 respectively.

TABLE 4.5(c)

Value of F_C

SH/TS SX/SY	SH/TS			
	1/5	1/4	1/3	1.2/5
0.5	0.204	0.256	0.39	0.547
1.0	0.34	0.446	0.718	1.07
1.5	0.560	0.772	1.331	2.090
2.0	0.888	1.28	2.34	3.810

TABLE 4.5(d)

Value of F_{TC}

SH/TS SX/SY	SH/TS			
	1/5	1/4	1/3	1/2.5
0.5	0.0360	0.059	0.124	0.218
1.0	0.0516	0.0843	0.177	0.313
1.5	0.0636	0.106	0.235	0.425
2.0	0.0798	0.14	0.326	0.610

where,

SH = Shear Wall Size,
 TS = Total Span, and
 SY and SX = Shear Wall size in Y-Y and X-X direction
 respectively.

TABLE 4.5(e)
Value of F_{BC}

SX/SY	SH/TS			
	1/5	1/4	1/3	1/2.5
0.5	0.0626	0.107	0.235	0.452
1.0	0.037	0.0624	0.141	0.262
1.5	0.0323	0.0561	0.132	0.251
2.0	0.0335	0.0598	0.145	0.284

where,

SH = Shear Wall Size,
TS = Total Span, and
SY and SX = Shear Wall size in Y-Y and X-X direction
respectively.

TABLE 4.6

EFFECT OF DIFFERENT PARAMETERS ON
BENDING STIFFNESS COEFFICIENTS

EFFECT OF COLUMN SIZE

$$K_{SS} = 27535.6 + 28043.0 (C/S) \quad (4.1.1)$$

$$K_{CC} = 1152.79 + 7454.25 (C/S) \quad (4.1.2)$$

$$K_{CS} = K_{SC} = 1262.32 + 6446.44 (C/S) \quad (4.1.3)$$

EFFECT OF SHEAR WALL SIZE

$$K_{SS} = -17148.9 + 144201.0 \left(\frac{SH}{TS}\right) \quad (4.2.1)$$

$$K_{CC} = 1181.22 + 1057.0 \left(\frac{SH}{TS}\right) \quad (4.2.2)$$

$$K_{CS} = K_{SC} = -141.05 + 5292.31 \left(\frac{SH}{TS}\right) \quad (4.2.3)$$

EFFECT OF SHEAR WALL SHAPE

$$K_{SS} = -3993.63 + 36932.0 \left(\frac{SX}{SY}\right) \quad (4.3.1)$$

$$K_{CS} = K_{SC} = 646.82 + 1186.22 \left(\frac{SX}{SY}\right) \quad (4.3.3)$$

where, K_{SS} and K_{CC} are direct stiffness coefficients at shear wall and column respectively,

K_{CS} = carry-over bending stiffness coefficients from shear wall to one column

K_{SC} = carry-over bending stiffness coefficient from one column to shear wall.

C = column size SH = size of square shear wall

S = clear span TS = total span

SY and SX = shear wall size in the Y-Y and X-X direction respectively.

4.2 Results for Experimental Study

The purpose of the Moiré experimental study was to provide a check of the direct stiffness coefficients determined in phase two of the analytical study. Known moments were applied to the shear wall and the resulting shear wall rotations were calculated for seven models, ES1 to ES7, which were similar in geometry to analytical models PS10-1, PS10-2, PS10-3, PS10-4, PS10-5, PS10-8 and PS10-9.

The values of the moments applied to the shear wall, the resulting rotations and the calculated direct stiffness coefficients are tabulated in Table 4.7. The values of direct stiffness coefficients were obtained by dividing the applied moments by the corresponding rotations as described in Section 2.3.1. The experimental values of slopes and deflections were plotted along the vertical lines passing through edges of shear walls and columns for the various models. These slope and deflection curves are given in Appendix 'B'.

TABLE 4.7

EXPERIMENTAL RESULTS

Model	Moment Applied to the Shear Wall	Rotation	Direct Stiffness
ES1	120 in. Lb.	0.0045 Rad.	26666.66
ES2	120 in. Lb.	0.00525 Rad.	22850.0
ES3	120 in. Lb.	0.00525 Rad.	22850.0
ES4	120 in. Lb.	0.090 Rad.	13333.3
ES5	120 in. Lb.	0.006 Rad.	20000.0
ES6	60 in. Lb.	0.006 Rad.	10000.0
ES7	60 in. Lb.	0.02325 Rad.	2580.0

CHAPTER V

DISCUSSION OF RESULTS

This chapter contains a discussion of the analytical and experimental results.

5.1 Effects of Column Size and Shear Wall Size

The first phase of the investigation was carried out to study the effect of column size and shear wall size and shape on the bending stiffness coefficients.

5.1.1 Direct Bending Stiffness Coefficients

It can be seen from Figures 4.1.1, 4.2.1 and 4.3.1 that the direct stiffness coefficient for the floor loaded through the shear wall is extremely sensitive to shear wall shape and size and is relatively insensitive to column size. The value of this stiffness coefficient is increased by approximately 120 percent as the shear wall size is changed from 9' x 9' to 18' x 18' and by approximately 75 percent as the shear wall dimension in the X - X direction is changed from 9 feet to 18 feet, with other dimensions kept constant. The increase is only about 10 percent when the column size is changed from 1 foot square to 2 feet square. This can be explained by the fact that as the shear wall size is changed,

the widths of both the bending and torsional panels change. Hence the stiffness is also changed. However, when the column size is changed only the clamped areas of the plate near the column supports change, and then by a very small amount. This does not affect the stiffness greatly.

The value of direct stiffness when the floor is loaded through the exterior columns is more sensitive to variations in column size relative to shear wall size and is independent of the shape of the shear wall. The reason is that the portion of the plate near the loaded columns, due to its free edges, is more flexible than the portion near the shear wall. Hence the deflections and rotations of the plate near the columns are sensitive more to column size than to shear wall size because any effect of change in shear wall size is absorbed mainly in the comparatively stiff portion of the plate near the shear wall. Further, this bending stiffness is mainly derived from bending and corner panels and changing the shear wall dimension in the X - X direction only, does not change the size of bending and corner panels. Hence the value of this stiffness coefficient is not affected by shear wall shape. The value of this stiffness is increased by approximately 30 percent as the column size is changed from 1 foot square to 2 feet square and by less than 15 percent when the shear wall size is changed from 9 feet square to 18 feet square.

Model P₁ of this investigation is similar to model P₄

tested experimentally by Nantasarn.⁽¹²⁾ The values of the bending stiffness coefficients for this model, obtained in the present investigation by the finite element technique, are compared in table 5.1, with those obtained experimentally by Nantasarn. His experimental value for the direct stiffness coefficient when the shear wall is loaded, is within 10 percent of the analytical value. However, his value for the direct stiffness coefficient when the exterior columns are loaded is 25 percent lower than the analytical value. This discrepancy is probably largely due to the fact that true fixed shear wall supports could not be achieved experimentally in the Moire' apparatus used by Nantasarn.

TABLE 5.1

STIFFNESS COEFFICIENTS FOR MODEL P1

Stiffness Coefficients	Values Obtained by Finite Element Procedure	Values Obtained by Nantasarn (12) experimentally	Difference	Percentage Difference	
Direct Stiffness Coefficient	Shear Wall Loaded	28915	26650	2265	8.4%
	Exterior Column Loaded	1562	12250	312	25%
Carry-Over Stiffness Coefficient	Shear Wall Loaded	1590	2007	417	26.0%
	Exterior Column Loaded	1618	1020	598	37.0%
	Average Value	1604	1513	91	5.6%

5.1.2 Carry-Over Bending Stiffness Coefficients

Tables 4.1, 4.2 and 4.3 show that the value of the carry-over stiffness coefficient from the shear wall to one exterior column is quite close to that from the exterior column to the shear wall. The maximum discrepancy is about 2 percent. This is to be expected in view of the Maxwell-Betti reciprocal theorem. Figures 4.1.3, 4.2.3 and 4.3.3 show that the carry-over stiffness coefficient is more sensitive to shear wall shape and size than to column size. The value of the carry-over stiffness is increased by approximately 70 percent as the shear wall size is changed from 9' x 9' to 18' x 18' and by approximately 45 percent as the shear wall dimension in the X - X direction is changed from 9 feet to 18 feet. The increase is only about 25 percent when the column size is changed from 1 foot square to 2 feet square. The reason is that as the shear wall shape or size is changed, the clamped area of the plate changes by a greater amount than when the column size is changed. The average values of carry-over stiffness coefficients obtained experimentally by Nantasarn ⁽¹²⁾ differ by about 5 percent from those obtained in this investigation. The experimental value of the carry-over stiffness from the exterior column to the shear wall obtained by Nantasarn ⁽¹²⁾ is quite low relative to the experimental value of carry-over stiffness from the shear wall to the exterior column. It is again probably largely due to the fact that true fixed shear wall could not be achieved experimentally.

5.2 CONTRIBUTIONS OF FLOOR PLATE ELEMENTS TO DIRECT BENDING STIFFNESS

The second phase of the investigation was concerned with determining the contributions of the various panels (bending panels, torsion panels and corner panels) and joints (continuity between adjacent panels) to the direct bending stiffness at the shear wall for the flat plate floor.

The percentage contributions of the various plate elements were determined by first calculating the direct stiffness coefficients at the shear wall for each of the nine model configurations show in Figure 2.5. Then, by combining the calculated stiffnesses for the various model configurations, as described in Section 2.5, the contributions of the various elements were determined. The above procedure was carried out sixteen times, for four different shear wall/total span ratios and four different shear wall shapes.

The percentage contributions of various elements are summarized in Table 5.2, for the various shear wall sizes and shapes. Figures 5.2.1 and 5.2.2 show the variation in the contributions of the various elements with shear wall shape, while Figures 5.2.3 and 5.2.4 show the variation with shear wall size.

From Figure 5.2.1 it can be seen that the contribution of the bending panel reduces rapidly, while the contribution

TABLE 5.2

PERCENTAGE CONTRIBUTION OF DIFFERENT PANELS AND JOINTS
TO THE TOTAL STIFFNESS WHEN SHEAR WALL LOADED

Model	$\frac{S_X}{S_Y}$	Shear Wall Size Total Span	Percentage Contribution of Different Panels to the Total Stiffness			Percentage Contribution of Different Joints to the Total Stiffness	
			Torsional Panels	Bending Panels	Corner Panels	Bending Joints	Torsion Joints
PS1-1	0.5	1/5	3.14	46.25	20.13	9.25	21.23
PS2-1	1.0	1/5	8.6	32.8	22.9	14.9	20.8
PS3-1	1.5	1/5	14.7	22.50	22.55	19.85	17.40
PS4-1	2.0	1/5	19.8	14.94	26.58	24.2	14.48
PS5-1	0.5	1/4	3.02	49.49	18.90	8.90	19.69
PS6-1	1.0	1/4	9.1	36.0	22.10	14.0	18.8
PS7-1	1.5	1/4	16.12	24.50	25.20	18.58	15.60
PS8-1	2.0	1/4	22.0	15.98	26.64	22.38	13.0
PS9-1	0.5	1/3	3.05	52.6	18.40	8.35	17.60
PS10-1	1.0	1/3	10.0	39.4	21.7	12.7	16.2
PS11-1	1.5	1/3	18.50	26.4	25.2	16.70	13.20
PS12-1	2.0	1/3	25.6	16.8	26.6	19.8	11.2
PS13-1	0.5	1/2.5	3.0	54.16	18.14	8.40	16.30
PS14-1	1.0	1/2.5	10.8	40.8	21.9	12.1	14.4
PS15-1	1.5	1/2.5	20.60	26.85	25.40	15.50	11.65
PS16-1	2.0	1/2.5	28.8	16.6	26.85	18.0	9.75

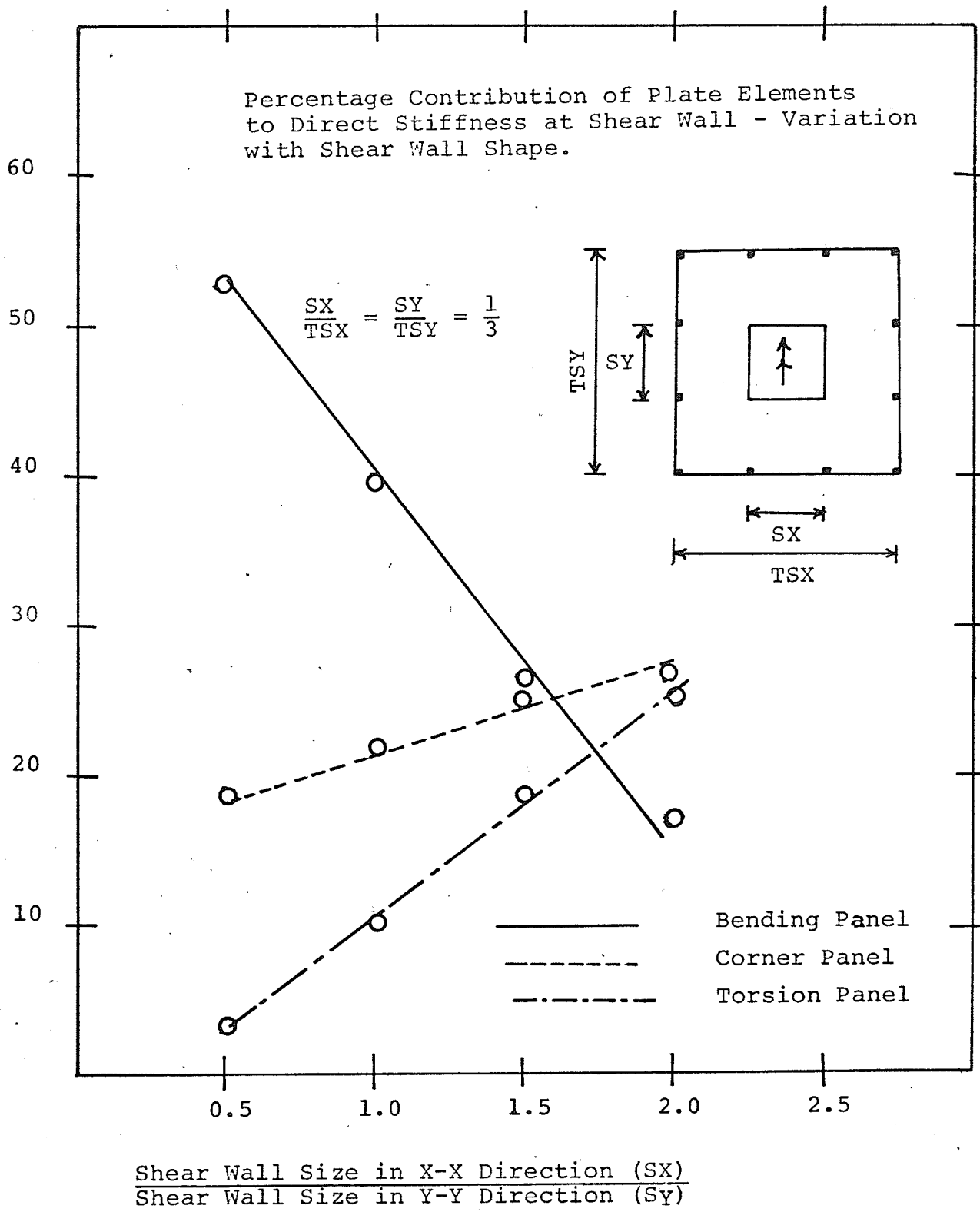


Fig. 5.2.1

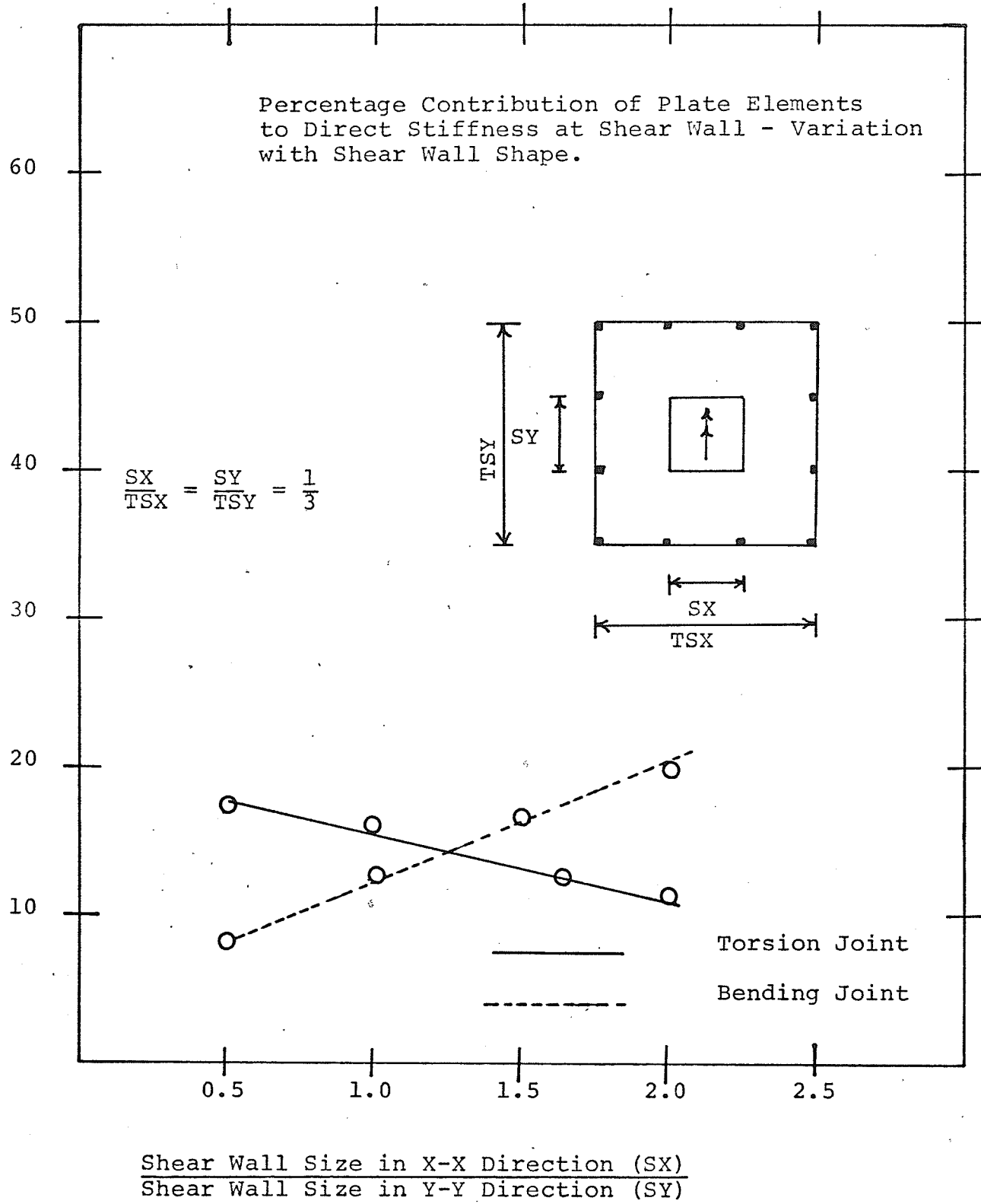


Fig. 5.2.2

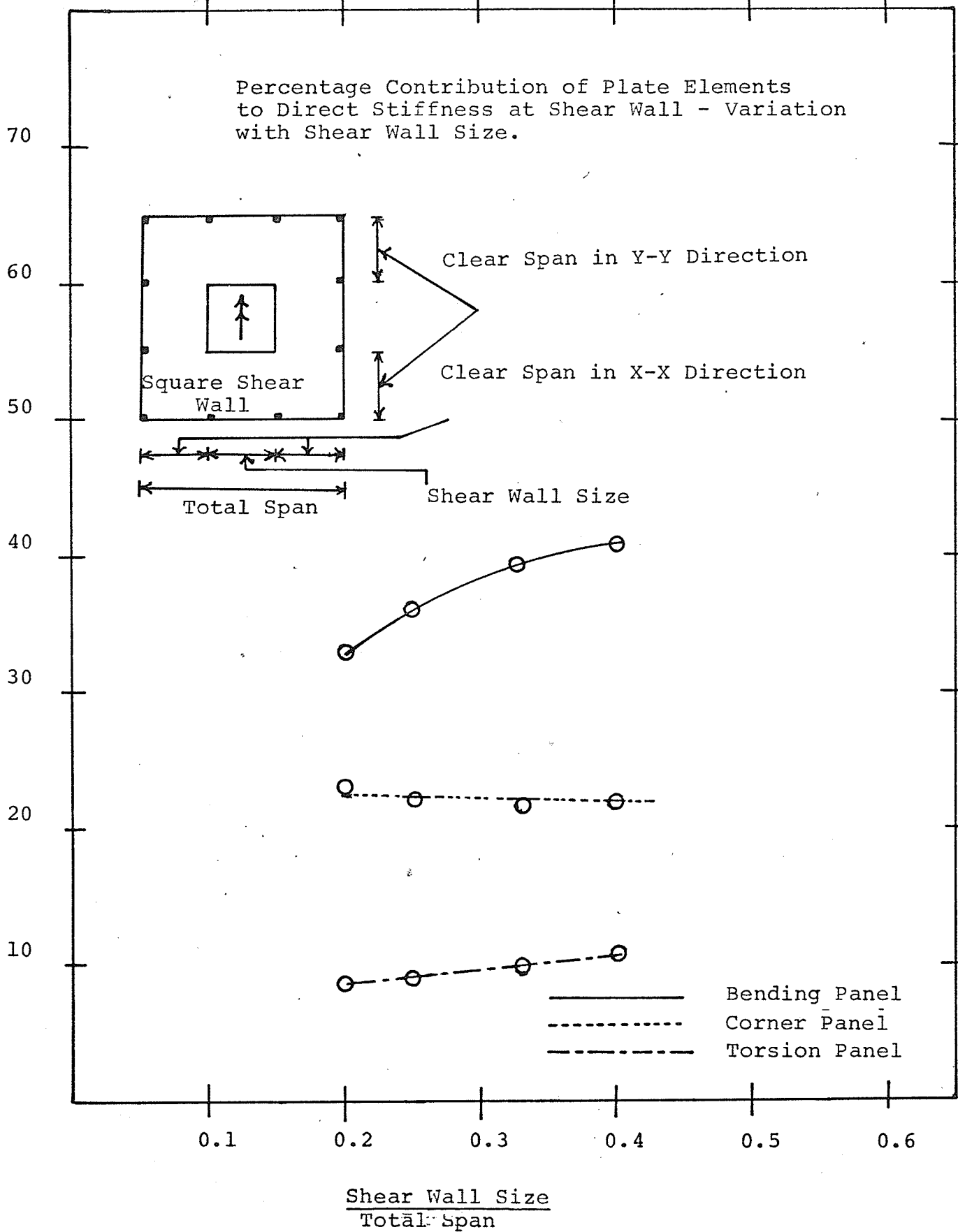


Fig. 5.2.3

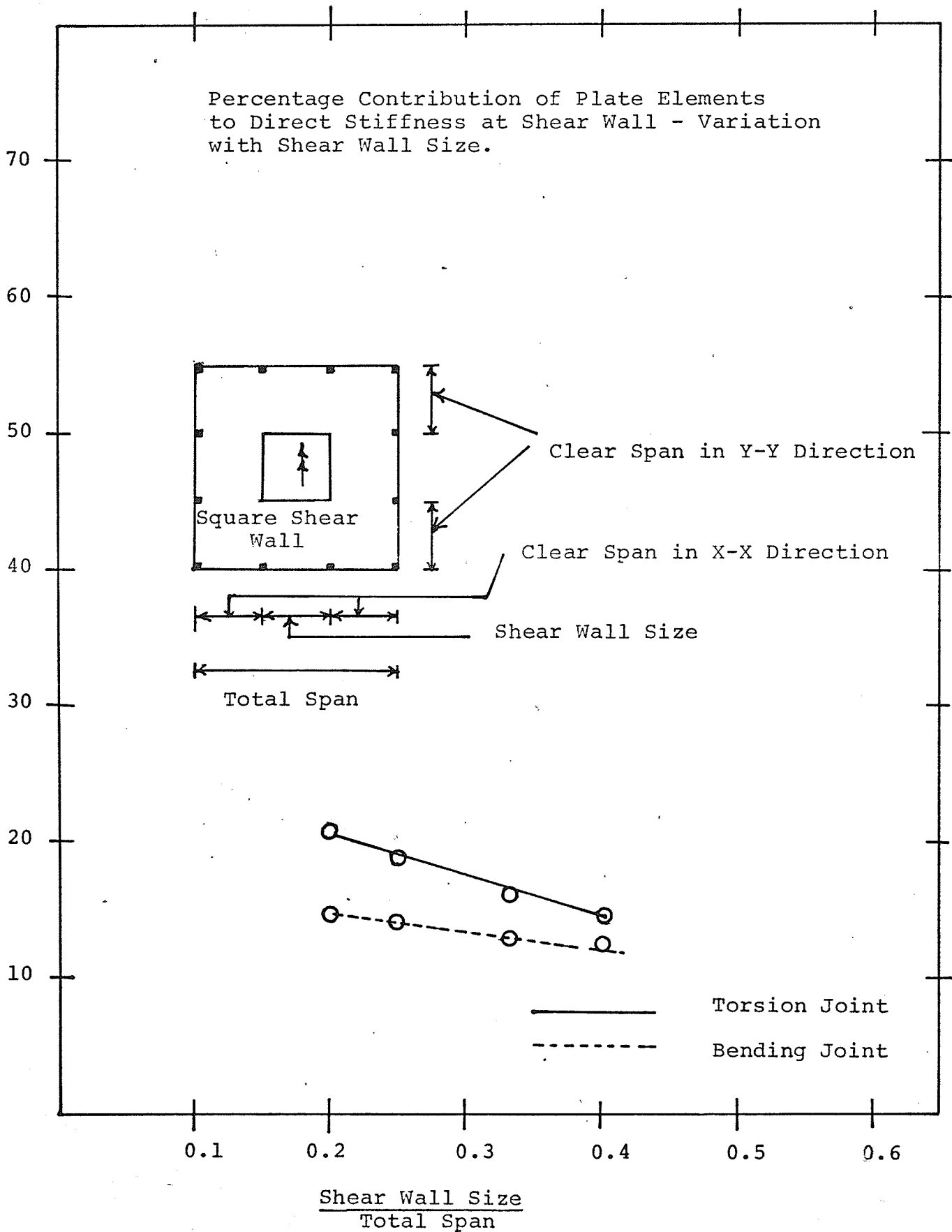


Fig. 5.2.4

of the torsional panel increases, as the shear wall dimension in the X-X direction increases. The reason is that as the shear wall dimension in the X-X direction increases, the span of the bending panel increases as does the width of the torsional panel. It is a well known fact that as the span of a panel increases, its bending stiffness gets reduced. Likewise, the torsional stiffness of a panel is increased by increasing the width of the panel. Figure 5.2.3 shows that for a floor system with a square shear wall for which the torsional panel is similar to bending panel in shape and size, the major contribution to direct stiffness comes from the bending panels while the torsion panels contribute little. It can be seen that the contribution of the corner panel is independent of the shear wall size. This is probably due to the fact that when the shear wall size was varied, the clear spans in both X-X and Y-Y directions were kept constant. Hence the dimensions of the corner panel (whose width is equal to the clear span in the Y-Y direction and whose span is equal to the clear span in the X-X direction), did not change as the shear wall size changed. It is evident from Figures 5.2.2, and 5.2.4 that the effect of continuity between the various panels is quite significant.

To corroborate the analytical results, Moiré[®] experimental models ES1 to ES7 which correspond to analytical models

PS10-1, PS10-2, PS10-3, PS10-4, PS10-5, PS10-8 and PS10-9, respectively, were tested. The experimentally and analytically obtained direct stiffness coefficients, and their ratios, are listed in Table 5.3.

It can be seen that the experimentally obtained stiffnesses are consistently lower than the analytical values. There are several probable reasons for this. Firstly, the finite element mathematical model of the structure is always stiffer than the actual structure. Secondly, it is impossible, in the experimental model to achieve truly fixed column supports. Hence the experimental model is more flexible than if it were completely fixed.

It should be expected that the analytical models would yield more accurate results for the idealized structure because of the various sources of experimental error associated with the Moire technique.

TABLE 5.3

COMPARISON OF EXPERIMENTAL AND ANALYTICAL RESULTS

Direct Stiffness Floor is Loaded by Shear Wall			Analytical
	Experimental	Analytical	Experimental
ES ₁	26666	30336	1.14
ES ₂	22850	26397	1.15
ES ₃	22850	25400	1.11
ES ₄	13333	14519	1.09
ES ₅	20000	22411	1.12
ES ₆	10000	11934	1.19
ES ₇	2580	3032	1.17

CHAPTER VI

ILLUSTRATIVE EXAMPLES

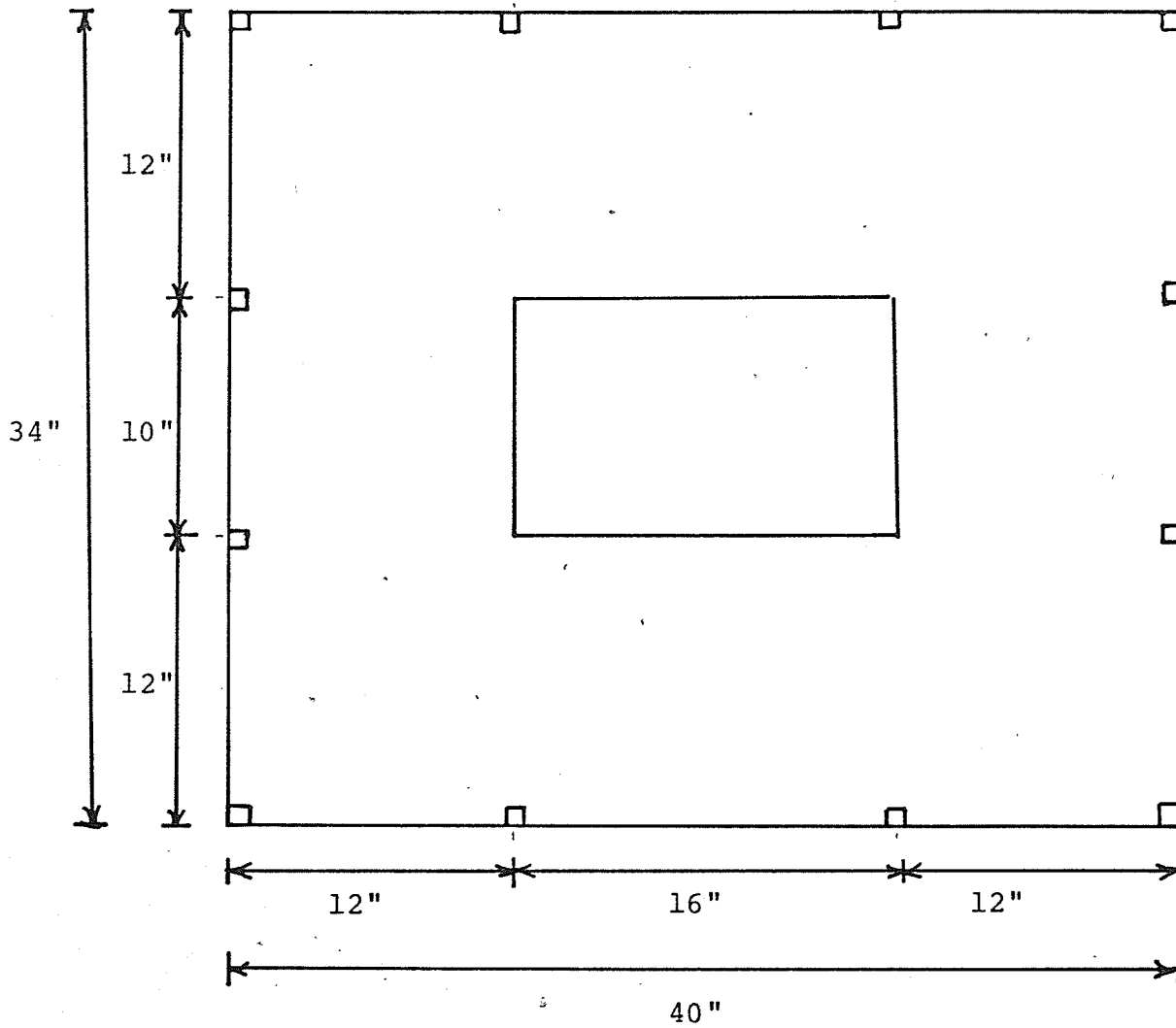
In this chapter, examples are given to illustrate the use of the analytically and experimentally obtained information including multiplying factors defined in this study, in calculating stiffness coefficients for a variety of flat plate floor systems.

6.1 Stiffness Coefficients For Basic Flat Plate Floor System

In this section, the use of the graphs shown in Figures 4.1.1, 4.1.2...4.3.3, in calculating the values of stiffness coefficients is illustrated with the help of two examples. In each example, stiffness values obtained by making use of the graphs are compared with those obtained by direct finite element analysis.

EXAMPLE 1

It is desired to calculate the direct stiffness coefficient at the shear wall and external column and the carry over stiffness coefficient for the floor system whose $\frac{1}{24}$ scale model is shown in Fig. 6.1.1. The procedure is to firstly obtain the values of the stiffness coefficients for model P1 from table 4.1 and then to modify them to account for differences in column size, shear wall size and shape, etc. to obtain the stiffness values for the floor system considered. The stiffness coefficients for model P1 from table 4.1 are;



Floor Thickness = 0.25 inches

Column Size = 0.75 inch square

All columns are of same size.

Fig. 6.1.1

Direct bending stiffness at shear wall, $K_{SS}=28915$ lb.inch.

Direct bending stiffness at column, $K_{CC}=1562$ lb. inch.

Carry-over bending stiffness coefficient $K_{SC}=K_{CS}=1604$ lb.inch.

Correction For Clear Span

Since the clear span for model P1 is 9 inches while that for the structure considered is 12 inches, the dimensions of the model P1, except for the floor thickness, are multiplied by the ratio $\frac{\text{Clear Span of the floor system in Fig. 6.1.1}}{\text{Clear Span of the floor system of model P1}} = \frac{12}{9}$

A modified "basic floor system" with the same slab thickness as model P1 but with the following dimensions, is obtained.

- (a) Shear Wall size = 12 inches square
- (b) Total span in both directions= 36 inches
- (c) Clear span in both directions= 12 inches
- (d) Column size = 0.666 inches square

Let this model be designated P₁'. Since, the bending stiffness of a plate panel does not change if all of the in-plane dimensions of the panel are changed in the same proportions, the stiffness coefficients of the model P₁' will be the same as those for model P1. Therefore, no correction is required for the stiffness values in this step.

Correction For Shear Wall Size

The shear wall size for model P₁' is next changed from 12 inches square to 10 inches square. Let this new model be designated P₁'.

The dimensions of P_1'' will be

- (a) Shear wall size=10 inch square
- (b) Total span in both directions=34 inches.
- (c) Clear span in both directions=12 inches.
- (d) Column size = 0.666 inches.

Hence,

the value of $\frac{\text{Shear Wall Size (SH)}}{\text{Total Span (TS)}}$ for model P_1' is $\frac{1}{3} = 0.333$

the value of $\frac{\text{SH}}{\text{TS}}$ for model P_1'' is $\frac{1}{3.4} = 0.294$

Thus,

from graph 4.2.1, the ratio of the value of K_{SS} corresponding to $\frac{\text{SH}}{\text{TS}} = 0.294$ to the value of K_{SS} corresponding to $\frac{\text{SH}}{\text{TS}} = 0.333$ is = 0.80

Therefore,

The value of K_{SS} for model $P_1'' = 28915.66 \times 0.80 = 23150.0$

Similarly, the value of direct stiffness at the exterior column for P_1'' is obtained by applying a correction for shear wall size with the help of graph in Fig. 4.2.2, to that for P_1' .

The value of K_{CC} for $P_1'' = 1562.50 \times 0.97 = 1519.0$

Like wise, the value of carry-over stiffness for model P_1' is modified with the help of graph 4.2.3, to obtain that for P_1'' .

The value of $K_{SC} = K_{CS}$ for $P_1'' = 1604.55 \times 0.875 = 1404.0$

Correction For Shear Wall Shape

The dimensions of the shear wall for model P_1'' are changed from 10" x 10" to 10" x 16". Let this new model be designated P_1''' .

The dimensions for P_1''' will thus be

- (a) Shear wall size in y-y direction is $SX=16$ inches.
- (b) Shear wall size in x-x direction is $SY=10$ inches.
- (c) Total span in x-x direction is $TSX = 40$ inches.
- (d) Total span in y-y direction is $TSY = 34$ inches.
- (e) Clear span in both directions = 12 inches.
- (f) Column size is 0.666 inch square.

Thus,

The value of $\frac{SX}{SY}$ for $P_1'' = 1.0$

The value of $\frac{SX}{SY}$ for $P_1''' = 1.6$

From graph 4.3.1, the ratio of the value of K_{SS} corresponding to $\frac{SX}{SY} = 1.6$ to the value of K_{SS} for $\frac{SX}{SY} = 1.0$ is = 1.67.

Therefore,

The value of K_{SS} for $P_1''' = 23150.0 \times 1.67 = 38600.0$

As indicated by graph 4.3.2 the value of K_{CC} is independent of shear wall shape.

Therefore,

the value of K_{CC} for $P_1''' = 1519.0$

Next,

From graph 4.3.3 the ratio of the value of K_{SC} or K_{CS} for $\frac{SX}{SY} = 1.6$ to the value of K_{SC} or K_{CS} for $\frac{SX}{SY} = 1.0$ is = 1.40

Therefore,

the value of K_{SC} or K_{CS} for $P_1''' = 1404 \times 1.40 = 1969.0$.

Correction For Column Size

The column size is next changed from 0.666 inches square to 0.75 inches square. Let the new model thus obtained be designated P_1^{1V} .

The dimensions of model P_1^{1V} are those for the floor system in Fig. 6.1.1.

Next,

The value of $\frac{\text{column size (C)}}{\text{clear span (S)}}$ for model P_1''' is $\frac{0.666}{12} = 0.055$

The value of $\frac{\text{column size (C)}}{\text{clear span (S)}}$ for P_1^{1V} is $\frac{0.75}{12} = 0.0625$

The values of the stiffness coefficients for P_1''' are thus modified for column size with the help of graphs in Figures 4.1.1, 4.1.2 and 4.1.3 to obtain the values for model P_1^{1V} .

The final values of stiffness coefficients for model P_1^{1V} , the floor system shown in Fig 6.1.1, are thus

(a) Direct Bending Stiffness at Shear Wall,

$$\begin{aligned} K_{SS} &= 38600.0 \times 1.01 \\ &= 39000.0 \text{ lb. inch.} \end{aligned}$$

(b) Direct Bending Stiffness at column

$$\begin{aligned} K_{CC} &= 1519.0 \times 1.05 \\ &= 1590.0 \end{aligned}$$

(c) Carry-over Bending Stiffness

$$\begin{aligned} K_{SC} = K_{CS} &= 1969.0 \times 1.03 \\ &= 2020.0 \text{ lb. inch.} \end{aligned}$$

The values of the direct and carry-over stiffness coefficients for the structure in Fig. 6.1.1 were calculated using finite element analysis. The values obtained are compared with the corresponding values calculated using the graphs,

as described above, in Table 6.1(a). The stiffness coefficients for the prototype of the model in Fig. 6.1.1 are obtained by multiplying the corresponding values for the model by the cube of the scale of the model.

Example 2 As a second example, a model of the floor system similar to that shown in Fig. 6.1.1 is considered. The dimensions of this model are,

- (a) Shear wall size in x-x direction = 10 inches.
- (b) Shear wall size in y-y direction = 12 inches.
- (c) Total span in x-x direction = 40 inches.
- (d) Total span in y-y direction = 42 inches.
- (e) Clear span in both direction = 15 inches
- (f) Column size = 1 inch square.
- (g) Floor thickness = 6 inches.

The values of the stiffness coefficients for this floor system are obtained using the graphs given in Figures 4.1.1 ...4.3.3, as explained in example 1, and are compared with those obtained directly, by finite element analysis in Table 6.1(b).

Tables 6.1(a) and 6.1(b) show a good agreement between the values obtained by making use of graphs and those obtained by finite element analysis.

TABLE 6.1 (a)
 STIFFNESS COEFFICIENTS FOR THE FLOOR SYSTEM OF EXAMPLE 1

Stiffness Coefficient	Values obtained from graphs	Values obtained by finite-element Analysis	Difference	Percentage Difference
Direct Stiffness at shear wall	39,000.0	38,277.51	722.49	1.9%
Direct stiffness at column	1590.0	1553.28	36.72	2.3%
carry-over stiffness	2000.0	1902.76	97.24	5.1%

TABLE 6.1 (b)

STIFFNESS COEFFICIENTS FOR THE FLOOR SYSTEM OF EXAMPLE 2

Stiffness Coefficients	Values obtained From Graphs	Values obtained by finite element Analysis	Difference	Percentage Difference
Direct Stiffness at shear wall	18,500.0	18,624.85	124.85	0.70%
Direct stiffness at column	1570.0	1569.69	0.31	0.02%
carry-over stiffness	1230.0	1248.22	18.22	1.46%

6.2 Accuracy of Multiplying Factors

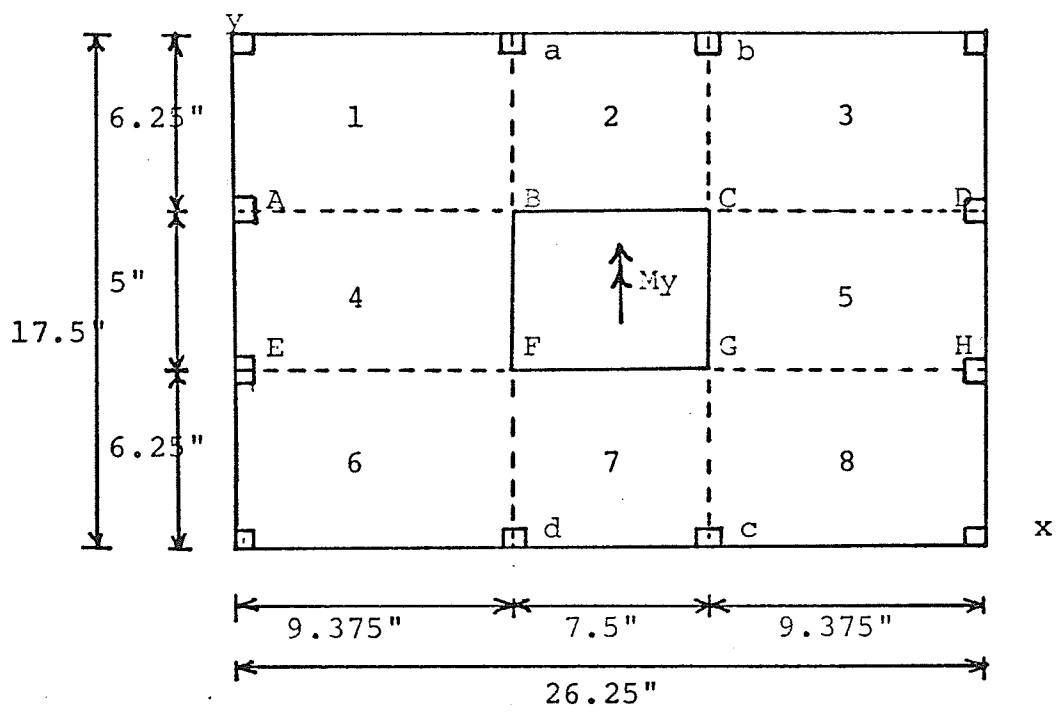
In this section two examples are presented to give an indication of the accuracy with which the direct bending stiffness coefficient at shear wall can be calculated by using the multiplying factors, listed in tables 4.5(a), 4.5(b), ... 4.5(e).

Example 3

In this example, the direct bending stiffness at the shear wall for the floor system shown in Fig. 6.2.1, is calculated with the help of multiplying factors. The contribution of different panels and joints to the total stiffness, obtained by making use of multiplying factors is compared with those obtained by direct finite element analysis.

The floor system in Fig 6.2.1 can be subdivided into eight different types of panels as described in section 2.4. Panels 1, 3, 6 and 8 are corner panels, 2 and 7 are torsional panels and 4 and 5 are bending panels. In addition, joints AB, CD, EF and GH are bending joints (joint between corner panels and bending panels), while joints aB, bC, dF and cG are torsion joints (Joints between corner panels and torsion panels). The contribution of the different panels and joints to the direct bending stiffness coefficient at shear wall is obtained employing multiplying factors as explained below.

Firstly, the value of the shear wall size to total span ratio, $(\frac{SH}{TS})$, and the ratio of shear wall dimension in the



Thickness of Slab = $\frac{1}{4}$ inch

All columns are of same size = 12" x 12"

Fig. 6.2.1

the x-x direction to that in the y-y direction, $(\frac{S_X}{S_Y})$, are calculated. The values of the multiplying factors corresponding to these ratios, are obtained from tables 4.5(a) ...4.5(e). For the floor system shown in Fig. 6.2.1

$$\frac{S_H}{T_S} = \frac{1}{3.5}, \quad \frac{S_X}{S_Y} = 1.5$$

and the values of the multiplying factors from tables 4.5(a) to 4.5(e) are found to be :

$$F_T = 2.033$$

$$F_{TC} = 0.162$$

$$F_B = 2.488$$

$$F_{BC} = 0.089$$

$$F_C = 0.959$$

Next, the values of KEB, the bending stiffness of a beam whose width, depth and span are equal to the width, thickness and span respectively of the bending panel, KEC, the bending stiffness of a beam whose width, depth and span are equal to those of the corner panel and KET, the torsional stiffness of a rectangular bar whose width, depth and span are equal to those of the torsional panel, are calculated as described in section 2.5.

For the floor system shown in Fig. 6.2.1, the span of the bending panel is $L_B = 9.375$ inches, the span of the corner panel is $L_C = 9.375$ inches and the span of the torsional panel is $L_T = 6.25$ inches.

The widths of the torsional, corner and bending panels are 7.5, 6.25 and 5 inches respectively. The modulus of elasticity, E , for the material is assumed to be 441000.0 PSI.

Thus,

$$K_{EB} = \frac{4EI}{L_B} = \frac{4 \times 441000.0 \times \frac{1}{12} \times 5 \times (0.25)^3}{9.375} = 1222.2 \text{ lb. inch,}$$

$$K_{EC} = \frac{4EI}{L_C} = \frac{4 \times 441000.0 \times \frac{1}{12} \times 6.25 \times (0.25)^3}{9.375} = 1530.0 \text{ lb. inch, and}$$

$$K_{ET} = (I_1 b t^3 G) / L_T$$

where,

b=width of torsional panel = 7.5"

c=thickness of the panel = 0.25"

$$G = \frac{E}{2(1+\nu)} = \frac{441000.0}{2(1+0.3)} = 163333.4 \text{ lb./ inch}^2$$

= shearing modulus for material

$$I_1 = \frac{1}{3}(1 - 0.63 \frac{t}{b}) = \frac{1}{3} (1 - 0.36 \times \frac{0.25}{7.5})$$

$$0.333 \text{ in.}^4$$

$$\text{Therefore } K_{ET} = \frac{0.333 \times 7.5 \times (0.25)^3 \times 163333.4}{6.25} \\ = 1020.0 \text{ lb. inch.}$$

Next, the contributions of the various panels and joints, to the total stiffness is calculated as explained in section 2.5.

The contribution of a bending panel is

$$K_B = F_B \times K_{EB} \\ = 2.488 \times 1222.2 \\ = 3040.0 \text{ lb. inch.}$$

The contribution of a torsional panel is

$$K_T = F_T \times K_{ET} \\ = 2.033 \times 1020 \\ = 2070.0 \text{ lb. inch}$$

The contribution of a corner panel is

$$\begin{aligned} K_C &= F_C \times K_{EC} \\ &= 0.959 \times 1530 \\ &= 1470.0 \text{ lb. inch.} \end{aligned}$$

The contribution of a bending joint (a joint between a corner and a bending panel) is

$$K_{BC} = \frac{F_{BC} \times L_B \times t^3 \times E}{B}$$

where,

B = width of bending panel = 5.0 inches

t = Floor thickness = 0.25 inches

therefore,

$$K_{BC} = \frac{0.089 \times 9.375 \times 0.25^3 \times 441000.0}{5.0} = 1150.0$$

Finally,

the contribution of a torsion joint (a joint between a corner and a torsional panel) is

$$\begin{aligned} K_{TC} &= \frac{F_{TC} \times L_T \times t^3 \times E}{b} \\ &= \frac{0.162 \times 6.25 \times 0.25^3 \times 441000.0}{7.5} \\ &= 928.0 \end{aligned}$$

The floor system shown in Fig 6.2.1 consists of four corner panels, two bending panels, two torsional panels, four torsion joints and four bending joints.

Thus, the total direct stiffness of the floor plate at the shear wall is

$$\begin{aligned} &= 4 \times K_C + 2 \times K_B + 2 \times K_T + 4 \times K_{BC} + 4 \times K_{TC} \\ &= 4 \times 1470 + 2 \times 3040 + 2 \times 2070 + 4 \times 1150.0 \\ &\quad + 4 \times 928.0 \\ &= 24212.0 \text{ lb. inch.} \end{aligned}$$

The contributions of different panels and joints to the total stiffness for the floor system shown in Fig. 6.2.1, obtained with the help of the multiplying factors and by finite element analysis are given in table 6.2(a)

Table 6.2(a)

CONTRIBUTION OF DIFFERENT PANELS AND JOINTS
TO THE TOTAL STIFFNESS

Different Panels and Joints	Obtained By Finite Elem. Procedure	Obtained From Multiplying Factors	Difference	Percentage Difference
Two Bending Panels	6412.66	6080.0	332.66	5.18%
Two Torsional Panels	4178.417	4140.0	38.47	0.92%
Four Corner Panels	6167.45	5880.10	287.45	4.65%
Four Bending Joints	4393.0	4600.0	207.0	4.7%
Four Torsional Joints	3479.0	3712.0	233.0	6.6%
Total	24630.527	24212.0	418.52	1.7%

Example 4

As a second example, a model that is identical to that shown in Fig 6.2.1, except for the plate thickness, is considered. The floor thickness for the model of examples 4 is 0.3 inches. The values of the contributions for different panels and joints to the total stiffness is calculated with the help of the multiplying factors, as in example 3. They are also compared, in table 6.2(b) with the values obtained by direct finite element analysis.

Table 6.2(b)

CONTRIBUTION OF DIFFERENT PANELS AND JOINTS
TO THE TOTAL STIFFNESS

Different Panels and Joints	Obtained By Finite Elem. Procedure	Obtained from multiplying Fractors	Difference	Percentage Difference
Two Bending Panels	10909.0	10500.0	409.0	3.75
Two Torsional Panels	7180.0	7160.0	20.0	0.278
Four Corner Panels	10548.5	10160.0	388.5	3.68
Four Bending Joints	7598.3	7900.0	301.7	4.0%
Four Torsional Joints	6128.3	6400.0	271.7	4.4%
TOTAL	42364.0	42120.0	244.0	1.05%

Tables 6.2(a) and 6.2(b) show that the values of the contributions of various panels to the total direct stiffness at shear wall, obtained with the help of multiplying factors, are quite close to those obtained by direct finite element analysis.

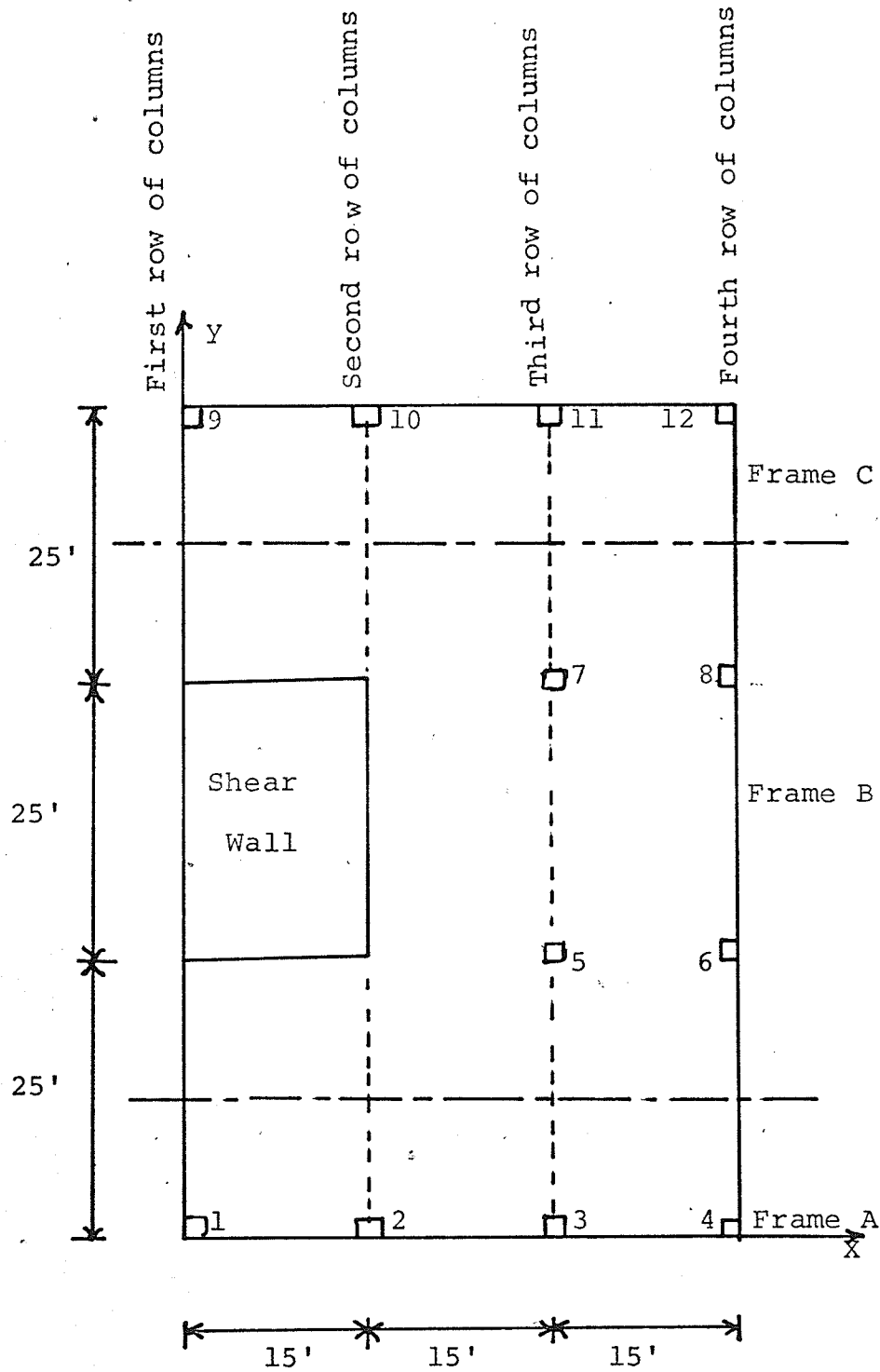
6.3 Lateral Load Analysis of a Frame Work

In this section, an example is given to demonstrate the use of the multiplying factors developed in this study, in the lateral load analysis of a multistorey flat-plate shear wall structure. The multiplying factors are used to determine direct stiffness coefficients for the shear wall. Procedures formulated in previous studies are used to determine the direct stiffness coefficients at the columns, as well as the carry over stiffness coefficients.

Example 5

In this example, a typical intermediate floor of a tall building shown in Fig 6.3.1 is considered. A common procedure in the lateral load analysis of flat plate multispan structure is to subdivide the whole structure into a series of parallel planar frames. Each such planar frame is analyzed separately and then the frames are combined in such way that compatibility and equilibrium conditions are fully satisfied.

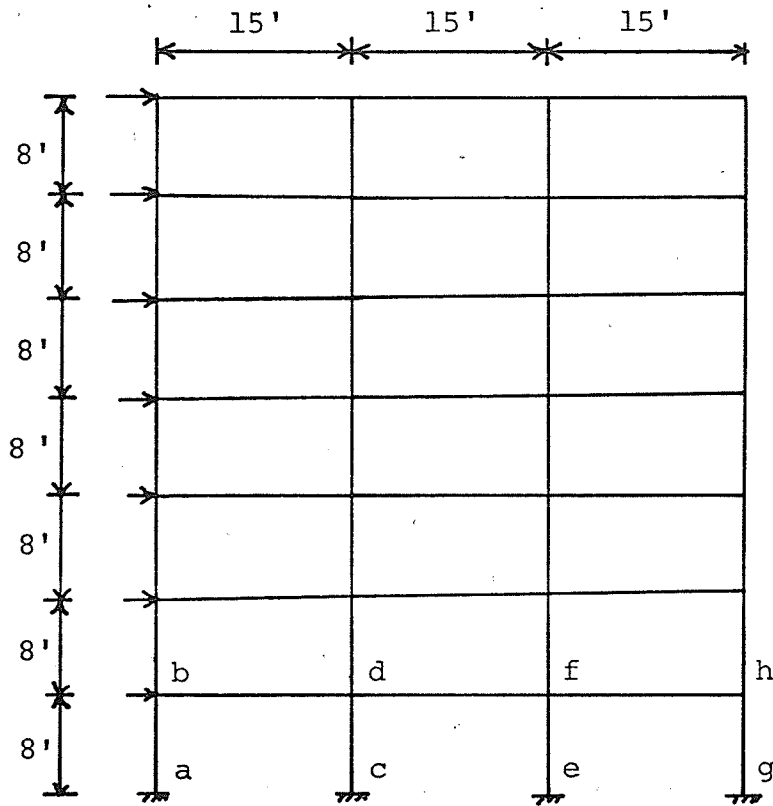
To carry out the lateral load analysis of the considered structure, the structure is subdivided into three parallel planar frames, A, B and C, as illustrated in Fig 6.3.1. Frame A, which is identical to frame C, and frame B are shown in elevation in Figures 6.3.2 and 6.3.3 respectively. The determination of the bending stiffness coefficients for each structural element in each frame is essential for the analysis.



All columns are of same size = 1' x 1'

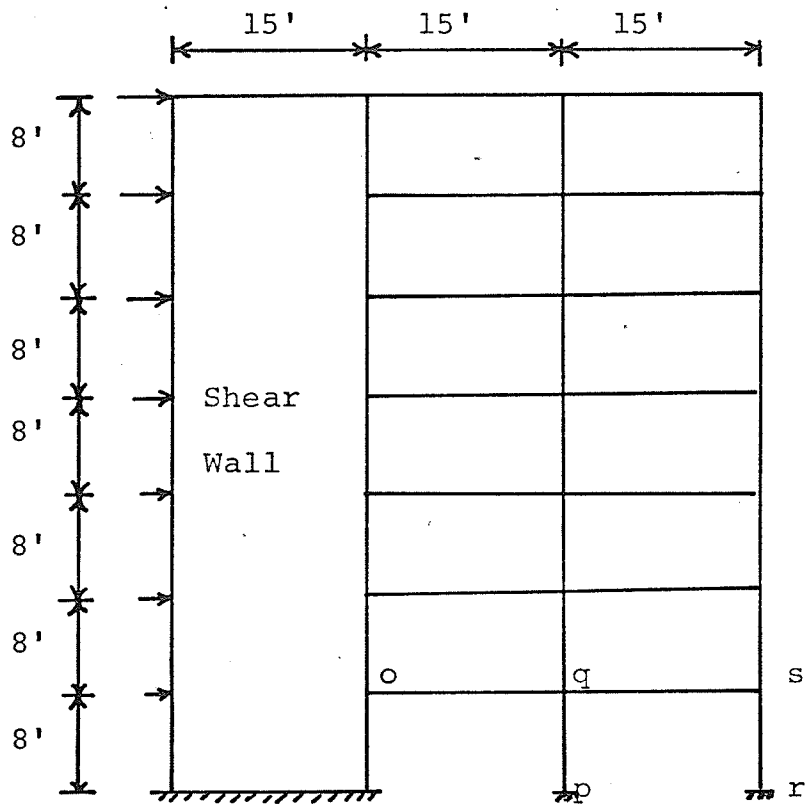
Thickness of Floor Slab = 6 inches

Fig. 6.3.1



Elevation of Planar Frame A

Fig. 6.3.2



Elevation of Planar Frame B

Fig. 6.3.3

6.3.1 Bending Stiffness Coefficients For the Floor Systems

Supported Only On Columns

The floor system of the planar frame A is supported only on columns and does not include any shear walls. Let it be assumed that the sizes of the columns, thickness of the slabs and floor plan are the same for each storey of the building. Calculations for the bending stiffness coefficients for the structural members in the first storey only are given below. In order to simplify the calculations, the moment of inertia of the uncracked sections has been used and at the same time the effects of reinforcement have been neglected.

Direct Bending Stiffness Coefficients

In Fig 6.3.2, the direct bending stiffness coefficients for columns ab, cd, ef and gh are equal to those for columns 1, 2, and 3, 4 respectively in the floor plan shown in Fig 6.3.1. Since all columns for the floor system shown in Fig 6.3.1 are of the same size, the stiffnesses of columns ab, cd, ef, and gh will also be equal.

Each column is 1 foot square. The moment of inertia of each column about the bending axis is

$$I = \frac{1}{12} \times (12) \times (12)^3 = 1728 \text{ inch}^4$$

The modulus of elasticity for concrete is assumed to be

$$4 \times 10^6 \text{ PSI.}$$

The storeyheight is 96 inches.

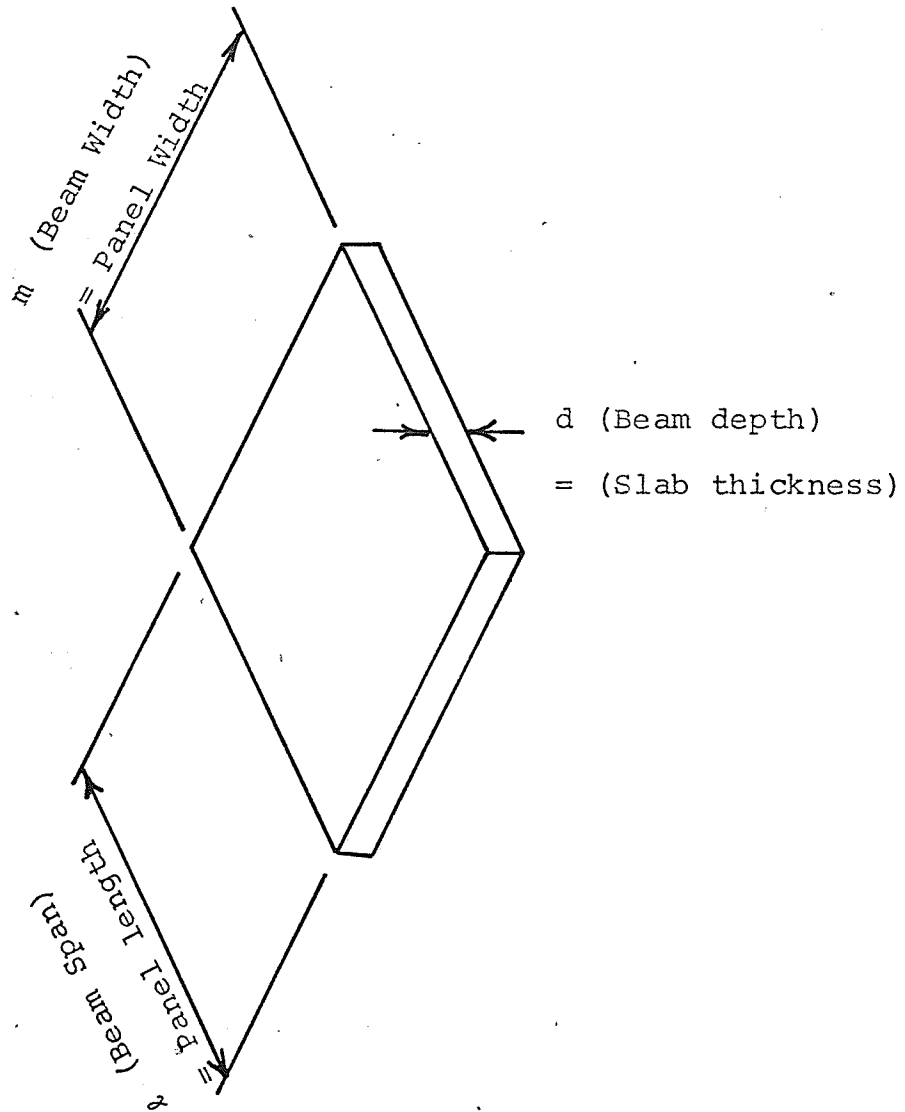
Therefore, the direct bending stiffness coefficient for each

column is

$$\begin{aligned}
 &= \frac{4 \times E \times I}{\text{storey height}} \\
 &= \frac{4 \times 4 \times 10^6 \times 1728}{96} \\
 &= 288 \times 10^6 \text{ lb. inch.}
 \end{aligned}$$

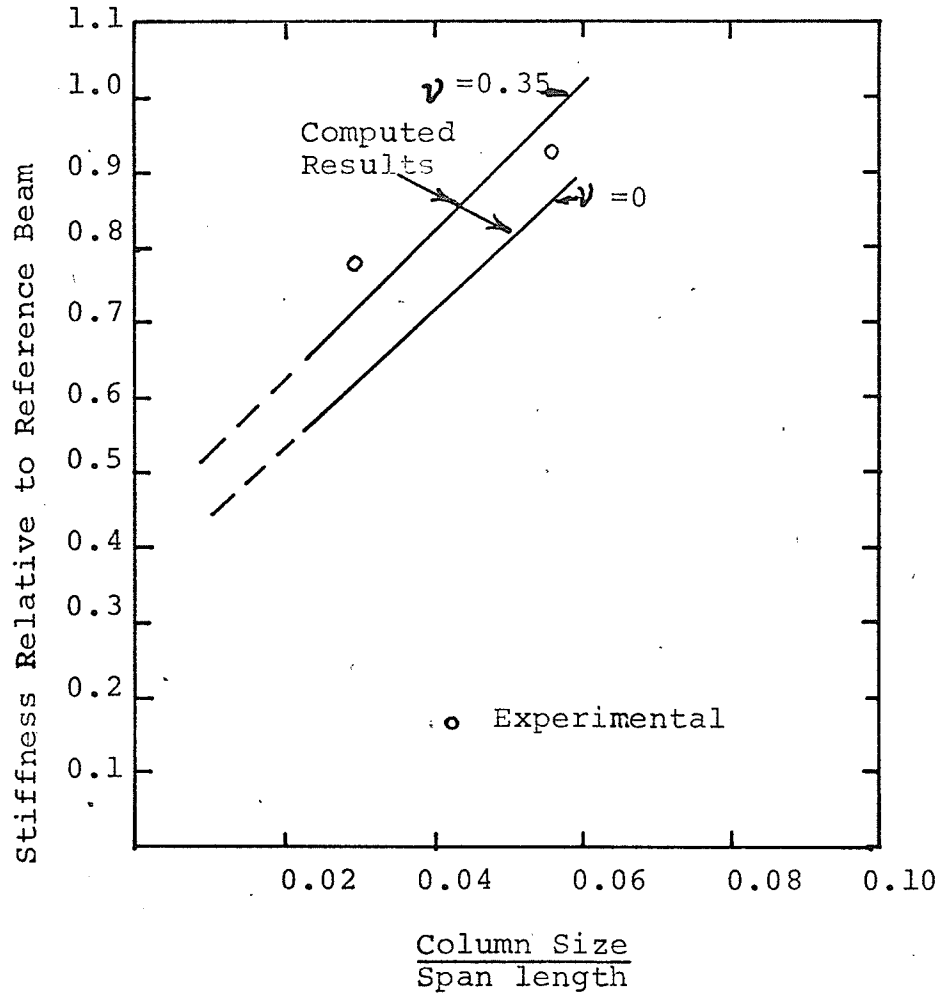
Next, the structural members bd, df and fh are assumed to be identical and to represent the floor slab between columns 1 and 2, 2 and 3, 3 and 4 respectively, in the floor system shown in Fig 6.3.1. Thus the direct bending stiffness of the floor member at b in Fig 6.3.2, will be equal to that at h, the value at d will be equal to that at f, and the total stiffness of the floor members at d or f will be double that at b or h. The reason is that at d or f two floor members frame into each of joints d and f, while one structural member frames into each of joints b and h. As the floor system in the planar frame A is supported on columns only, the concept of a reference beam, used by Carpenter⁽¹⁰⁾ can be employed. Carpenter defined a reference beam, as shown in Fig 6.3.4, as a hypothetical wide, shallow structural member whose width, depth and span are equal to the width, thickness and length of the flat plate floor panel. He presented a graph of the variation of the stiffness of the floor panel relative to that of the reference beam with the ratio of column size to span length. This graph has been reproduced in Fig 6.3.5.

The dimensions of the reference beam for member bd in Fig 6.3.2 are:



Reference Beam

Fig. 6.3.4



Variation of Direct Stiffness relative to Reference Beam
Fig. 6.3.5

width of reference beam, $m = 12.5$ feet

span of reference beam, $l = 15$ feet

depth of reference beam, $d = 6$ inches

Therefore,

The direct bending stiffness of the reference beam is

$$\frac{4 \times E \times m \times d^3}{l \times 12} = \frac{4 \times 4 \times 10^6 \times 12.5 \times 12 \times 6^3}{15 \times 12 \times 12}$$

$$= 24.0 \times 10^7 \text{ lb. inch.}$$

Next,

$$\frac{\text{column size}}{\text{span length}} = \frac{1}{15} = 0.066.$$

Thus, from the graph in Fig 6.3.5, the ratio of the direct stiffness of the floor plate to that of the reference beam for the present case is 1.0.

Therefore,

the direct bending stiffness at b or h in Fig 6.3.2 is $24.0 \times 10^7 \times 1.0 = 24.0 \times 10^7$ lb. inch.

Consequently,

the direct bending stiffness at d or f in Fig 6.3.2 is 48.0×10^7 lb. inch.

Carry-Over Bending Stiffness Coefficients

Since columns ab, cd, ef and gh in Fig 6.3.2 are prismatic members, the value of the carry-over bending stiffness coefficient column is

$$= \frac{2 \times E \times I}{\text{Storey height}}$$

$$= \frac{2 \times 4 \times 10^6 \times 1728}{96}$$

$$= 144 \times 10^6 \text{ lb. inch.}$$

As yet no direct information is available concerning carry-over bending stiffness coefficients for floor systems. However, carry-over factors for floor systems such as that in frame A, have been presented by carpenter⁽¹⁰⁾. He has presented a graph relating carry-over factors to the ratio of column size to span length.

For the floor system of frame A

$$\frac{\text{column size}}{\text{span length}} = \frac{1}{15} = 0.0666.$$

From Carpenter's graph, reproduced in Fig 6.3.6, the value of the carry-over factor is 0.32.

Therefore,

the carry over bending stiffness coefficient for members bd, df or fh, in Fig 6.3.2, is equal to the direct bending stiffness coefficient times the carry-over factor

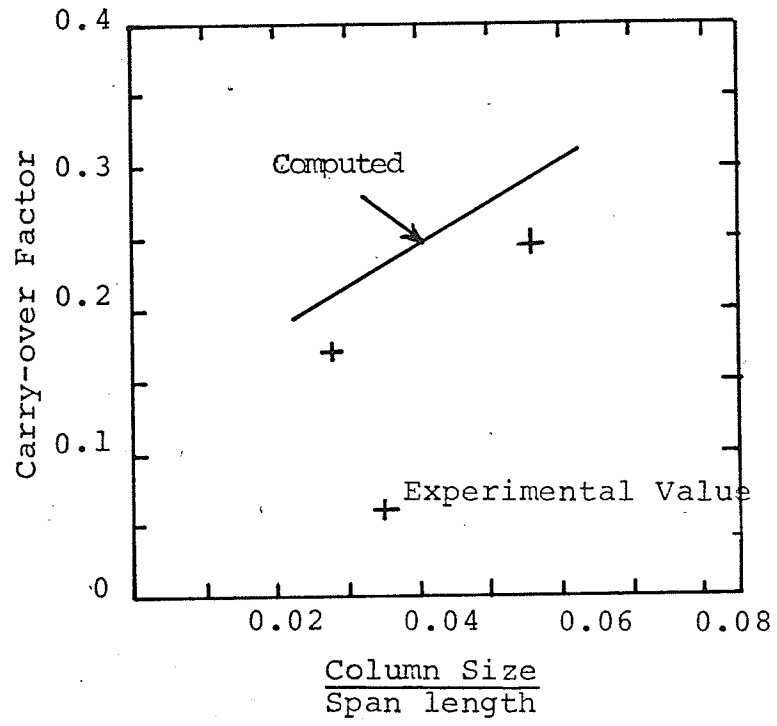
$$= 24.0 \times 10^7 \times 0.32$$

$$= 7.67 \times 10^7 \text{ lb. inch.}$$

6.3.2 Bending Stiffness Coefficients For Floor Systems

With Shear Wall

The floor system of planar frame B has a box type shear wall and columns located on a rectangular grid, as shown in Fig 6.3.1. Structural member oq of the frame B, shown in Fig 6.3.3, represents the floor slab between the first and third rows of columns in Fig 6.3.1, while member qs in Fig 6.3.3 represents the floor slab between the third and fourth rows.



Carry-Over Factor
of Slab Element

Fig. 6.3.6

Direct Bending Stiffness Coefficients

In Fig 6.3.3, the direct bending stiffness coefficient for columns pq and rs is equal to the sum of stiffnesses of columns 5 and 7, 6 and 8, respectively, in the floor system shown in Fig 6.3.1. Since all columns in the floor system shown in Fig 6.3.1 are assumed to be the same size, the stiffnesses for columns pq and rs also be the same.

The size of each column is 1 ft. square. The moment of inertia of each column about its bending axis is

$$I = \frac{1}{12} \times 12 \times (12)^3$$

$$= 1728 \text{ inch.}^4$$

The modulus of elasticity for concrete is again

$$4 \times 10^6 \text{ PSI}$$

Also, the length of each column is 96 inches.

Therefore,

the direct bending stiffness coefficient for each

$$\text{column is } = \frac{4 \times E \times I}{\text{span}}$$

$$= \frac{4 \times 4 \times 10^6 \times 1728}{96}$$

$$= 288 \times 10^6 \text{ lb. inch.}$$

Thus, the direct bending stiffness coefficient for structural member pq or rs in Fig 6.3.3 is

$$= 2 \times 288 \times 10^6$$

$$= 576 \times 10^6 \text{ lb. inch.}$$

Structural member qs of planar frame B shown in Fig 6.3.3 represents a floor system supported on columns only. The direct bending stiffness coefficient can be calculated

using the concept of the reference beam as explained in section 6.3.1. The dimensions of the reference beam for member qs in Fig 6.3.3 will be:

width of reference beam, $m = 50$ feet

span of reference beam, $l = 15$ feet

depth of the reference beam, $d = 6$ inches

Therefore ,

the direct bending stiffness of the reference beam is

$$\frac{4 \times E \times m \times d^3}{l \times 12} = \frac{4 \times 4 \times 10^6 \times 50 \times 12 \times 6^3}{15 \times 12 \times 12}$$

$$= 96.0 \times 10^7 \text{ lb. inch.}$$

Next,

$$\frac{\text{column size}}{\text{span length}} = \frac{1}{15} = 0.066.$$

From the graph in Fig 6.3.5, the value of the ratio of the direct stiffness of the floor plate to that of the reference beam is 1.0

Therefore,

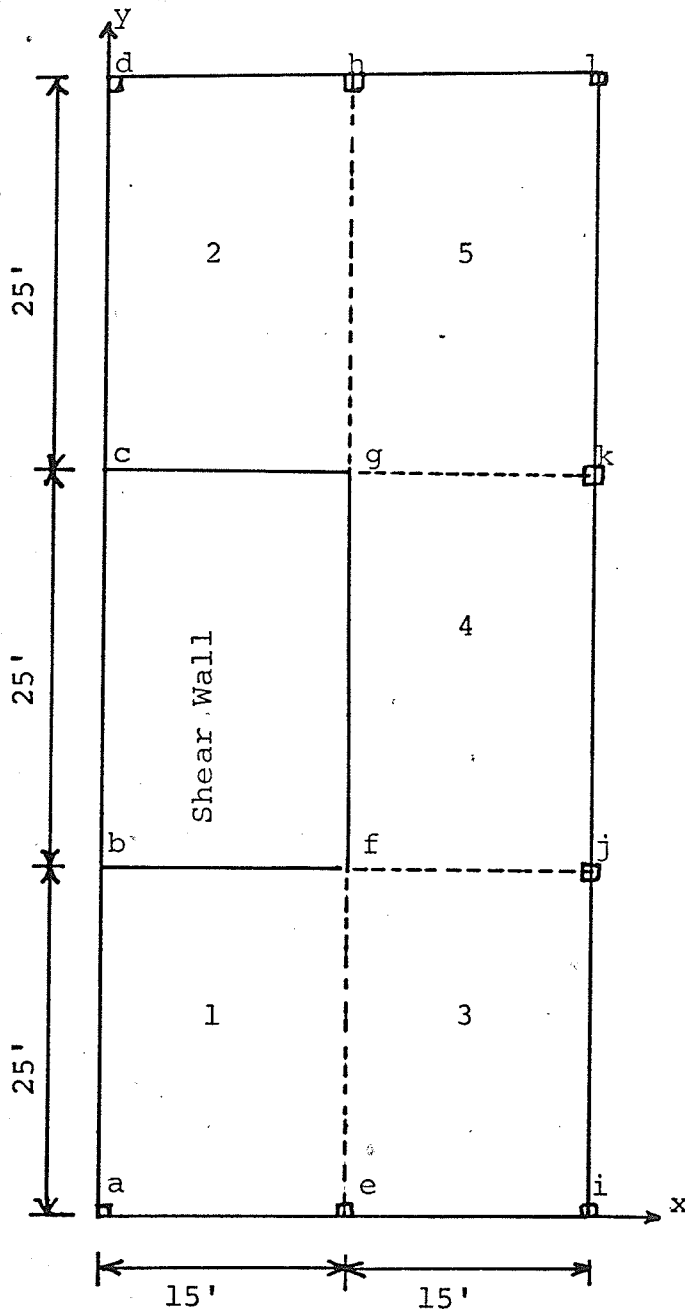
the direct bending stiffness at s in Fig 6.3.3 is $96.0 \times 10^7 \times 1.0 = 96.0 \times 10^7$ lb. inch.

Since two floor members meet at joint q, the direct bending stiffness at q will be twice that at s.

Therefore,

the direct stiffness at q is $= 192.0 \times 10^7$ lb. inch.

The direct stiffness coefficient at the shear wall, for member oq in frame B, can be calculated using multiplying factors. Fig 6.3.7 shows the portion of the



Panels 1 and 2 are torsional panels

Panels 3 and 5 are corner panels

Panel 4 is a bending panel

Fig. 6.3.7

original floor plan extending one panel in each direction from the shear wall. The various floor panels are next classified according to their contributions to the direct bending stiffness at the shear wall. Panels 1 and 2 will be torsional panels, panels 3 and 5 will be corner panels and panel 4 will be a bending panel. In addition, joints gk and fj are bending joints, the joint between a corner panel and a bending panel, while joints gh and ef will be torsion joints, the joint between a corner panel and a torsional panel.

Next, the value of the shear wall size to total span ratio ($\frac{SH}{TS}$) and the shear wall dimension in the x - x direction to shear wall dimension in the y - y direction ratio ($\frac{SX}{SY}$) are calculated. The values of the multiplying factors corresponding to these ratios are obtained from tables 4.5(a) ,...4.5(e). For the floor system shown in

Fig 6.3.7
$$\frac{SH}{TS} = \frac{1}{3} \quad , \quad \frac{SX}{SY} = 0.6$$

and the values of the multiplying factors from tables 4.5(a) ...4.5(e) are found to be:

$$\begin{aligned} F_T &= 1.457 & F_{TC} &= 0.134 \\ F_B &= 2.308 & F_{BC} &= 0.216 \\ F_C &= 0.445 & & \end{aligned}$$

Now the values of KE_B , the bending stiffness of a beam whose width, depth and span are equal to the width, thickness and span, respectively, of the bending panel, KE_C , the

bending stiffness of a beam whose width, depth and span are equal to these of the corner panel and K_{ET} , torsional stiffness of a rectangular bar whose width, depth and span are equal to those of the torsional panel are calculated as described in section 2.5.

For the floor system considered,

span of bending panel, $L_B = 180$ inches

span of corner panel, $L_C = 180$ inches

span of torsion panel, $L_T = 300$ inches

Modulus of elasticity, $E = 4 \times 10^6$ PSI

Modulus of Rigidity, $G = \frac{E}{2(1+\nu)} = \frac{4 \times 10^6}{2(1+0.3)}$
 $= 1.54 \times 10^6$ PSI

Thus

$$K_{EB} = \frac{4EI}{L_B} = \frac{4 \times 4 \times 10^6 \times \frac{1}{12} (25 \times 12) (6)^3}{180} = 48 \times 10^7 \text{ lb. inch.}$$

$$K_{EC} = \frac{4EI}{L_C} = \frac{4 \times 4 \times 10^6 \times \frac{1}{12} (25 \times 12) (6)^3}{180} = 48 \times 10^7 \text{ lb. inch.}$$

$$= 4 \times 10^7 \text{ lb. ft.}$$

$$K_{ET} = \frac{I_1 b t^3 G}{L_T}$$

where,

$b =$ width of torsional panel = 180 inches.

$t =$ thickness of torsional panel = 6 inches.

$$I_1 = \frac{1}{3} (1 - 0.63 \frac{t}{b}) = \frac{1}{3} (1 - 0.63 \times \frac{6}{180}) = 0.333$$

Therefore,

$$K_{ET} = \frac{0.333 \times 180 \times (6)^3 \times 1.54 \times 10^6}{300} = 5.4 \times 10^7 \text{ lb. ft.}$$

Next, the contributions of the various panels and joints of the floor system to the total direct stiffness are obtained as explained in section 2.5.

(i) The contribution of one bending panel is

$$\begin{aligned} K_B &= F_B \times KEB \\ &= 2.308 \times 4 \times 10^7 \\ &= 9.232 \times 10^7 \text{ lb. ft.} \end{aligned}$$

(ii) The contribution of one corner panel is

$$\begin{aligned} K_C &= F_C \times KEC \\ &= 0.445 \times 4 \times 10^7 \\ &= 1.78 \times 10^7 \text{ lb. ft.} \end{aligned}$$

(iii) The contribution of one torsional panel is

$$\begin{aligned} K_T &= F_T \times KET \\ &= 1.457 \times 5.4 \times 10^7 \\ &= 7.85 \times 10^7 \text{ lb. ft.} \end{aligned}$$

(iv) The contribution of a bending joint is

$$K_{BC} = \frac{F_{BC} \times L_B \times t^3 \times E}{B}$$

where,

B = width of the bending panel = 300 inches

t = floor thickness = 6 inches

therefore,

$$\begin{aligned} K_{BC} &= \frac{0.216 \times 180 \times 6^3 \times 441000.0}{300} \\ &= 1.03 \times 10^6 \text{ lb. ft.} \end{aligned}$$

(v) The contribution of a torsion joint is

$$\begin{aligned} K_{TC} &= \frac{F_{TC} \times L_T \times t^3 \times E}{b} \\ &= \frac{0.134 \times 300 \times 6^3 \times 441000.0}{180.0} \\ &= 1.76 \times 10^6 \text{ lb. ft.} \end{aligned}$$

Finally the contributions of the various panels and joints, in the floor system are summed to obtain the total stiffness. Since the floor system consists of two torsional panels, two corner panels, one bending panel, two torsion joints and two bending joints,

The total direct bending stiffness at the shear wall is

$$\begin{aligned}
 K_{SS} &= 2 \times K_T + 2 \times K_C + K_B + 2 \times K_{TC} + 2 \times K_{BC} \\
 &= 2 \times 7.85 \times 10^7 + 2 \times 1.78 \times 10^7 + 9.232 \times 10^7 \\
 &\quad + 2 \times 1.76 \times 10^6 + 2 \times 1.03 \times 10^6 \\
 &= 29.05 \times 10^7 \text{ lb. ft.}
 \end{aligned}$$

Since tables 4.5(a), 4.5(b)...4.5(e) for the multiplying factors are developed for a 2 foot square column, whereas the floor system considered had 1 foot square columns, the value of K_{SS} must be corrected for the effect of column size. The correction can be determined from table 10. Table 10 shows that the value of K_{SS} reduces from 31421 to 28915 as the column size changes from 2 feet square to 1 foot square.

Thus the value of K_{SS} should be reduced in this case, by

$$\frac{(31421 - 28915)}{31421} \times 100 = 8\%$$

Therefore

for the floor system considered, the corrected value of K_{SS} will be

$$\begin{aligned}
 &= 29.05 \times 10^7 \times 0.92 \\
 &= 26.7 \times 10^7 \text{ lb. ft.}
 \end{aligned}$$

Carry-Over Bending Stiffness Coefficients

Since the frame in Fig 6.3.3 consists of the shear wall, a 50 ft. wide section of the floor slab and two column lines parallel to the plane of the frame, the carry-over bending stiffness coefficients for structural members pq or rs in Fig 6.3.3 are each twice the value for a single column.

Since the columns are prismatic, the carry-over stiffness coefficient for one column is

$$\begin{aligned}
 &= \frac{2 \times E \times I}{\text{storey height}} \\
 &= \frac{2 \times 4 \times 10^6 \times 1728}{96} \\
 &= 144.0 \times 10^6 \text{ lb. inch.}
 \end{aligned}$$

Therefore,

the carry-over bending stiffness coefficient for member pq or rs is 288×10^6 lb. inch.

Member qs in Fig 6.3.3 is similar to member bd in Fig 6.3.2 and represents a floor system supported on columns only. Therefore, the value of carry-over stiffness for such a member can be obtained as explained in section 6.3.1.

For this floor system

$$\frac{\text{column size}}{\text{total span}} = \frac{1}{15} = 0.0666$$

Thus from Fig 6.3.6, the value of the carry over factor is 0.32, and the value of direct bending stiffness for member qs from section 6.3.2 is 96.0×10^7 lb. inch.

Therefore,

$$\begin{aligned} & \text{the carry over bending stiffness for member qs is} \\ & \text{equal to the direct stiffness x carry over factor} \\ & = 96.0 \times 10^6 \times 0.32 \\ & = 30.8 \times 10^6 \text{ lb. inch.} \end{aligned}$$

The member oq of planar frame B, shown in Fig 6.3.3 represents a floor system shown in Fig 6.3.7. A general procedure for calculating carry-over stiffness coefficient for such members in situations when one or more floor panels are missing, can not be established with the help of the available information. However, the member is similar to member qs except that it's one end is supported on shear wall rather than two columns. Therefore, the carry-over stiffness for oq is approximately equal to that of member qs.

CHAPTER VII

CONCLUSIONS AND RECOMMENDATIONS FOR FURTHER STUDY

7.1 Conclusions

In this investigation, the bending stiffness characteristics of flat plate floor systems in laterally loaded shear wall-frame structures have been studied and the following conclusions reached.

1. The direct bending stiffness coefficients when the floor is loaded through the shear wall are highly sensitive to shear wall shape and size and are relatively insensitive to the column size.
2. The direct bending stiffness coefficients when the floor is loaded through exterior columns are independent of the shear wall shape.
3. The carry-over bending stiffness coefficients are more sensitive to the shear wall shape and size than the column size.
4. The experimental models used in determining some of the stiffness coefficients are 10 to 20 percent more flexible than the corresponding analytical models.
5. The direct bending stiffness coefficients for a variety of flat plate floor plans can be easily calculated with reasonable accuracy using the multiplying factors defined and evaluated in this study.

6. For a flat plate structure with a square shear wall, the major contributions to total direct bending stiffness at the shear wall comes from the bending panels (as defined in this study), while the contribution of the torsional panel is minimal.
7. The effect of continuity between the different floor panels has a very significant effect on the stiffness of the floor system.
8. The bending stiffness coefficients for the basic flat plate floor plan with square corner panels, but a wide range of dimensions, can be calculated with reasonable accuracy with the help of graphs given in the fourth chapter of this study.

7.2 RECOMMENDATIONS FOR FURTHER STUDY

1. The primary purpose of this study has been to develop shear wall stiffness coefficients for use in analyzing shear wall-frame structures. The ultimate objective of further work in this area should be to permit the calculation of these coefficients for structures with arbitrary floor plans and shear wall shapes and sizes and for flat slab and waffle slab as well as flat plate floors to be usefully applied, the coefficients should then be incorporated into a structural analysis computer program.
2. Non-dimensional factors for use in determining direct bending stiffness coefficients at the shear walls were evaluated in this study. A further study should be carried out to establish similar multiplying factors for carry-over stiffness coefficients and direct bending stiffness coefficients at exterior columns.
3. In this study, structures with plates extending a maximum of three panels in each direction were considered. Further studies should be carried out to investigate the effect of continuity when additional panels are added.
4. The behaviour of the flat plate floor systems with shear walls in the inelastic region is still an interesting area of research.
5. Possible failures of the floor slab due to punching

shear and diagonal tension at the junction of the shear wall and the floor slab and the possible buckling failure of the slab requires considerably more study.

6. The dynamic behaviour of floor systems with shear walls should be studied.

REFERENCES

1. Dowell, Henry D., and Hamil, Harold B., "Flat Slabs and Supporting Columns and Walls Designed as Indeterminate Structural Frames", Journal of the American Concrete Institute, Proc. 34, pp.321-344, January-February, 1938.
2. Sozen, Mete A., and Siess, Chester P., "Investigation of Multi-Panel Reinforced Concrete Floor Slabs: Design Methods - Their Evolution and Comparison", Journal of the American Concrete Institute, Proc. 60, No.8, pp. 999-1028, August, 1963.
3. Frederick, G.R. and Pollauf, F.P., "Experimental Determination of the Transmission of Column Moments to Flat Plate Floors", University of Toledo, (Unpublished Report, May, 1959).
4. Blakey, Frank A., "Australian Experiments With Flat Plates", Journal of the American Concrete Institute, Proc. 60, No. 4, pp.515-523.
5. American Concrete Institute, "Building Code Requirements for Reinforced Concrete", ACI Standard 318-63, June, 1963.
6. Di Stasio, Joseph and Van Buren, M.P., "Transfer of Bending Moment Between Flat Plate Floor and Column", Journal of the American Concrete Institute, Proc. 57, No.3, pp.299-314, September, 1960.
7. Tsuboi and Kawaguchi, "On Earthquake Resistant Design of Flat Slabs and Concrete Shell Structures", The Second World Conference on Earthquake Engineering, Tokyo, 1960.
8. Khan Fazlur, R., and Sbarounis, John A., "Interaction of Shear Walls and Frames", Journal of the Structural Division, ASCE Proceedings, Vol.90, ST 3, June, 1964.
9. Brotchie, John F., and Russell, J.J., "Flat Plate Structures", Part I., Journal of the American Concrete Institute, Proc. 61, No.8, August, 1964.
Part II, available from American Concrete Institute, Detroit, Michigan.

10. Carpenter J. E., "Flexural Characteristics of Flat Plate Floors in Buildings Subjected to Lateral Loads", Ph. D. Thesis, Purdue University, June, 1965.
11. Bernard, P. R., and Schweighofer, J., "Interaction of Shear Walls Connected Solely to Slabs", The International Symposium on Tall Buildings, University of Southampton, London, April, 1966.
12. Nantasarn, R., and Parnichkul, A., "Effective Stiffness and Carry-Over Factors for Flat Plates", Master of Science Thesis, University of Manitoba, April, 1969.
13. Gouwens, Albert J., "Lateral Load Analysis of Multistory Frames with Shear Walls", Portland Cement Association, July, 1968.
14. Wiebe, J. D., "Preparation of Influence Surfaces for a Simply Supported Square Plate by the Moiré Method," M. Sc. Thesis, University of Manitoba, 1967.
15. Ligtenberg, F. K., "The Moiré Method, a New Experimental Method for the Determination of Moments in Small Slab Models," Proc. Soc. Exp. Stress Analysis, XII (2), 1954.
16. Timoshenko, S., and Goodier, J. N., "Theory of Elasticity", (second edition) New York, McGraw-Hill Book Company, 1951.

APPENDICES

APPENDIX A

COMPUTER PROGRAM USER'S GUIDE

IDENTIFICATION

GENDEK 3 - Finite Element Analysis of
Stiffened Plates

PROGRAMMED

Ian G. Buckle, July 1969

ORGANIZATION OF GUIDE

	Page
1.0 Program Purpose and Structure Idealization	143
2.0 Program Input Data	144
3.0 Explanatory Notes	152
3.1 NQUAD Significance	152
3.2 Coordinate Systems and Sign Convention	153
3.3 Nodal Point Coordinate Generation	154
3.4 Element Nodal Point Array Generation	155
3.5 Slab Elastic Axes and Properties	156
4.0 Output Description	156
5.0 Program Restrictions and Capacity Changes	157

1.0 PROGRAM PURPOSE AND STRUCTURE IDEALIZATION

The primary purpose of this program is the analysis of highway girder bridge decks of arbitrary geometry. The program may, however, be used for the analysis of general slab systems under lateral load, including slabs which are stiffened by discrete ribs.

The deck slab is idealized by a mesh of plate bending finite elements. The stiffness of each quadrilateral element is computed and assembled into the structure stiffness matrix. Variation in deck slab properties from element to element is permitted. The program makes use of the Felippa Q-19 plate bending element with orthotropic elastic properties.

The girders and diaphragms are idealized by beam finite elements joining the nodal points of the deck slab elements. Again, each element stiffness is individually computed and assembled into the structure stiffness matrix. The beams are assumed to be in the plate midsurface for the purposes of idealization and analysis. However, eccentrically connected ribs can be considered by assigning appropriate effective stiffnesses. These effective stiffnesses can be specified as input data or they can be computed automatically within the program. Ribs which are too closely spaced to be represented as individual beams can be "smeared" by assigning appropriate anisotropic properties to the plate elements.

Written in FORTRAN IV, the program presently uses the overlay feature to economize computer storage requirements. If necessary, substitution of "subroutine" for "overlay" statements will convert the program to the standard subroutine form.

Other important features of the program are:

- (a) For regular meshes, automatic generation is available for nodal point coordinates, nodal point arrays, support conditions, and load data. Data preparation effort may be considerably reduced if these options are used.
- (b) Multiple load cases can be considered without redefining the structure data for each case. Five load options are available, which include single loads, uniformly distributed loads, truck loading, and any combination of these.
- (c) Internal hinge lines can be specified.
- (d) The program can be used directly for the analysis of arbitrary anisotropic slabs, arbitrary beam gridworks, and arbitrary combinations of slabs and beams.

2.0 PROGRAM INPUT DATA

Input to the program is by punched cards. Standard FORTRAN format has been used throughout, and is identified for each card by A, E, F or I specifications.

Basically the data deck will consist of operation control cards, structure definition cards, and load case cards. The organization of data on each type of card is described in the following paragraphs.

- A. Start Card (A8) - One card at the beginning of each problem.
Cols 1-5 punch the word 'START'
- B. Title Card (10A8) - One card for each new problem.
Cols 1-80 any heading to be printed at beginning of output,
all keypunch symbols are acceptable.
- C. Basic Control Card (10I5) - One card for each problem.
- | | |
|----------|--|
| Cols 1-5 | NPEL number of plate elements |
| 6-10 | NBEL number of beam elements |
| 11-15 | NJ number of nodal points |
| 16-20 | NJBC number of supported nodal points |
| 21-25 | NPT number of different plate element types |
| 26-30 | NBT number of different beam element types |
| 31-35 | ISO if set to 0, the elastic properties of the plate elements will be defined directly by the thickness, elastic moduli and Poisson's ratio of the plate material. |
| | if set to 1, these properties will be defined by equivalent flexural and torsional inertias per unit length of plate. |
| 36-40 | NHNP number of nodal point pairs which are connected by hinges (see Card L). |
| 41-45 | NQUAD if set to 0, plates specified to have identical elastic properties (see Card D.) are also assumed to have identical shape. |
| | if set to 1, all plates are assumed to be of different shape. See Note 3.1 for discussion of significance. |

Cols 45-50 MPRINT if set to 0, only the average value of the plate element moments at each nodal point are printed.

if set to 1, not only the average moments but also the moments from each contributing element at each nodal point are printed.

A value of 0 is recommended.

- D. Plate Properties Card - Variation in plate properties from element to element is defined by assignment of plate property type numbers to elements of different properties. For uniform properties (no variation) the number of different plate element types (NPT, Card C) is 1, for non-uniform properties NPT will be greater than 1, and it will be necessary to input one plate property card for each plate type.

Either: Orthotropic plate properties - (ISO = 0, Card C)
(F10.5, 2E10.4, 3F10.5) - one card for each plate type.

Cols 1-10	T	slab thickness
11-20	E1	elastic modulus in principal direction 1
21-30	E2	elastic modulus in principal direction 2
31-40	U1	Poisson's ratio in principal direction 1
41-50	U2	Poisson's ratio in principal direction 2
51-60	ALPHAT	torsion parameter, if not specified it is set to 1.0, the correct value for a solid slab.

Or: Equivalent plate properties - (ISO = 1, Card C)
(E10.4, 6F10.5) one card for each plate type.

Cols 1-10	E	elastic modulus of slab material
11-20	U	Poisson's ratio of slab material
21-30	T	slab thickness
31-40	I1	equivalent flexural inertia per unit length in principal direction 1

41-50	I2	equivalent flexural inertia per unit length in principal direction 2
51-60	J1	equivalent torsional inertia per unit length in principal direction 1
61-70	J2	equivalent torsional inertia per unit length in principal direction 2

Note that in cases where several property cards are necessary, only a few parameters may vary. In this event those that are constant may be left blank on the second and succeeding cards. The program will then set these parameters equal to those specified on the first property card.

E. Plate Properties Distribution Cards (40I2) - as many cards as needed. Omit if there is only one plate type (NPT = 1).

Cols 1-80 plate element type numbers,
 40 type numbers per card in numerical order
 of element number.

F. Beam Properties Cards (8E10.4) - one card for each beam type.

Either - for beams eccentric to plate midsurface

Cols 1-10	A	cross sectional area
11-20	I	flexural moment of inertia with respect to the beam's neutral axis
21-30	J	torsional moment of inertia
31-40	EXEN	eccentricity of beam neutral axis from plate midsurface
41-50	D	distance from beam neutral axis to lower fiber
51-60	W	effective width of slab that can be assumed to act as an upper flange to the beam.
61-70	BE	elastic modulus of beam material
71-80	BNU	Poisson's ratio of beam material

Or - for beams symmetric about plate midsurface

Cols 1-10	A	cross sectional area
11-20	I	flexural moment of inertia

Cols 21-30	J	torsional moment of inertia
31-40	Y1	distance from neutral axis to lower fiber
41-50	Y2	distance from neutral axis to upper fiber
51-60		blank
61-70	BE	elastic modulus of beam material
71-80	BNU	Poisson's ratio of beam material

If there is a variation in the beam properties, several property cards may be necessary. In this event, a beam element type number is assigned to each element to describe the distribution of these properties. Note that these property cards are input in numerical order of the type number; and further note that if either BE or BNU are omitted from the second and succeeding cards, the value(s) from the first card will be assumed by the program.

- G. Beam Properties Distribution Cards (40I2) - as many cards as needed. Omit if there is only one beam type (NBT = 1).

Cols 1-80	beam element type numbers, 40 type numbers per card, in numerical order of element number.
-----------	--

- H. Nodal Point Coordinate Cards (I5, 2F10.5, 2I5, 2F10.5) - one card for each nodal point unless the generation options are used.

Cols 1-5	nodal point number
6-15	x-coordinate of point
16-25	y-coordinate of point
26-55	used for layered generation, otherwise leave blank

These cards are input in numerical sequence. If any card is omitted, straight line equal increment generation of coordinates takes place, or, if cols 26-55 have been used, layered generations occur. Refer to Note 3.2 for explanation of the coordinate system to be used and to Note 3.3 for details of generation options.

I. Plate Nodal Point Array Cards (5I5, 2F5.0, 2I5) - one card for each element unless the generation options are used.

Cols 1-5	element number
6-10	nodal point I
11-15	nodal point J
16-20	nodal point K
21-25	nodal point L
26-30	angle ϕ in degrees
31-35	angle α in degrees
36-45	used for layered generation, otherwise leave blank.

These cards are also input in numerical sequence. If a card or group of cards is omitted, layer generation takes place (refer to Note 3.4.1). The four nodal point numbers I, J, K and L must be input in counter-clockwise sequence. The angle ϕ is the angle between the global x-axis and the direction of the principal orthotropic axis (1-axis) of the plate material. The angle α is the angle between the principal axes of the plate material. If cols 31-35 are left blank, angle α is assumed to be 90 degrees (refer to Fig. 3).

J. Beam Nodal Point Array Cards (4I5) - one card for each element unless the generation option is used.

Cols 1-5	element number
6-10	nodal point I
11-15	nodal point J
16-20	used for line generation, otherwise leave blank, refer Note 3.4.2 for details.

K. Support Condition Cards (I5, 3I1, 22X, 2I5) - one card for each supported nodal point unless generation option is used.

Cols 1-5	nodal point number
6	set to 1 if vertical deflection is to be restrained; otherwise leave blank
7	set to 1 if rotation about x-axis (fig. 1)

is to be restrained, otherwise leave blank

8 set to 1 if rotation about y-axis (fig.1) is to be restrained, otherwise leave blank

Cols 9-30 blank

31-40 used for line generation as noted below, otherwise leave blank

31-35 increment between two successive nodal point numbers which have same support condition as that just described

36-40 number of the last nodal point in this sequence to have this support condition

L. Hinge Line Data Cards

First Card (E10.3)

Cols 1-10 spring constant approximating stiffness of hinge linkage. For an assumed rigid linkage enter 10^8 k/in. A larger value may cause numerical instability.

Each hinge is defined by two nodal points located on either side of the hinge. These pairs of nodal points are identified on the following set of cards.

Remaining Cards (16I5) - as many cards as needed

Cols 1-5 number of first nodal point in first hinge pair
 6-10 number of second nodal point in first hinge pair
 11-15 number of first nodal point in second hinge pair
 and so on for as many hinges as specified.

M. Load Card (A8) - one card at beginning of each new load case

Cols 1-4 punch the word "LOAD"

9-80 any title describing this loadcase - all key-punch symbols are acceptable.

N. Basic Load Data Card (5I5) - one card for each load case.

Cols 1-5 number of single loads applied at nodal points

Cols 6-10	number of uniformly loaded areas for which the load is to be distributed to the nodal points in proportion to the tributary area of each point.
11-15	number of single loads applied at arbitrary points (x,y)
16-20	number of uniformly loaded areas for which the load is to be distributed to the nodal points by consistent load theory
21-25	number of trucks

O. Single, Nodal Point Load Cards (I5, 3E10.3) - one card for each loaded nodal point

Cols 1-5	nodal point number
6-15	applied vertical load
16-25	applied moment about global x-axis
26-35	applied moment about global y-axis

P. Uniform Tributary Area Load Cards (I5, F10.5, 3I5) - one card for each uniformly loaded area

Cols 1-5	element number	
6-15	intensity of uniform load expressed in units of load per unit area.	
16-20	N2	} used for generation as described below, otherwise leave blank.
21-25	MOD	
26-30	NLIM	

N2 is the number of the last element, in the direction of element numbering, to have the same load intensity.

MOD is the element number difference across element layers within the same area.

NLIM is the last element number in the area.

Q. Single, Arbitrary Load Cards (3E10.3) - One card for each load.

Cols 1-10	x - coordinate of load
11-20	y - coordinate of load
21-30	applied vertical load

R. Uniform, Consistent Load (I5, F10.5, 3I5)

Cols 1-5	element number
6-15	intensity of uniform load expressed in units of load per unit area
16-20	N2 used for generation as described for Card P
21-25	MOD
26-30	NLIM

S. Truck Load Cards - one set for each truck

Vehicle Identity (A8, 2X, F10.5)

Cols 1-8	Punch identity of vehicle, two options are presently available: If HS20 is used, program assumes that the standard AASHO HS20 vehicle, has been requested, and does not require the dimensions or wheel loads to be input. These are available to the program in units of inches and kips. If SPCIAL is used, program requires that the vehicle dimensions and wheel loads be specified as noted below.
----------	---

11-20	If HS20 option has been requested, the wheel base length for the rear axle must be punched in these columns, otherwise leave blank.
-------	---

Vehicle Properties

These cards are omitted if HS20 vehicle has been requested on the previous card.

(a) one card for each truck (I5)

Cols 1-5	number of axles
----------	-----------------

(b) one card for each axle (E10.3, I5)

Cols 1-10 wheel base length (for first axle this length is zero)

11-15 number of pairs of wheels on axle

(c) one card for each wheel pair on each axle (2E10.3)

Cols 1-10 axle length between wheels in each pair

11-20 wheel load (both wheels in pair are assumed to have equal load)

Vehicle coordinates (3F10.5)

Cols 1-10 x - coordinate of center of front axle

11-20 y - coordinate of center of front axle

21-30 angle of attack of vehicle with respect to positive direction of x-axis

T. Next Operation Card (A8) - one card

Cols 1-6 Select next operation and punch appropriate word. Possible operations are:

START: commence a new analysis with a new data deck.

LOAD: rerun the same problem for a new load case

STOP: stop program execution

3.0 EXPLANATORY NOTES

3.1 NQUAD Significance

The variable NQUAD has been defined on Card C of the Input Data Deck. If set to 0, plate elements which have consecutive element numbers and also have identical plate type numbers are assumed to be of identical shape. The program does not re-compute the element stiffness, and hence computer time is saved. If NQUAD is set to 1, each element is assumed to be different and a new stiffness matrix is computed for each element.

In cases where there are few geometrically different elements it will be advantageous to assign separate plate property numbers to plates of identical shape, even if they actually have the same properties, since by setting NQUAD to 0, the structure stiffness formation time is reduced.

3.2 Coordinate Systems and Sign Convention

The slab is referenced by a global right-handed cartesian (x-y-z) system of axes with the x-y plane lying in the midsurface of the slab. Positive sign conventions for displacements and rotations of this mid-surface are indicated in Fig. 1.

Applied concentrated loads have the same sign convention as the corresponding displacements.

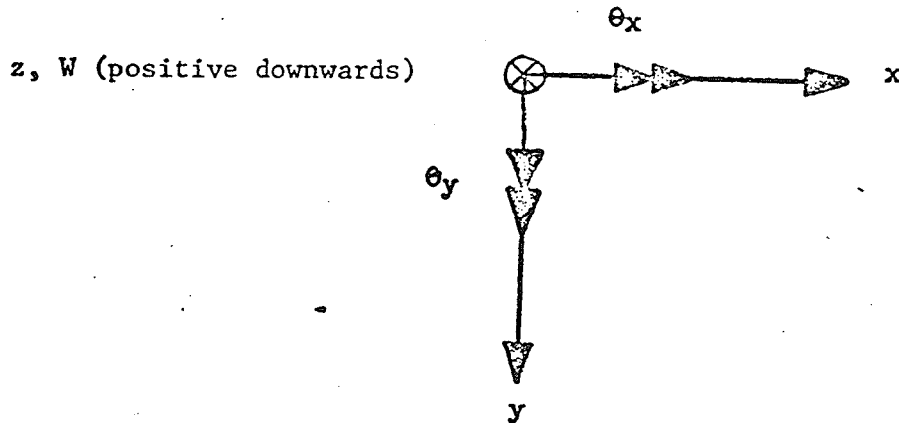


Fig 1. Global Coordinate System and Displacement Sign Convention

Sign conventions for slab moments are shown in Fig. 2. Positive bending moments produce compression in lower fibers.

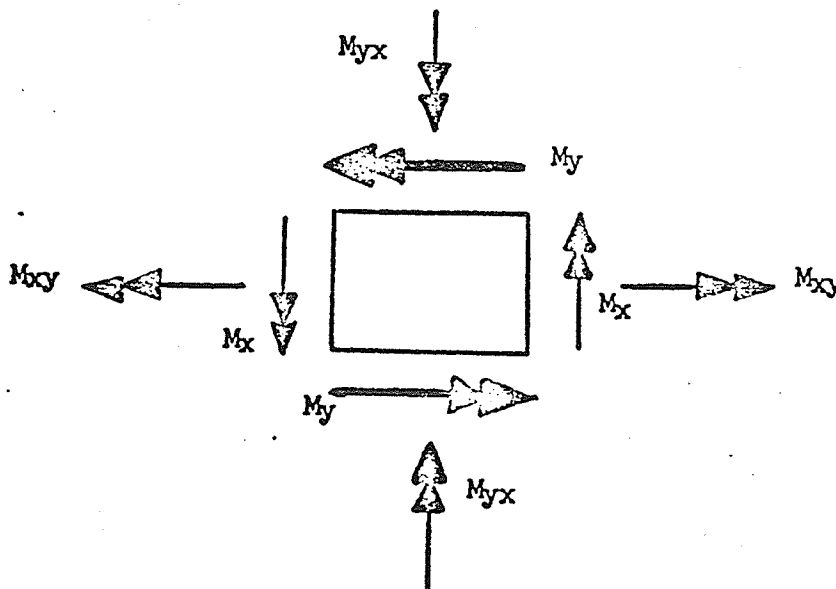


Fig. 2. Slab moments per unit length

Engineering convention has been used for the signs of the beam moments and stresses. That is, a positive bending moment causes a positive (tensile) stress in the lower fibers of the beam.

3.3 Nodal Point Coordinate Generation

Two types of coordinate generation are available:

3.3.1 Straight line generation

If the (L-1) nodal cards for points N+1, N+2 N+L-1 are omitted and cols 26-55 of the N-th Card are left blank, the missing coordinates will be generated as those of (L-1) equally spaced points on a line joining N and (N+L). That is

$$x_{N+k} = x_{N+k-1} + dx$$

$$y_{N+k} = y_{N+k-1} + dy$$

where $dx = (x_{N+L} - x_N)/L$ $dy = (y_{N+L} - y_N)/L$ for $k = 1, 2 \dots L-1$

3.3.2 Layer generation

This can be used after two "lines" of sequential nodal points have been previously defined, to construct the complete mesh or part of it by extrapolation. If on the card for point N we specify

Col 26-30	MOD	module $m > 0$	
31-35	NLIM	limit of generation ($> N$) -	
36-45	FACX	amplification factor f_x	(set to 1 if blank)
46-55	FACY	amplification factor f_y	

the x-y coordinates of points N+1, N+2 NLIM will be generated by the formulas

$$x_k = x_{k-m} + f_x (x_{k-m} - x_{k-2m})$$

$$y_k = y_{k-m} + f_y (y_{k-m} - y_{k-2m})$$

for $k = N+1, \dots, NLIM$. If $NLIM = NJ$ no more nodal cards are needed. If $NLIM < NJ$, the card for point (NLIM+1) must follow.

3.4 Element Nodal Point Array Generation

3.4.1 Plate Elements

Two types of plate elements generation are also available

3.4.1.1 Layer generation

If element cards N+1, N+2 N+L-1 are left out and cols 36-45 of the card for element N are left blank, the missing (L-1) elements will be generated by increasing the nodal numbers I, J, K, L of the preceding element by 1, ending with (N+L-1). The plate type number and angles ϕ and α are set equal to those read for element N.

3.4.1.2 Modular generation

This option can be used when two "layers" of sequentially numbered elements have been previously defined. If on the card for element N we specify

Cols 36-40 MOD module $m > 0$

41-45 NLIM limit of generation ($> N$)

the I-J-K-L nodal numbers of elements N+1, N+2 NLIM will be generated by the formula

$$I_k = I_{k-m} + (I_{k-m} - I_{k-2m})$$

(where I_k means nodal number I for the k-th element) and similarly for J-K-L, for $k = N+1$ NLIM. The plate type number and the angles ϕ and α are set equal to their values for element (k-m).

3.4.2 Beam Elements

If the beam elements in the structure are arranged in clearly defined lines, generation is possible for a complete line of elements provided the nodal point difference is the same for each element in the line.

In this event, for Card J:

Col 16-20 last element number in line to have same
nodal point difference as first element

Note that the beam elements must be numbered sequentially along the line to be generated.

3.5 Slab Elastic Axes and Properties

The principal elastic axes are assumed to be 1, 2, z, where the 1-axis forms an angle ϕ with the global x-axis, and the 2-axis forms an angle α with the 1-axis, as shown in Fig. 3.

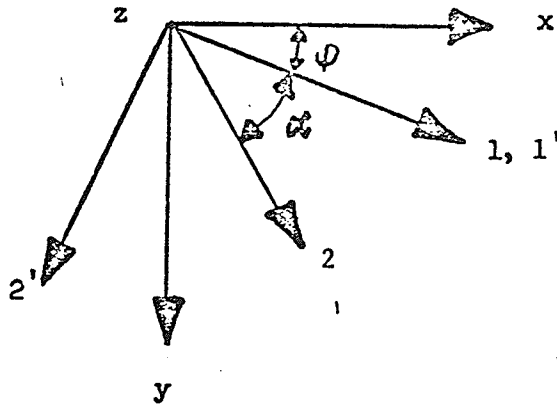


Fig. 3. Principal Elastic Axes for Orthotropic Material

The plate properties, input on Cards D and E, must be relative to these axes. If angle ϕ (Card I) is zero and angle α is 90° , the principal and global axes coincide.

Note that if the slab is isotropic, $E_1=E_2=E$, $U_1=U_2=U$ and the angles ϕ and α have no significance. (Leave blank on Card I).

Estimation of the equivalent flexural and torsional inertias (I_1 , I_2 , J_1 , J_2 - Card D) for a beam stiffened slab is made by spreading the beam properties over an assumed effective width of slab. The program approximates the reduced torsional stiffness in the equivalent slab by defining a torsion parameter (ALPHAT). Nevertheless, unreliable results may occur, particularly if the spacing between beam centerlines is large. In this event, the discrete beam representation should be used.

4.0 OUTPUT DESCRIPTION

The following is output by the program:

1. A complete printout of all input data, including all quantities calculated by the various generation routines.
2. A listing of the applied loading for every load case.
3. The displacements (vertical deflection, and rotations about the two global axes) for all nodal points. Included here are the reaction forces at each supported node.
4. The moments M_x , M_y and M_{xy} (Fig. 2) at the center of each plate element, are listed.

5. The moments M_x , M_y and M_{xy} (Fig. 2) at each nodal point are listed (on control of MPRINT, Card C of the Input Data Deck).
6. The shear force, torsion moment and bending moments acting on each beam element are listed. Further, the stresses at two fibers (distance Y_1 and Y_2 from the neutral axis of the combined section, Card F of the Input Data Deck) are computed and listed.

5.0 PROGRAM RESTRICTIONS AND CAPACITY CHANGES

Apart from restrictions imposed by the structure idealization and the method of analysis, the program is also restricted by the size of problem it can analyze.

Dimensioned arrays in labelled COMMON blocks have presently set the following restrictions on the finite element mesh:

Maximum number of plate elements	(NPEL)	is	551
Maximum number of beam elements	(NBEL)	is	648
Maximum number of nodal points	(NJ)	is	1225
Maximum number of supported nodal points	(NJEC)	is	200
Maximum number of plate element types	(NPT)	is	20
Maximum number of beam element types	(NBT)	is	30
Maximum nodal point difference in one element	(MAXPD)	is	18
Maximum number of hinges	(NHNP)	is	50

To change these limits the following cards should be repunched:

```
COMMON /MESH/      XORD (NJ), YORD (NJ), CONLD (3*NJ) NDEC (3*NJBC),
                   NPH (NHNP,2)

COMMON /PLATE/     NP (NPEL, 4), NPTYP (NPEL), PHGL (NPEL, 2)
                   PPROP (NPT, 7), ZPB (19, 19)

COMMON /BEAM/      NB (NBEL, 2), NBTYP (NBEL), EPROP (NBT, 8), ZB (6, 6)

COMMON /BANAB/     B (2*BW), A (2*BW, BW)
```

where $BW =$ one half of the bandwidth of the structure stiffness matrix $= 3 (MAXPD + 1)$

In addition the following statements should be changed:

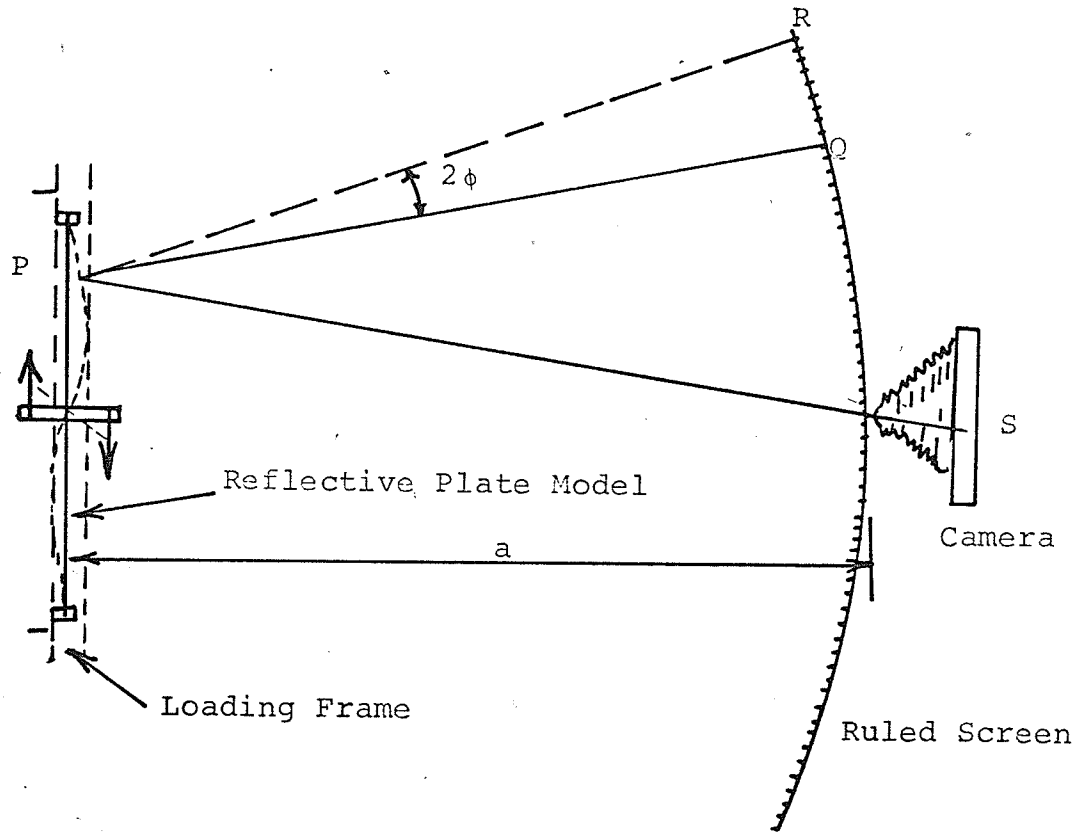
```
in subroutine SETUP:      MAXPD = MAXPD
in overlay   STIFF:       NX = MAXPD + 1
in overlay   LDSL:        DO 100I = 1, NJ
in subroutine BANSOL:     NN = 3* (MAXPD + 1)
in overlay   STRESS:      COMMON /BANAB/ STRESS (3,4, NPFL)
```

APPENDIX B

B - 1 Basic Principle of the Moiré Method. The Moiré Method is an experimental procedure for measuring the slopes of a deflected plexiglas plate model. If the slopes are established along a set of parallel lines, a slope diagram can be drawn. The slope curve along any given line can then be integrated to obtain a deflection diagram along that line.

A model plate with a reflecting surface is clamped to a loading frame in front of a ruled screen, as shown in Fig. B1. The unloaded model is photographed through a small opening in the screen, and a reflected image of the ruled dark and light lines on the screen obtained. For example, the image of a dark line at point Q would be reflected from point P on the plate and would appear at point S on the film. The model is then loaded and rephotographed. If point P on the model rotates through an angle ϕ , the image of a new point R appears at S. If point R on the screen coincides with a dark line, point S on the photo will be dark. Otherwise it will be somewhat lighter in color. This gives interference patterns on the photographic plate and produces Moiré fringes as shown in Figs. B2(a), B3(a), B4(a), etc. These fringes represent contours of constant slope, and since the slope along each fringe is constant, it follows that the change of slope between the contours corresponding to two consecutive fringes must also be constant. This constant "C" is dependent on the interval of ruling screen, "d" and on the distance between the screen and the model plate, "a" shown in Fig. B1.

The evaluation of the constant "C" is described by J. Weibe⁽¹⁴⁾ and for the M 1/03 apparatus used in this study $C = 0.0015$.



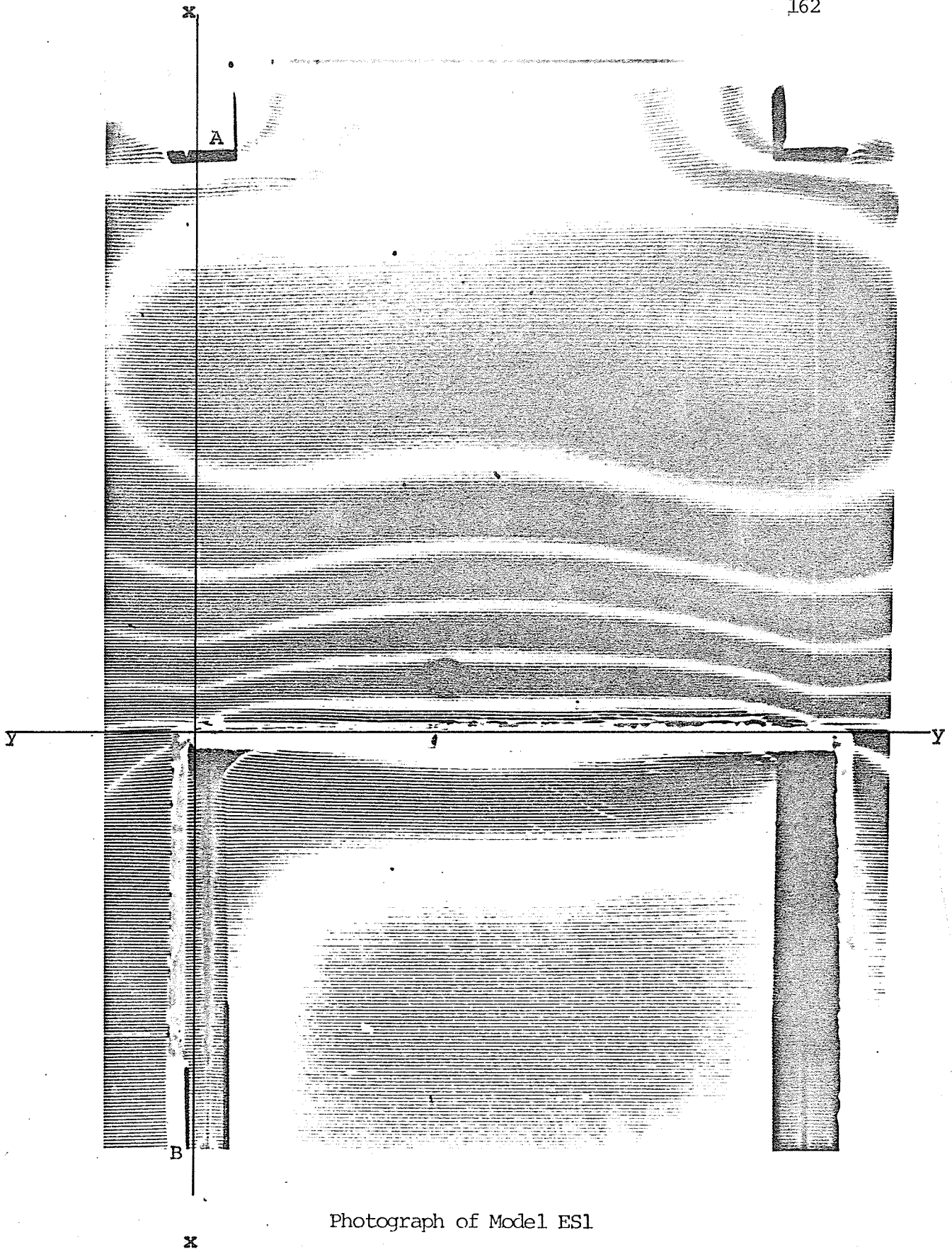
Basic Principle of Morie Method

Fig B1

B - 2 Determination of Slope Curve from Moiré Photographs. If a Moiré photograph of a model plate is taken with the rulings of the screen in the y- direction (horizontal), a curve of $\partial w / \partial x$ along a line parallel to the x- direction (vertical) may be obtained as follows:

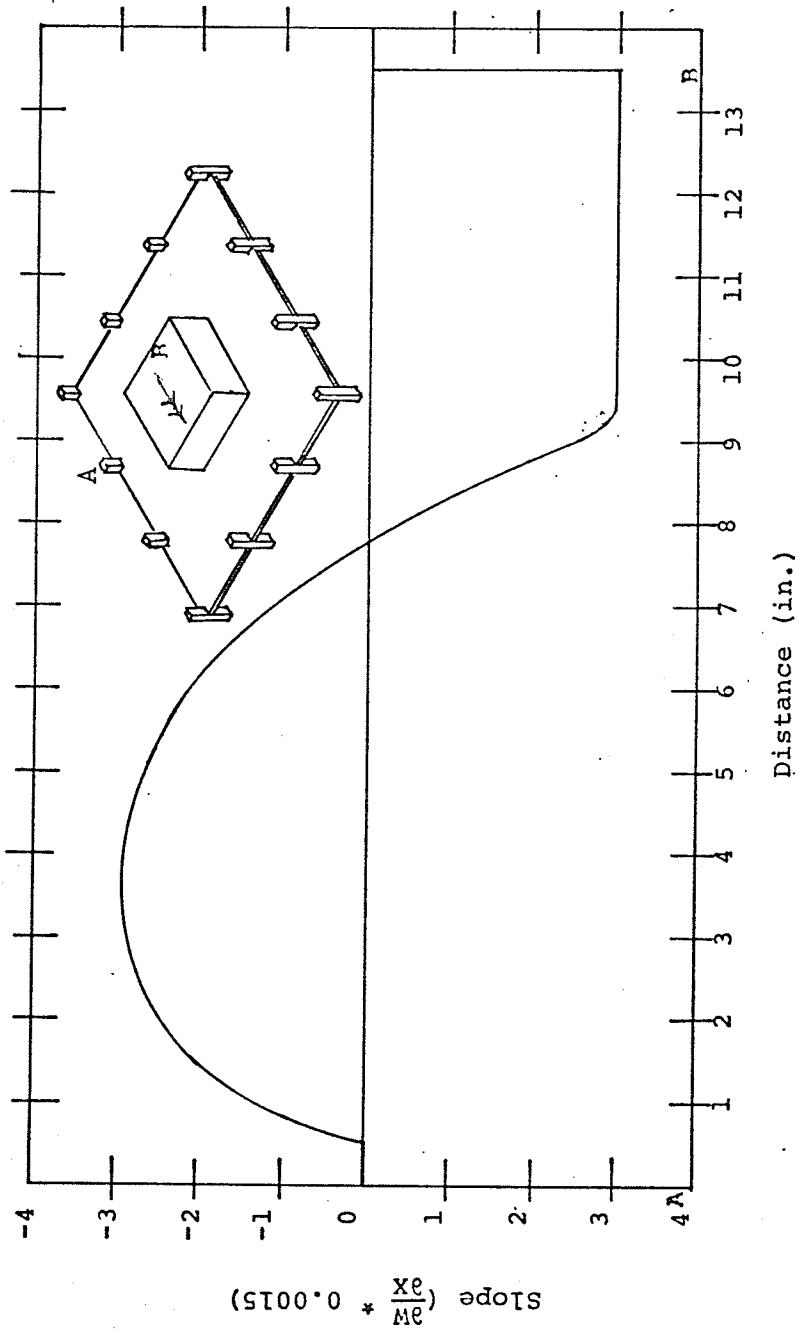
A line is drawn parallel to the x-axis as shown in Figs. B2(a), B3(a), B4(a), etc., this line intersects a number of fringes. The centres of the fringes along the line are then projected downward and plotted as shown in Figs. B2(b), B3(b), B4(b), etc. Values of slope are then plotted to obtain a curve of slope ϕ_x vs distance along the line.

The fringes are numbered starting from the zero fringe, which represents zero slope (i.e. a zero value for QR in Fig. B1). In Figs. B2(a), B3(a), B4(a), etc., for example, the zero fringe is the one that extends from the exterior fixed columns. The slope (in a direction perpendicular to the ruled lines on the screen) at any point is thus the fringe order at the point times C.

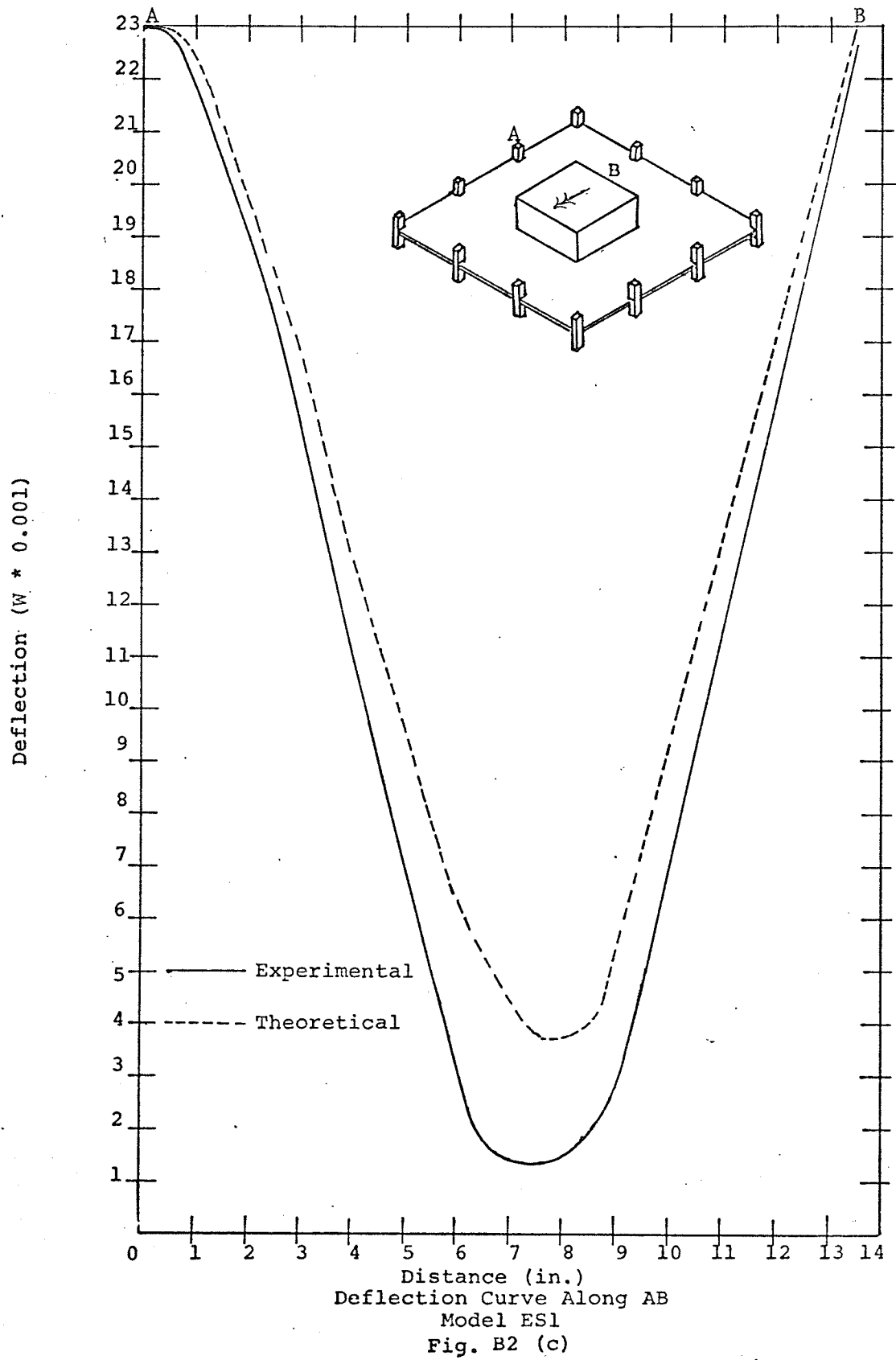


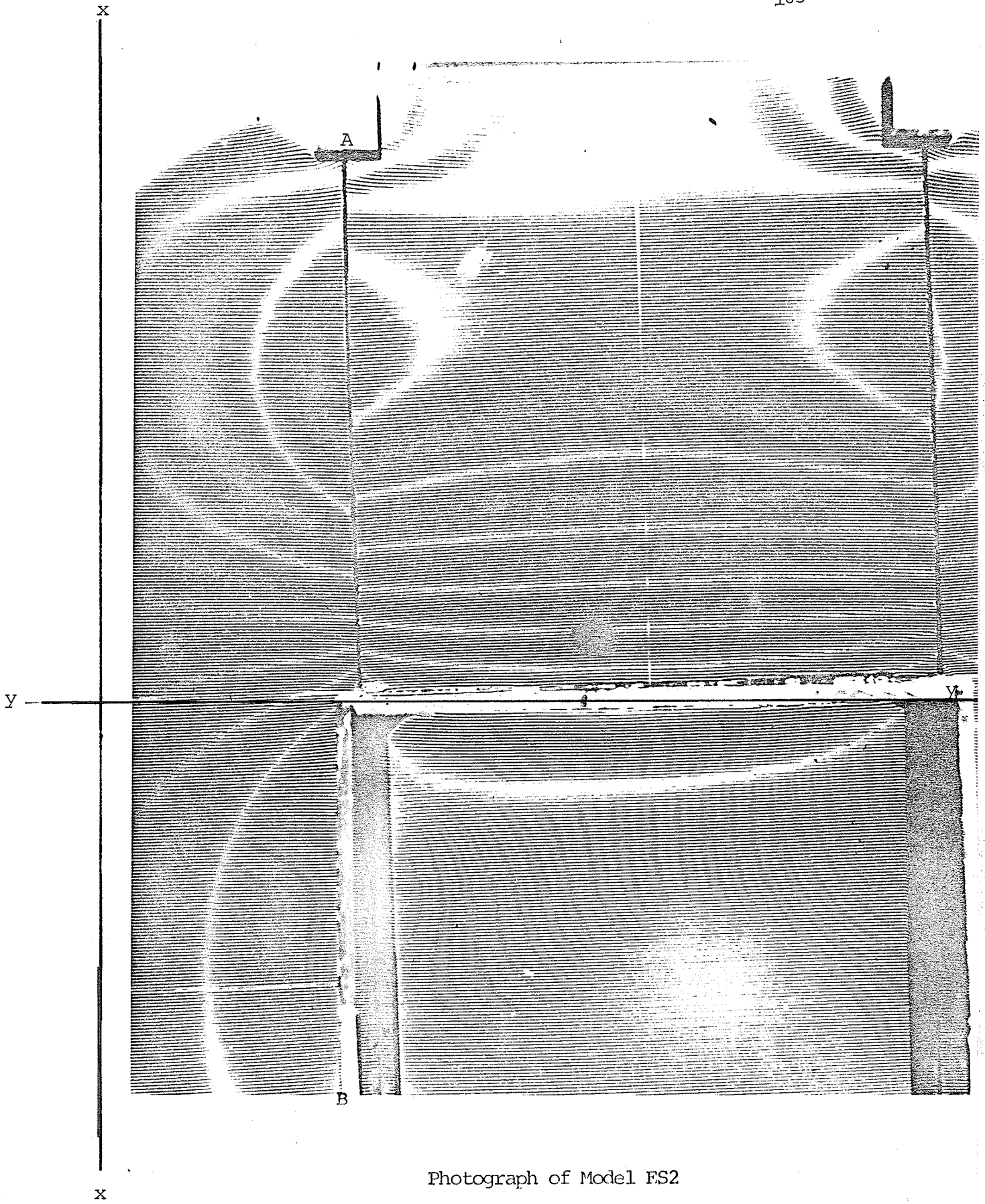
Photograph of Model ES1

Fig. B2(a)



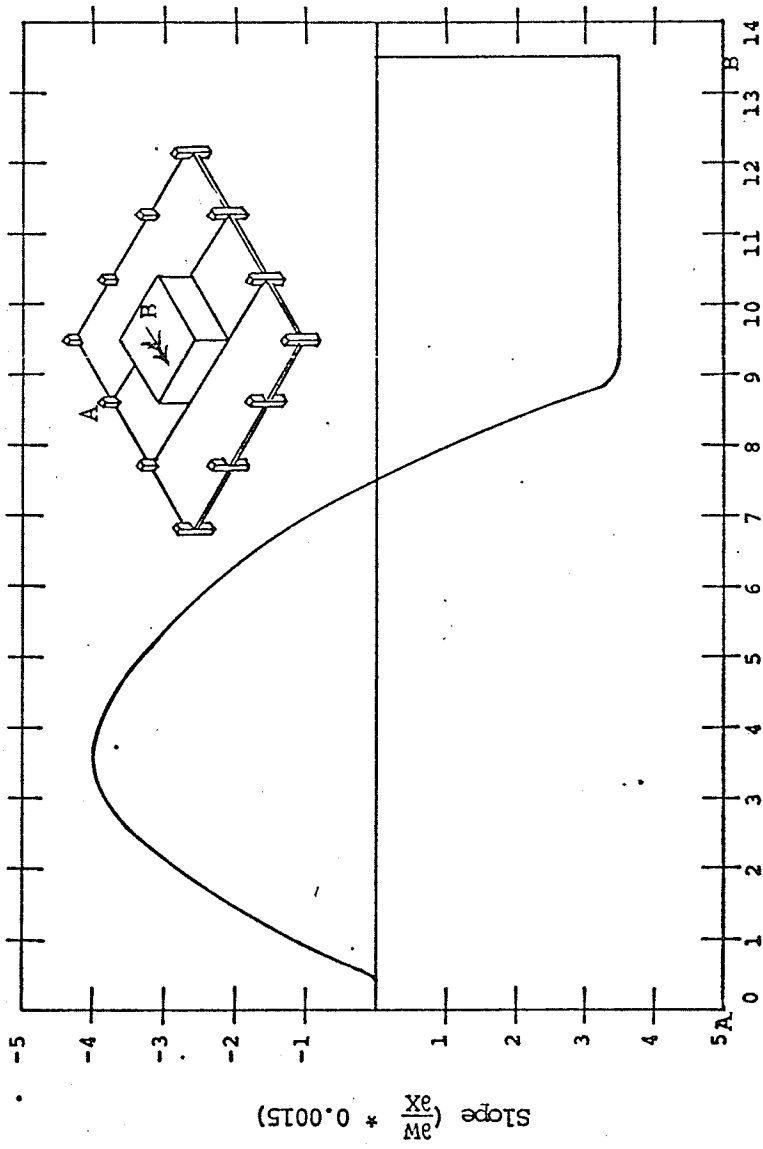
Slope Along AB
Model ES1
Fig. B2 (b)



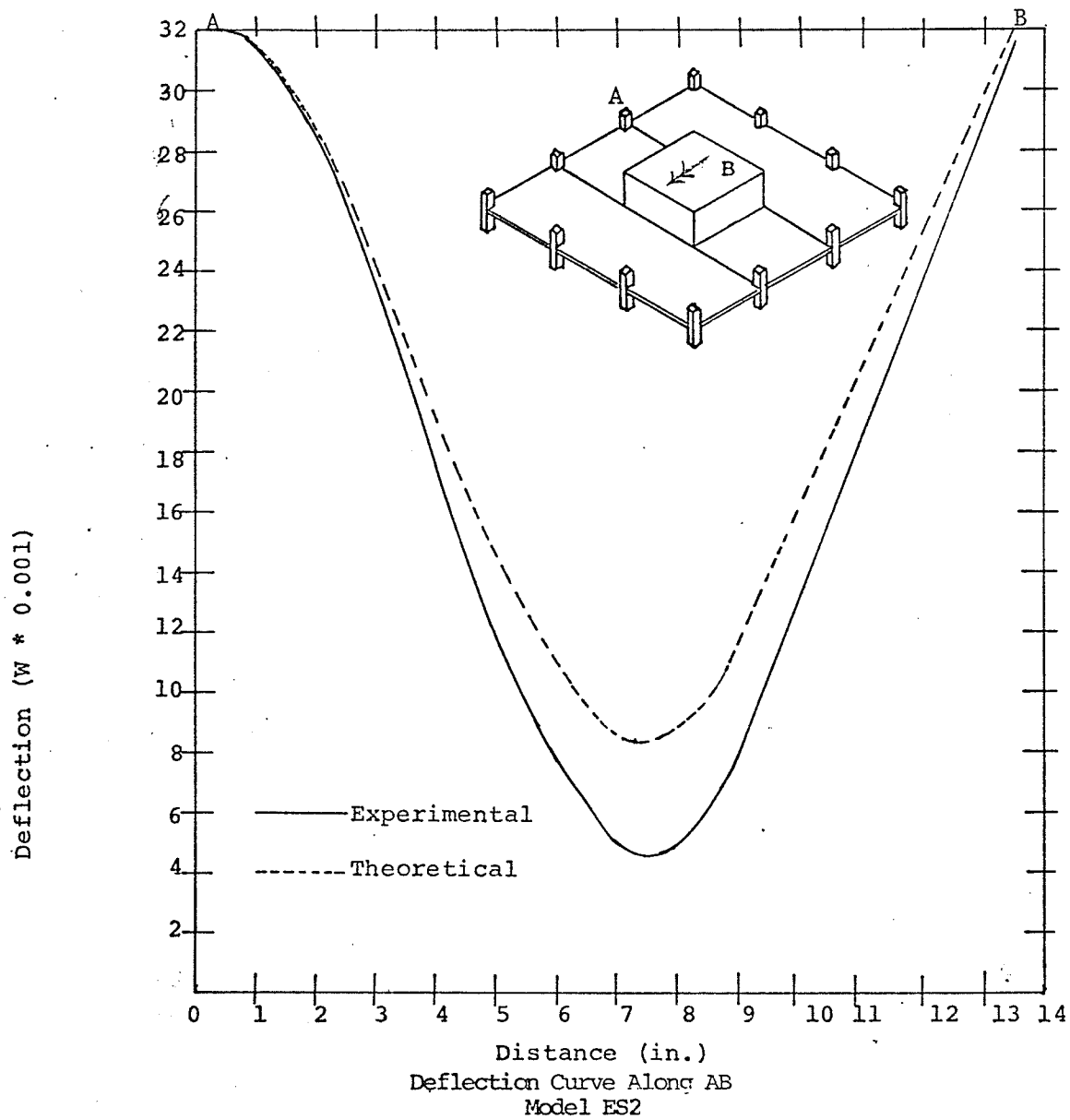


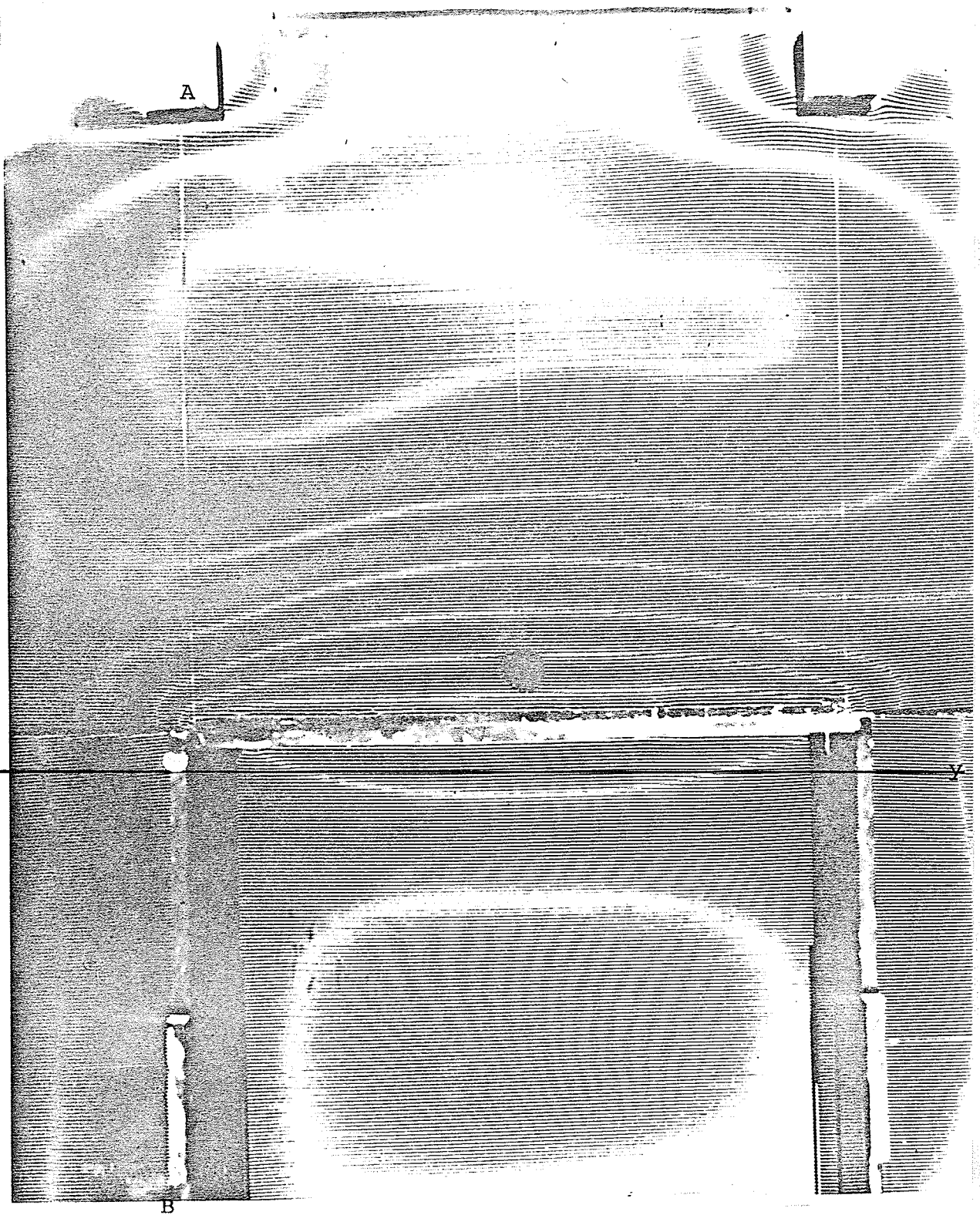
Photograph of Model FS2

Fig. B3(a)



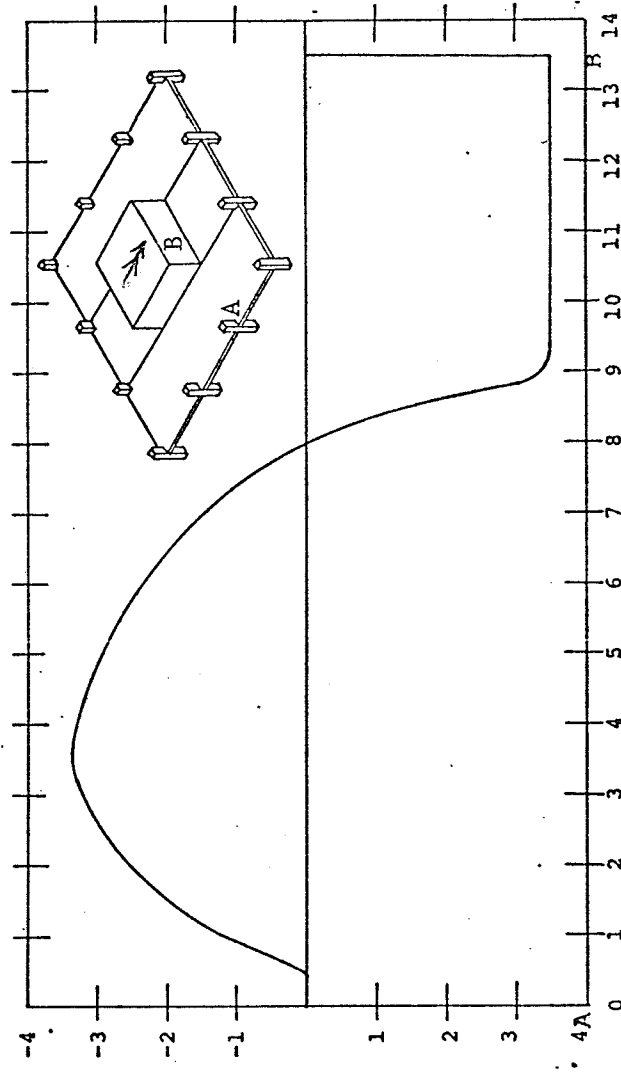
Distance (in)
Slope Along AB
Model ES2
Fig. B3 (b)





Photograph of Model ES3

Fig. B4(a)



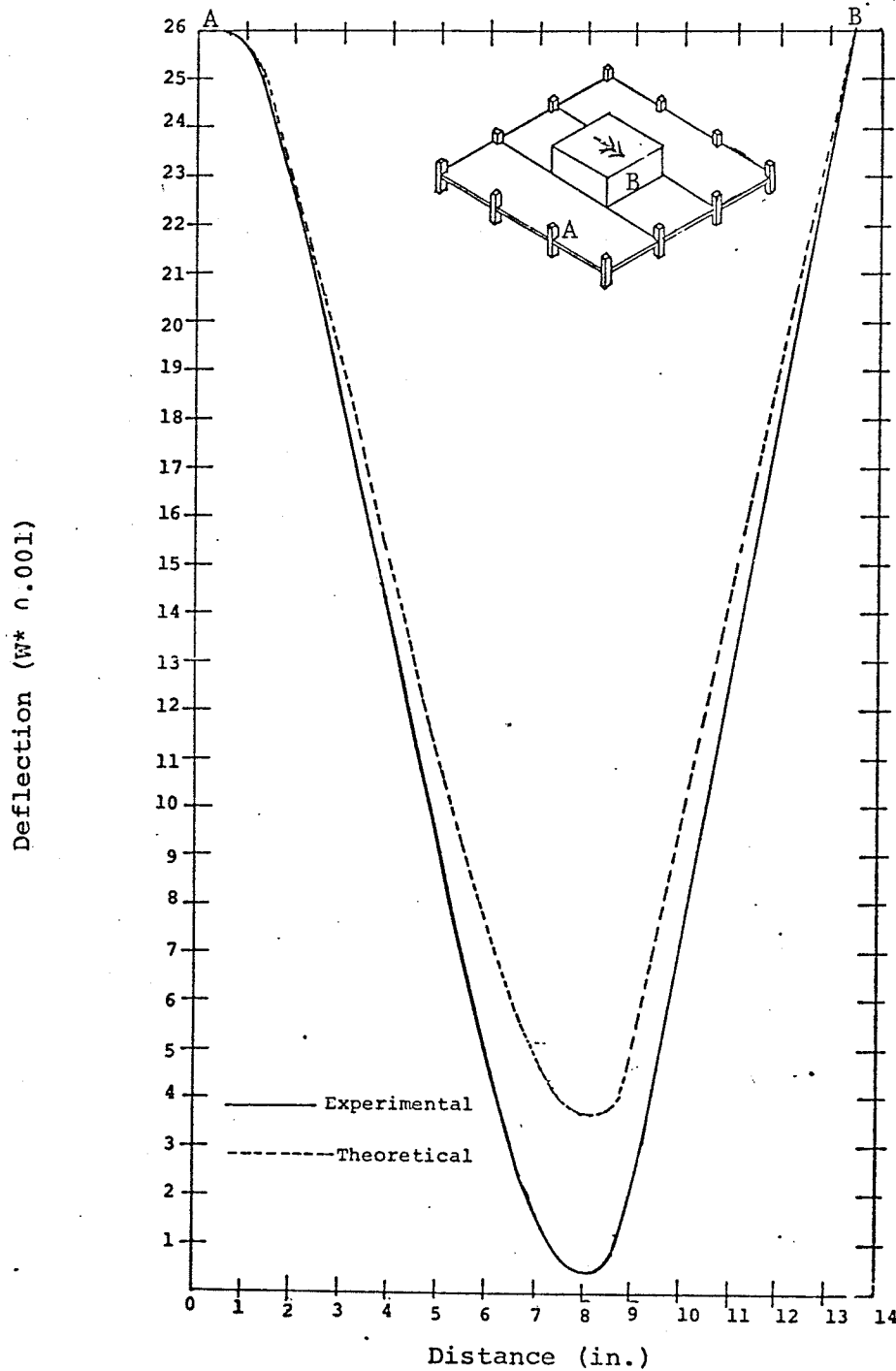
Slope ($\frac{3W}{X} * 0.0015$)

Distance (in.)

Slope Along AR

Model ES3

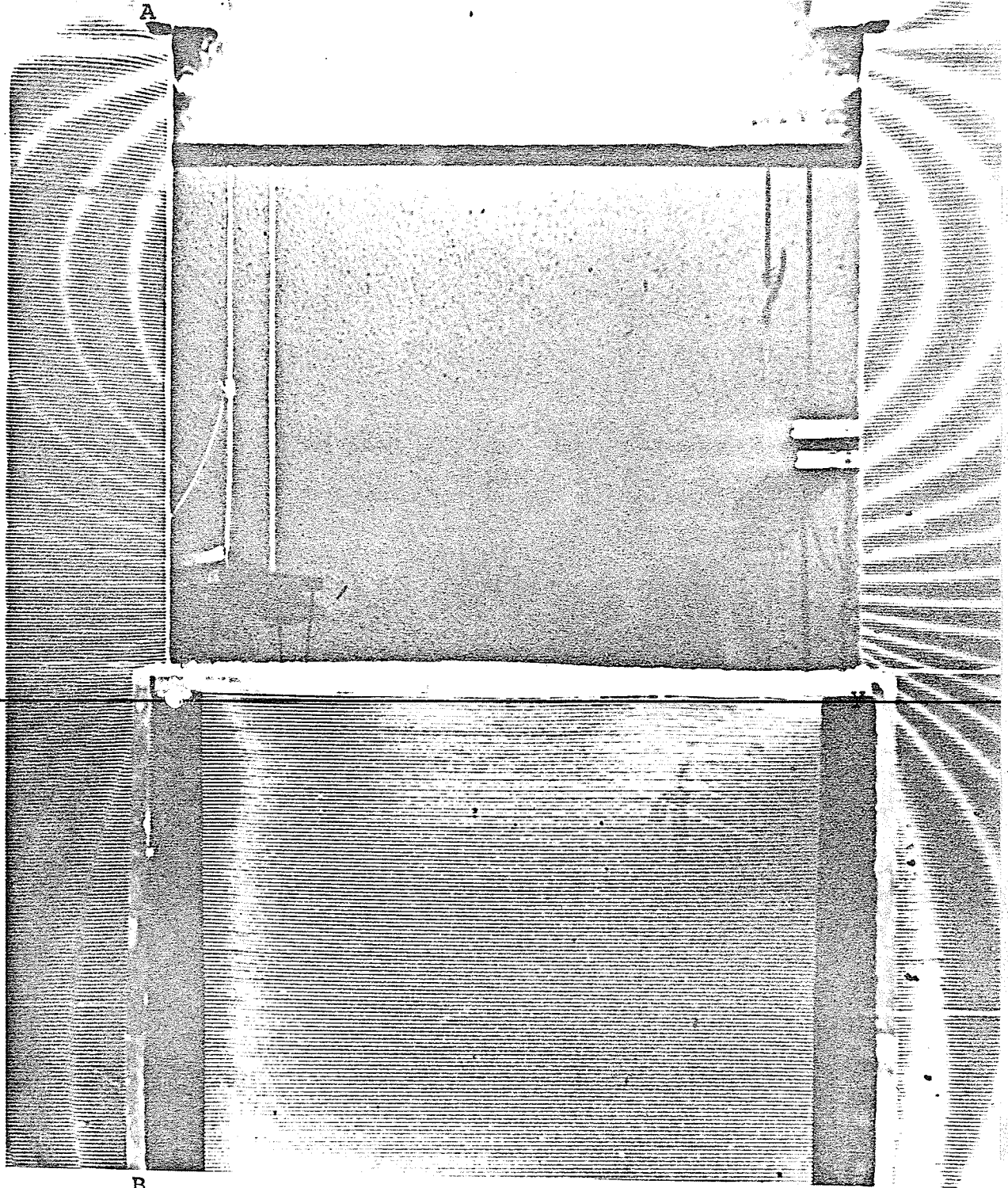
Fig. B4 (b)



Deflection Curve Along AB
Model ES3

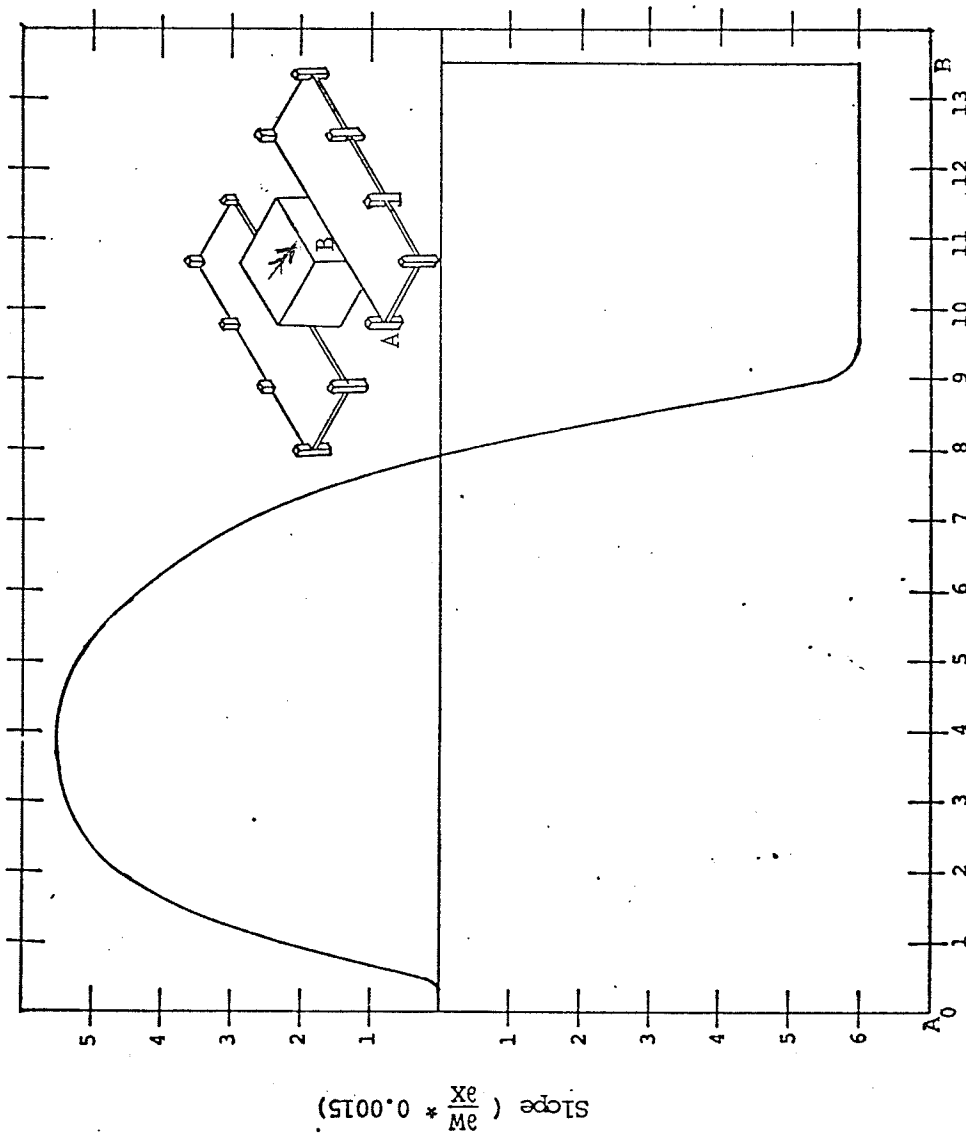
Fig. B4 (c)

x
y
x



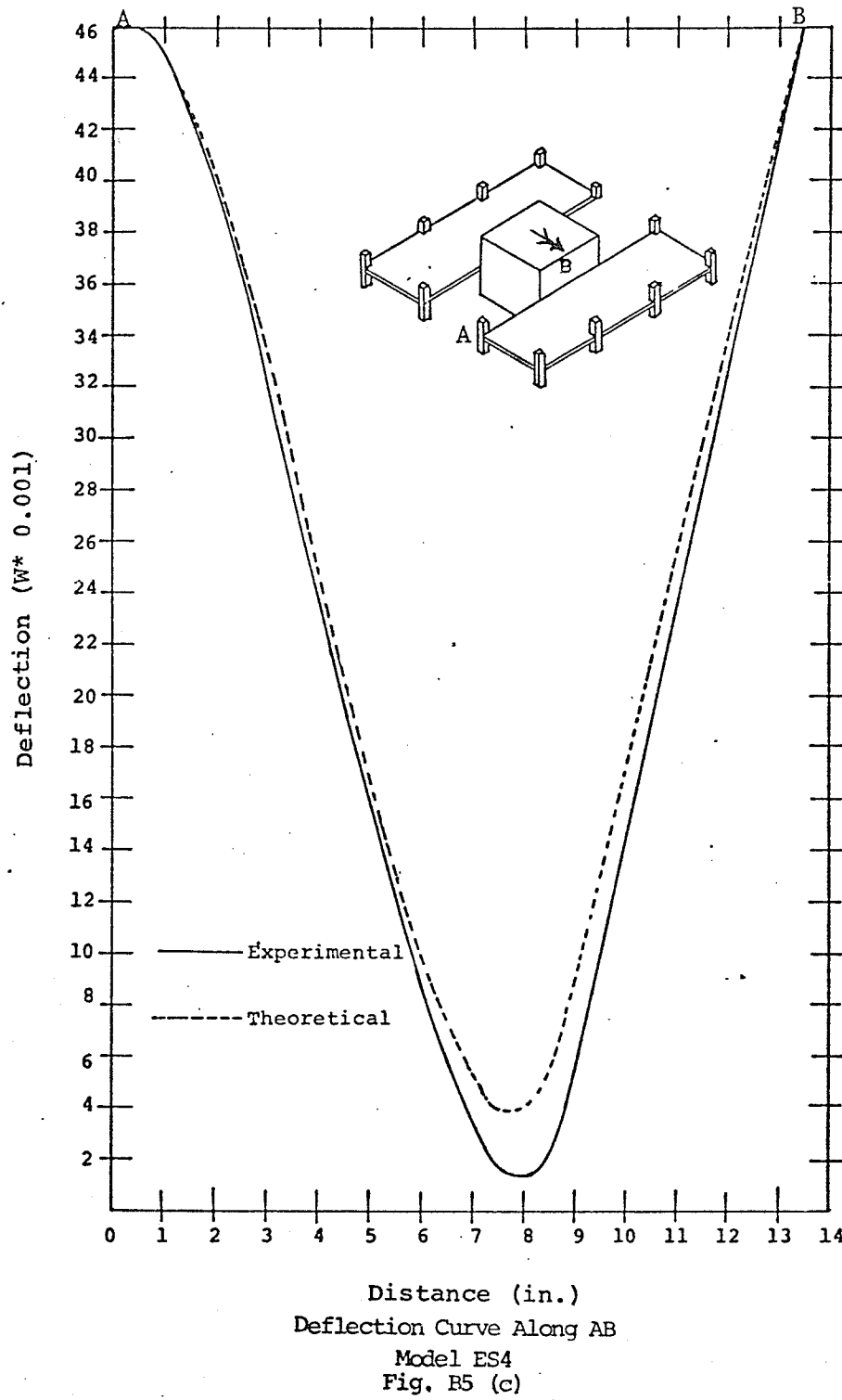
Photograph of Model ES4

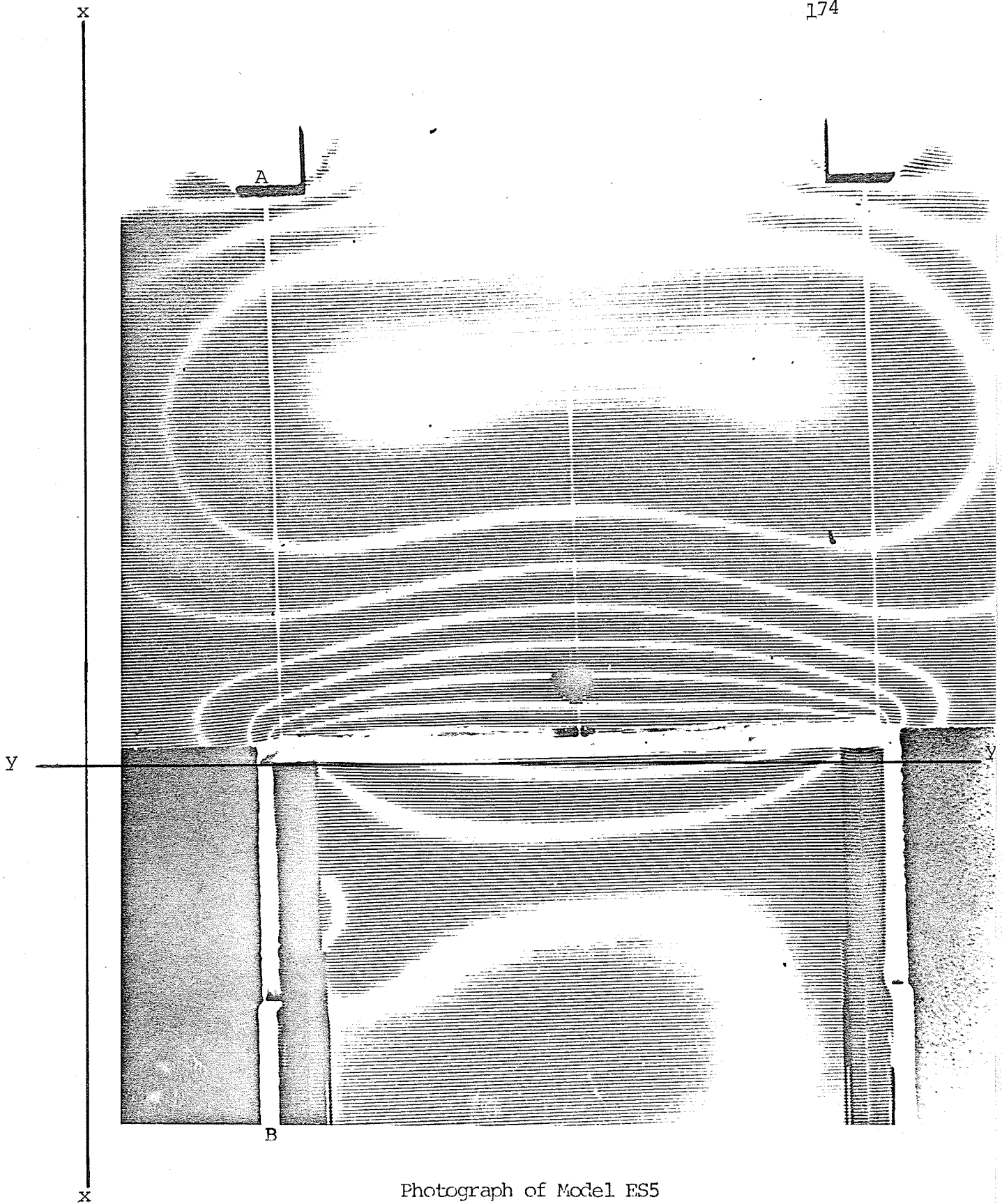
Fig. B5(a)



Distance (in.)
Slope Along AB
Model ES4

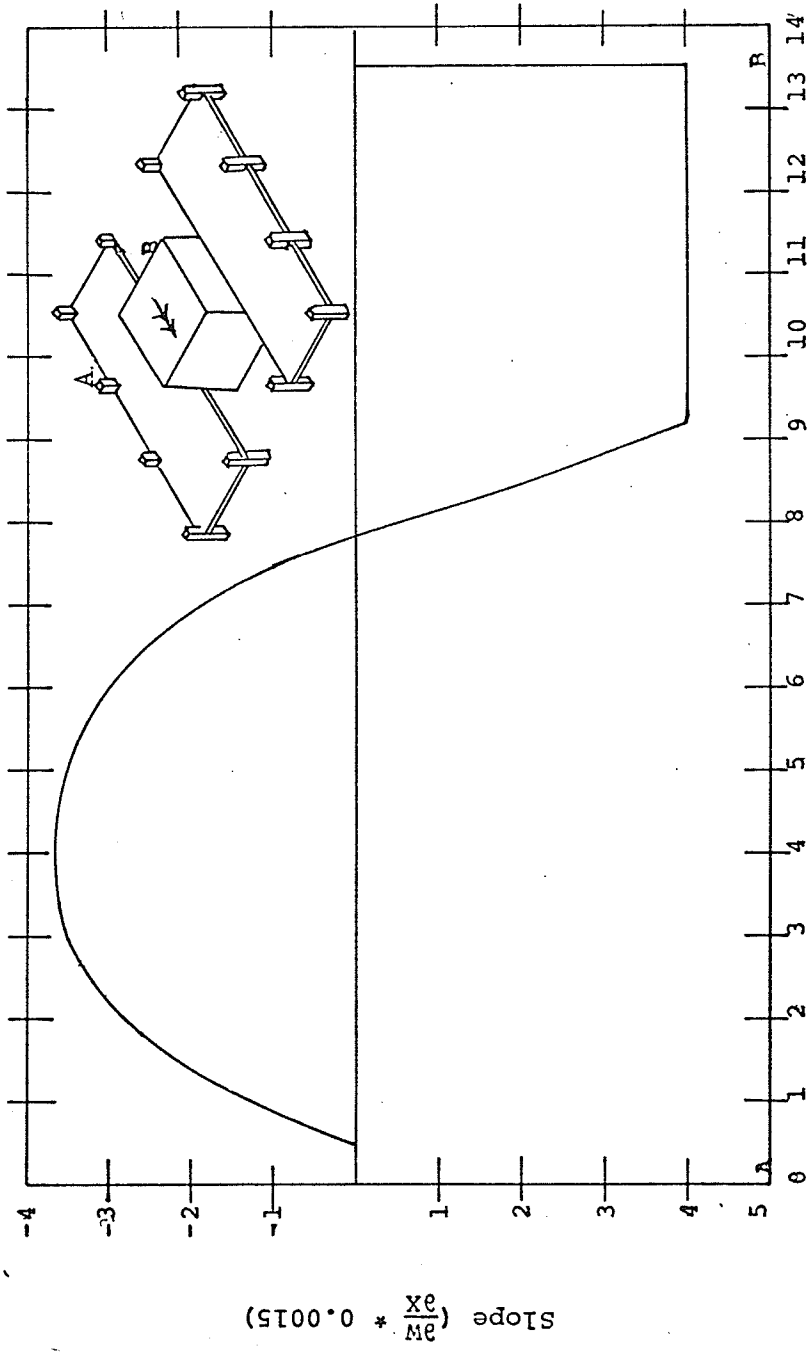
Fig. B5 (b)



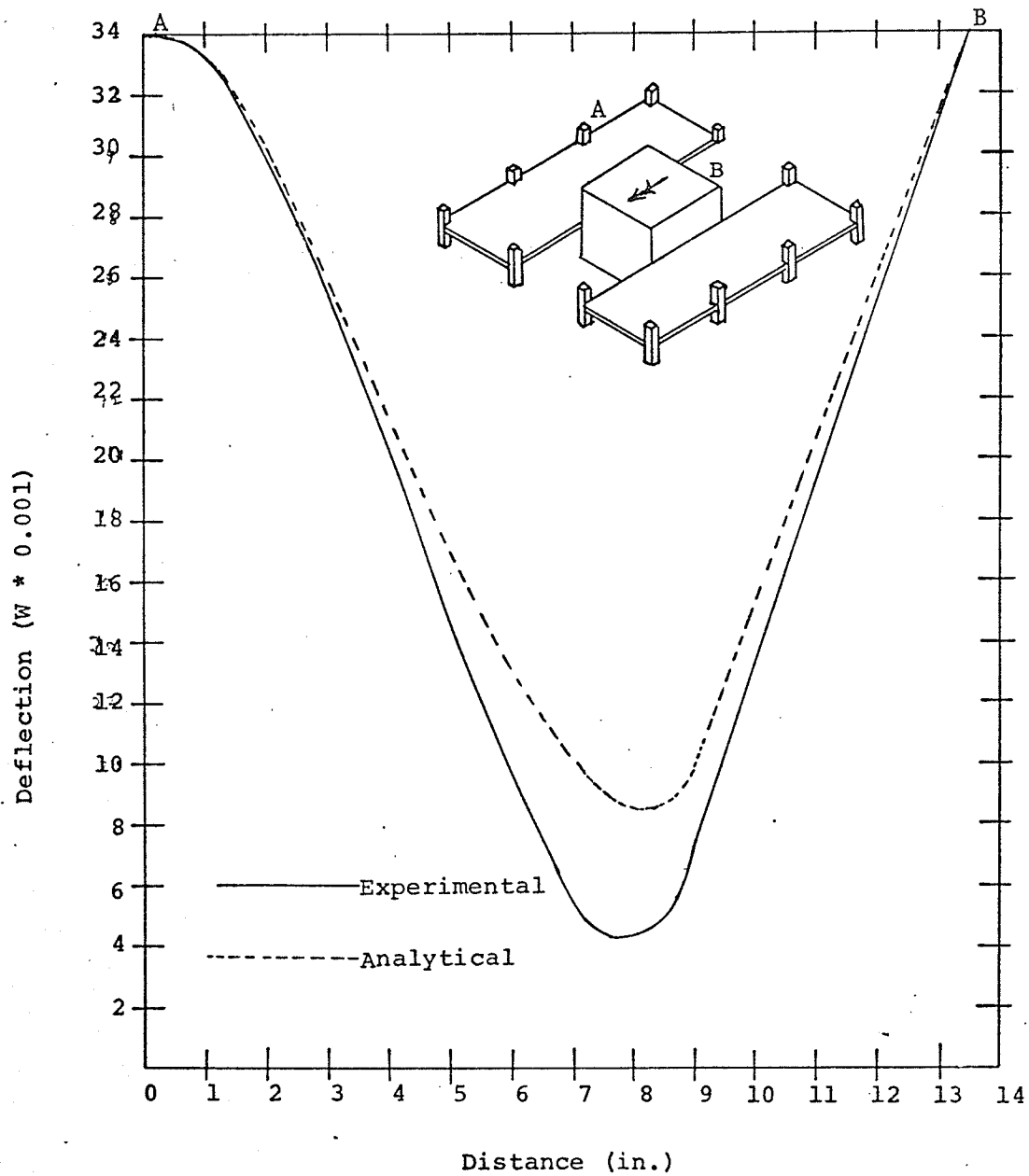


Photograph of Model ES5

Fig. B6(a)

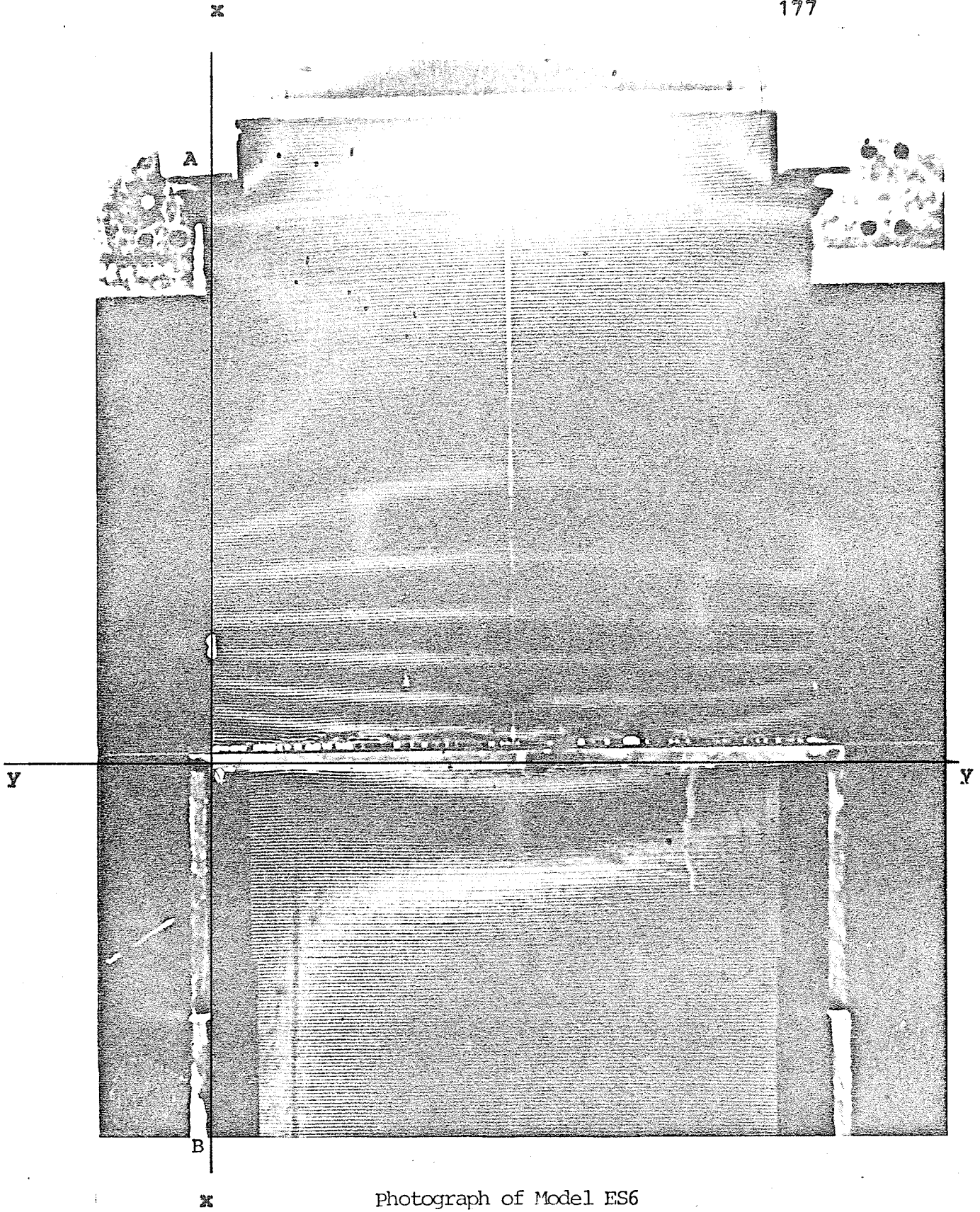


Distance (in.)
Slope Along AB.
Model ES5
Fig. D6 (b)



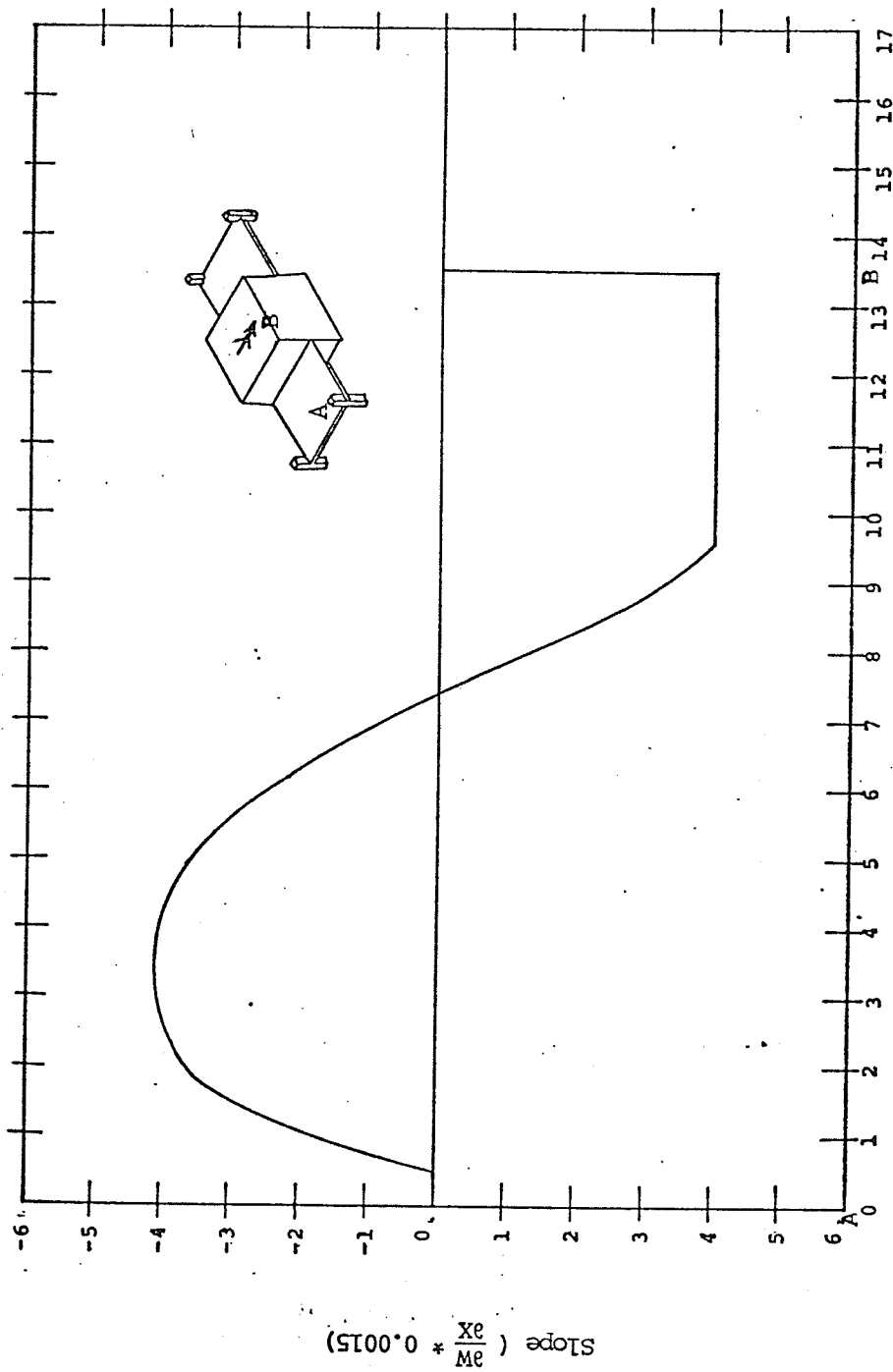
Deflection Curve Along AB
Model ES5

Fig. B6 (c)



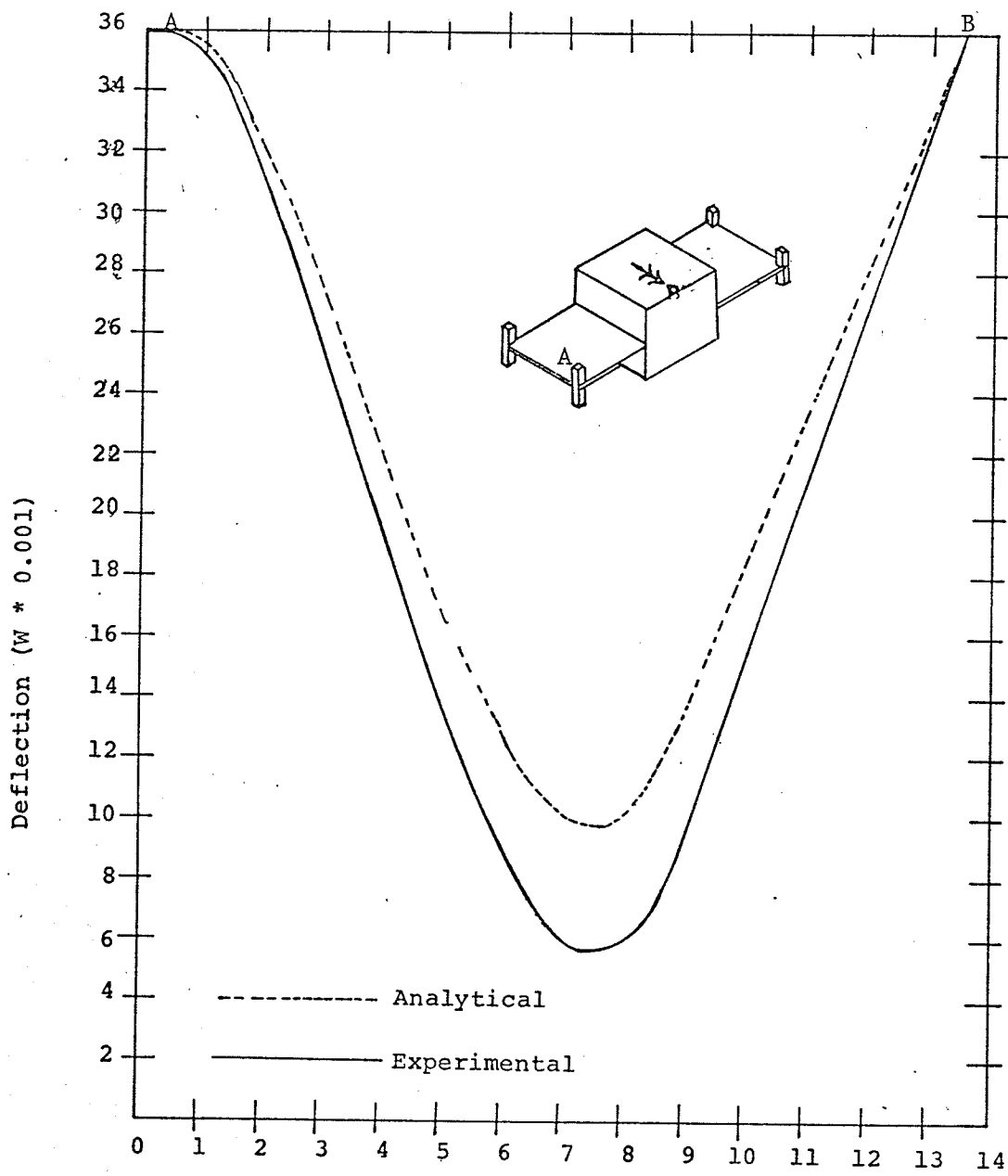
Photograph of Model ES6

Fig. B7(a)

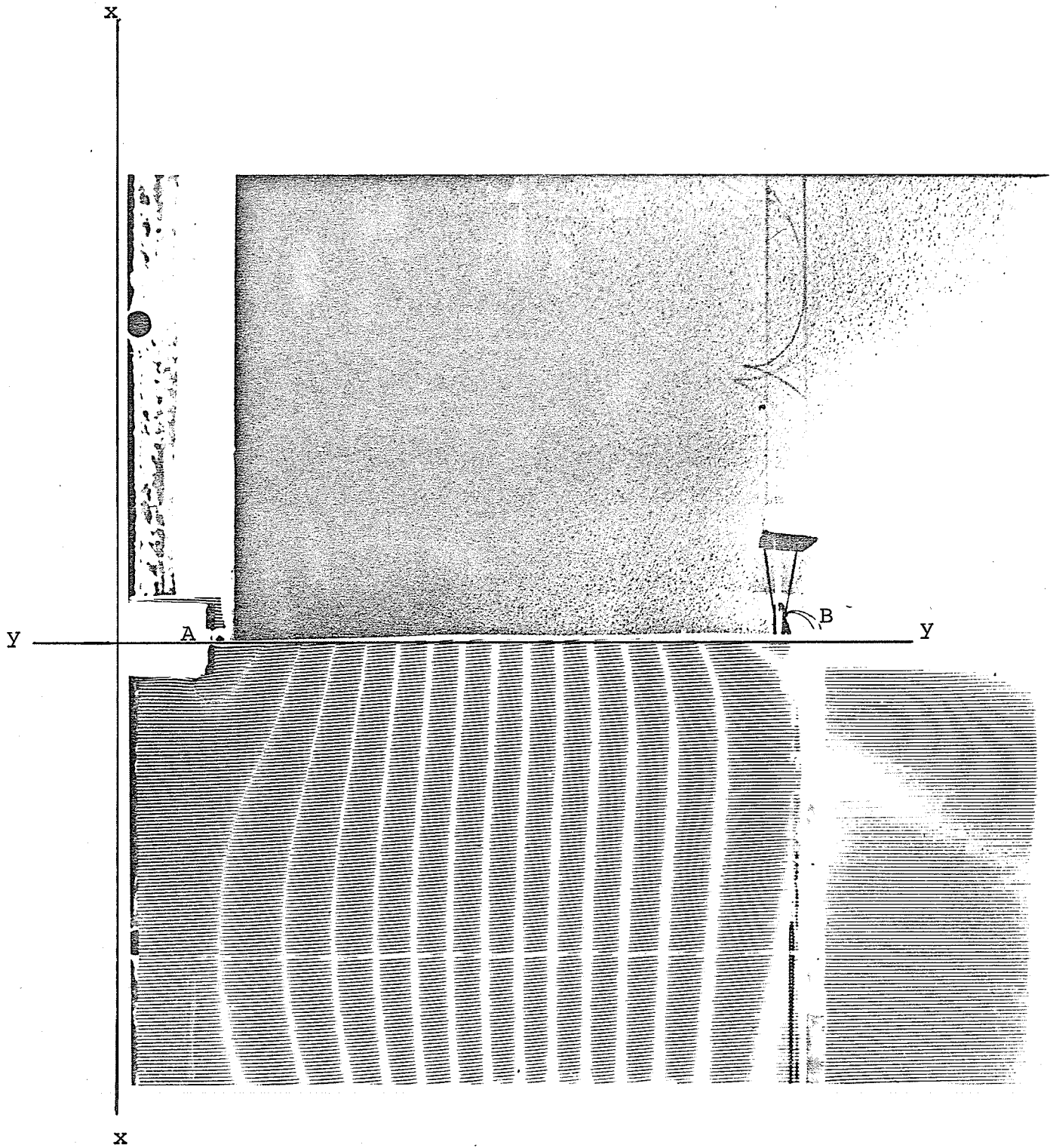


Distance (in.)
Slope Along AB
Model ES6

Fig. B7 (b)

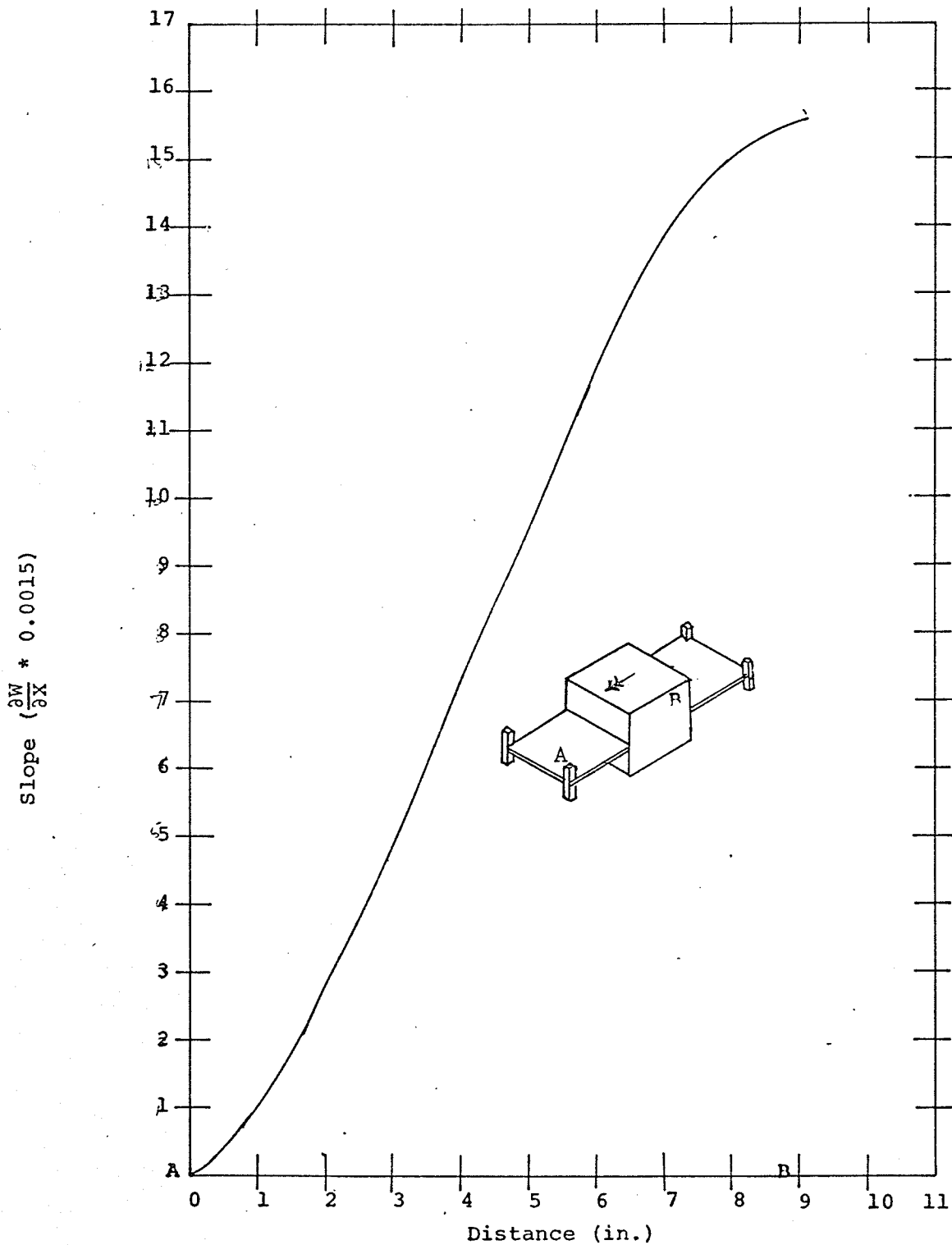


Distance (in.)
 Deflection Curve Along AB
 Model ES6
 Fig. B7 (c)



Photograph of Model ES7

Fig. B8(a)



Slope Curve Along AB

Model ES7

Fig. B8 (B)

APPENDIX C

Tables For Applied Moments and Resulting Rotations

TABLE C1

APPLIED MOMENTS AND ROTATIONS
EFFECT OF COLUMN SIZE

LOAD TYPE MODEL	A	B	C	D
P1	$M_B = 120 \text{ in.-Lb.}$ $\theta_B = 0.00415 \text{ Rad.}$	$M_B = 120 \text{ in.-Lb.}$ $\theta_{A_1} = \theta_{C_1} = 0.0056 \text{ Rad.}$ $\theta_{B_1} = 0.0054 \text{ Rad.}$	$M_A = M_C = 15 \text{ in.-Lb.}$ $\theta_{A_2} = \theta_{C_2} = 0.0126 \text{ Rad.}$ $\theta_{B_2} = 0.0028 \text{ Rad.}$	$M_A = M_C = 15 \text{ in.-Lb.}$ $\theta_A = \theta_C = 0.0096 \text{ Rad.}$
P2	$M_B = 120 \text{ in.-Lb.}$ $\theta_B = 0.00405 \text{ Rad.}$	$M_B = 120 \text{ in.-Lb.}$ $\theta_{A_1} = \theta_{C_1} = 0.0054 \text{ Rad.}$ $\theta_{B_1} = 0.0053 \text{ Rad.}$	$M_A = M_C = 15 \text{ in.-Lb.}$ $\theta_{A_2} = \theta_{C_2} = 0.01147 \text{ Rad.}$ $\theta_{B_2} = 0.0027 \text{ Rad.}$	$M_A = M_C = 15 \text{ in.-Lb.}$ $\theta_A = \theta_C = 0.0085 \text{ Rad.}$
P3	$M_B = 120 \text{ in.-Lb.}$ $\theta_B = 0.00382 \text{ Rad.}$	$M_B = 120 \text{ in.-Lb.}$ $\theta_{A_1} = \theta_{C_1} = 0.0053 \text{ Rad.}$ $\theta_{B_1} = 0.0052 \text{ Rad.}$	$M_A = M_C = 15 \text{ in.-Lb.}$ $\theta_{A_2} = \theta_{C_2} = 0.0103 \text{ Rad.}$ $\theta_{B_2} = 0.0026 \text{ Rad.}$	$M_A = M_C = 15 \text{ in.-Lb.}$ $\theta_A = \theta_C = 0.0074 \text{ Rad.}$
P4	$M_B = 120 \text{ in.-Lb.}$ $\theta_B = 0.00376 \text{ Rad.}$	$M_B = 120 \text{ in.-Lb.}$ $\theta_{A_1} = \theta_{C_1} = 0.0051 \text{ Rad.}$ $\theta_{B_1} = 0.0052 \text{ Rad.}$	$M_A = M_C = 15 \text{ in.-Lb.}$ $\theta_{A_2} = \theta_{C_2} = 0.0099 \text{ Rad.}$ $\theta_{B_2} = 0.0025 \text{ Rad.}$	$M_A = M_C = 15 \text{ in.-Lb.}$ $\theta_A = \theta_C = 0.0063 \text{ Rad.}$

TABLE C2

APPLIED MOMENTS AND ROTATIONS
EFFECT OF SHEAR WALL SIZE

MODEL	A	B	C	D
P5	$M_B = 120 \text{ in.-Lb.}$ $\Theta_B = 0.00907 \text{ Rad.}$	$M_B = 120 \text{ in.-Lb.}$ $\Theta_{A1} = \Theta_{C1} = 0.0076 \text{ Rad.}$ $\Theta_{B1} = 0.0112 \text{ Rad.}$	$M_A = M_C = 15 \text{ in.-Lb.}$ $\Theta_{A2} = \Theta_{C2} = 0.0135 \text{ Rad.}$ $\Theta_{B2} = 0.0038 \text{ Rad.}$	$M_A = M_C = 15 \text{ in.-Lb.}$ $\Theta_C = 0.0108 \text{ Rad.}$
P6	$M_B = 120 \text{ in.-Lb.}$ $\Theta_B = 0.00676 \text{ Rad.}$	$M_B = 120 \text{ in.-Lb.}$ $\Theta_{A1} = \Theta_{C1} = 0.0069 \text{ Rad.}$ $\Theta_{B1} = 0.00857 \text{ Rad.}$	$M_A = M_C = 15 \text{ in.-Lb.}$ $\Theta_{A2} = \Theta_{C2} = 0.01326 \text{ Rad.}$ $\Theta_{B2} = 0.00345 \text{ Rad.}$	$M_A = M_C = 15 \text{ in.-Lb.}$ $\Theta_A = \Theta_C = 0.0104 \text{ Rad.}$
P1	$M_B = 120 \text{ in.-Lb.}$ $\Theta_B = 0.00415 \text{ Rad.}$	$M_B = 120 \text{ in.-Lb.}$ $\Theta_{A1} = 0.0056 \text{ Rad.}$ $\Theta_{B1} = 0.0054 \text{ Rad.}$	$M_A = M_C = 15 \text{ in.-Lb.}$ $\Theta_{A2} = \Theta_{C2} = 0.0126 \text{ Rad.}$ $\Theta_{B2} = 0.0028 \text{ Rad.}$	$M_A = M_C = 15 \text{ in.-Lb.}$ $\Theta_A = \Theta_C = 0.0096 \text{ Rad.}$
P7	$M_B = 120 \text{ in.-Lb.}$ $\Theta_B = 0.00284 \text{ Rad.}$	$M_B = 120 \text{ in.-Lb.}$ $\Theta_{A1} = \Theta_{C1} = 0.00477 \text{ Rad.}$ $\Theta_{B1} = 0.00374 \text{ Rad.}$	$M_A = M_C = 15 \text{ in.-Lb.}$ $\Theta_{A2} = \Theta_{C2} = 0.0126 \text{ Rad.}$ $\Theta_{B2} = 0.00237 \text{ Rad.}$	$M_A = M_C = 15 \text{ in.-Lb.}$ $\Theta_A = \Theta_C = 0.00946 \text{ Rad.}$

TABLE C3

APPLIED MOMENTS AND ROTATIONS
EFFECT OF SHEAR WALL SHAPE

MODEL	A	B	C	D
P8	$M_B = 120 \text{ in.-Lb.}$ $\Theta_B = 0.00725 \text{ Rad.}$	$M_B = 120 \text{ in.-Lb.}$ $\Theta_{A_1} = \Theta_{C_1} = 0.00645 \text{ Rad.}$ $\Theta_{B_1} = 0.00916 \text{ Rad.}$	$M_A = M_C = 15 \text{ in.-Lb.}$ $\Theta_{A_2} = \Theta_{C_2} = 0.0109 \text{ Rad.}$ $\Theta_{B_2} = 0.0032 \text{ Rad.}$	$M_A = M_C = 15 \text{ in.-Lb.}$ $\Theta_A = \Theta_C = 0.00854 \text{ Rad.}$
P2	$M_B = 120 \text{ in.-Lb.}$ $\Theta_B = 0.00405 \text{ Rad.}$	$M_B = 120 \text{ in.-Lb.}$ $\Theta_{A_1} = \Theta_{C_1} = 0.0054 \text{ Rad.}$ $\Theta_{B_1} = 0.0053 \text{ Rad.}$	$M_A = M_C = 15 \text{ in.-Lb.}$ $\Theta_{A_2} = \Theta_{C_2} = 0.01147 \text{ Rad.}$ $\Theta_{B_2} = 0.0027 \text{ Rad.}$	$M_A = M_C = 15 \text{ in.-Lb.}$ $\Theta_A = \Theta_C = 0.0085 \text{ Rad.}$
P9	$M_B = 120 \text{ in.-Lb.}$ $\Theta_B = 0.0023 \text{ Rad.}$	$M_B = 120 \text{ in.-Lb.}$ $\Theta_{A_1} = \Theta_{C_1} = 0.0044 \text{ Rad.}$ $\Theta_{B_1} = 0.00318 \text{ Rad.}$	$M_A = M_C = 15 \text{ in.-Lb.}$ $\Theta_{A_2} = \Theta_{C_2} = 0.0111 \text{ Rad.}$ $\Theta_{B_2} = 0.00219 \text{ Rad.}$	$M_A = M_C = 15 \text{ in.-Lb.}$ $\Theta_A = \Theta_C = 0.0079 \text{ Rad.}$
P10	$M_B = 120 \text{ in.-Lb.}$ $\Theta_B = 0.00169 \text{ Rad.}$	$M_B = 120 \text{ in.-Lb.}$ $\Theta_{A_1} = \Theta_{C_1} = 0.00386 \text{ Rad.}$ $\Theta_{B_1} = 0.00233 \text{ Rad.}$	$M_A = M_C = 15 \text{ in.-Lb.}$ $\Theta_{A_2} = \Theta_{C_2} = 0.0117 \text{ Rad.}$ $\Theta_{B_2} = 0.0019 \text{ Rad.}$	$M_A = M_C = 15 \text{ in.-Lb.}$ $\Theta_A = \Theta_C = 0.00836 \text{ Rad.}$

TABLE C4

$$\frac{\text{Shear Wall Size}}{\text{Total Span}} = 1/5$$

Model	Shear Wall Size in X-X Direction (SX) Shear Wall Size in X-X Direction (SY)	Applied Moment to the Shear Wall	Rotation	Direction Stiffness Coefficient
PS1-1	0.5	120 in. Lb.	0.00643 Rad.	18666.92
PS1-4	0.5	120 in. Lb.	0.0144 Rad.	8308.26
PS1-5	0.5	120 in. Lb.	0.0085 Rad.	14117.64
PS1-8	0.5	60 in. Lb.	0.0069 Rad.	8633.09
PS1-9	0.5	60 in. Lb.	0.1033 Rad.	580.45
PS2-1	1.0	120 in. Lb.	0.0088 Rad.	13642.56
PS2-4	1.0	120 in. Lb.	0.0168 Rad.	7149.24
PS2-5	1.0	120 in. Lb.	0.0124 Rad.	9623.86
PS2-8	1.0	60 in. Lb.	0.0134 Rad.	4455.0
PS2-9	1.0	60 in. Lb.	0.0512 Rad.	1171.53
PS3-1	1.5	120 in. Lb.	0.0089 Rad.	13445.37
PS3-4	1.5	120 in. Lb.	0.0154 Rad.	7757.55
PS3-5	1.5	120 in. Lb.	0.0131 Rad.	9125.47
PS3-8	1.5	60 in. Lb.	0.0199 Rad.	3015.22
PS3-9	1.5	60 in. Lb.	0.0302 Rad.	1980.26
PS4-1	2.0	120 in. Lb.	0.0078 Rad.	15290.71
PS4-4	2.0	120 in. Lb.	0.0129 Rad.	9314.10
PS4-5	2.0	120 in. Lb.	0.0119 Rad.	10055.51
PS4-8	2.0	60 in. Lb.	0.0263 Rad.	2280.62
PS4-9	2.0	60 in. Lb.	0.0198 Rad.	3033.36

TABLE C5

$\frac{\text{Shear Wall Size}}{\text{Total Span}} = 1/4$

Model	Shear Wall Size in X-X Direction (SX) Shear Wall Size in Y-Y Direction (SY)	Applied Moment to the Shear Wall	Rotation	Direction Stiffness Coefficient
PS5-1	0.5	120 in. Lb.	0.0048 Rad.	24880.78
PS5-4	0.5	120 in. Lb.	0.0116 Rad.	10348.39
PS5-5	0.5	120 in. Lb.	0.0062 Rad.	19246.19
PS5-8	0.5	60 in. Lb.	0.00487 Rad.	12321.83
PS5-9	0.5	60 in. Lb.	0.0796 Rad.	753.20
PS6-1	1.0	120 in. Lb.	0.00648 Rad.	18521.37
PS6-4	1.0	120 in. Lb.	0.0129 Rad.	9274.28
PS6-5	1.0	120 in. Lb.	0.0089 Rad.	13349.64
PS6-8	1.0	60 in. Lb.	0.0090 Rad.	6666.66
PS6-9	1.0	60 in. Lb.	0.0356 Rad.	1685.39
PS7-1	1.5	120 in. Lb.	0.0064 Rad.	18782.57
PS7-4	1.5	120 in. Lb.	0.0112 Rad.	10695.18
PS7-5	1.5	120 in. Lb.	0.0093 Rad.	12816.4
PS7-8	1.5	60 in. Lb.	0.0130 Rad.	4604.76
PS7-9	1.5	60 in. Lb.	0.0197 Rad.	3033.36
PS8-1	2.0	120 in. Lb.	0.0054 Rad.	22113.30
PS8-4	2.0	120 in. Lb.	0.0088 Rad.	13636.36
PS8-5	2.0	120 in. Lb.	0.0083 Rad.	14361.12
PS8-8	2.0	60 in. Lb.	0.0170 Rad.	3529.41
PS8-9	2.0	60 in. Lb.	0.0123 Rad.	4878.44

TABLE C6

$$\frac{\text{Shear Wall Size}}{\text{Total Span}} = 1/3$$

Model	Shear Wall Size in X-X Direction (SX) Shear Wall Size in Y-Y Direction (SY)	Applied Moment to the Shear Wall	Rotation	Direction Stiffness Coefficient
PS9-1	0.5	120 in. Lb.	0.0031 Rad.	38986.35
PS9-4	0.5	120 in. Lb.	0.0079 Rad.	15099.27
PS9-5	0.5	120 in. Lb.	0.0039 Rad.	30953.36
PS9-8	0.5	60 in. Lb.	0.0029 Rad.	20547.94
PS9-9	0.5	60 in. Lb.	0.0512 Rad.	1170.85
PS10-1	1.0	120 in. Lb.	0.0039 Rad.	30336.97
PS10-4	1.0	120 in. Lb.	0.0082 Rad.	14519.92
PS10-5	1.0	120 in. Lb.	0.0053 Rad.	22411.46
PS10-8	1.0	60 in. Lb.	0.0050 Rad.	11934.12
PS10-9	1.0	60 in. Lb.	0.0198 Rad.	3032.29
PS11-1	1.5	120 in. Lb.	0.0037 Rad.	32490.40
PS11-4	1.5	120 in. Lb.	0.0065 Rad.	18482.86
PS11-5	1.5	120 in. Lb.	0.0054 Rad.	22160.66
PS11-8	1.5	60 in. Lb.	0.0070 Rad.	8555.53
PS11-9	1.5	60 in. Lb.	0.0099 Rad.	6012.8
PS12-1	2.0	120 in. Lb.	0.0029 Rad.	40367.33
PS12-4	2.0	120 in. Lb.	0.00468 Rad.	25617.00
PS12-5	2.0	120 in. Lb.	0.0047 Rad.	25501.52
PS12-8	2.0	60 in. Lb.	0.0089 Rad.	6719.67
PS12-9	2.0	60 in. Lb.	0.0058 Rad.	10364.48

TABLE C7

$$\frac{\text{Shear Wall Size}}{\text{Total Span}} = 1/2.5$$

Model	Shear Wall Size in X-X Direction (SX) Shear Wall Size in Y-Y Direction (SY)	Applied Moment to the Shear Wall	Rotation	Direct Stiffness Coefficient
PS13-1	0.5	120 in. Lb.	0.0022 Rad.	55435.95
PS13-4	0.5	120 in. Lb.	0.0058 Rad.	20761.24
PS13-5	0.5	120 in. Lb.	0.0027 Rad.	44732.88
PS13-8	0.5	60 in. Lb.	0.0020 Rad.	30003.74
PS13-9	0.5	60 in. Lb.	0.0356 Rad.	1683.88
PS14-1	1.0	120 in. Lb.	0.0027 Rad.	44923.28
PS14-4	1.0	120 in. Lb.	0.0056 Rad.	21192.8
PS14-5	1.0	120 in. Lb.	0.0036 Rad.	33570.18
PS14-8	1.0	60 in. Lb.	0.0033 Rad.	18312.22
PS14-9	1.0	60 in. Lb.	0.0123 Rad.	4878.44
PS15-1	1.5	120 in. Lb.	0.0024 Rad.	50316.57
PS15-4	1.5	120 in. Lb.	0.0041 Rad.	29028.99
PS15-5	1.5	120 in. Lb.	0.0035 Rad.	34092.94
PS15-8	1.5	60 in. Lb.	0.0044 Rad.	13501.35
PS15-9	1.5	60 in. Lb.	0.0058 Rad.	10368.24
PS16-1	2.0	120 in. Lb.	0.0018 Rad.	65111.22
PS16-4	2.0	120 in. Lb.	0.0028 Rad.	42553.18
PS16-5	2.0	120 in. Lb.	0.0030 Rad.	40058.75
PS16-8	2.0	60 in. Lb.	0.0055 Rad.	10810.80
PS16-9	2.0	60 in. Lb.	0.0032 Rad.	18750.00